AD-766 467

MECHANISMS OF COMBUSTION

T. L. Boggs, et al

Georgia Institute of Technology

Prepared for:

Naval Weapons Center

July 1973

Mechanisms of Combustion

Final Report

by

T. L. Boggs
D. E. Zurn
Naval Weapons Center

and

W. C. Strahle
J. C. Handley
T. T. Milkie
Georgia Institute of Technology

Naval Weapons Center
CHINA LAKE, CALIFORNIA ■ JULY 1973

ABSTRACT

This report summarizes studies of the combustion of ammonium perchlorate-polymeric binder-ammonium perchlorate sandwiches. The first section describes the combustion of sandwiches utilizing polyurethane, carboxyl-terminated polybutadiene, hyroxyl-terminated polybutadiene, or polybutadiene acrylic acid binders. The second section deals with the deflagration of sandwiches with Fe_2O_3 or Shaw Cu0202 catalysts incorporated in the ammonium perchlorate, the HTPB binder, or at the AP-HTPB interface. The third section is concerned with the combustion of sandwiches incorporating as-received or a special preoxidized aluminum within the HTPB binder. The final section is comprised of an analytical modeling of the sandwich combustion.

NWC Technical Publication 5514

Published by.....Research Department
Collation.....Cover, 62 leaves, DD Form 1473, abstract cards
First printing.....250 unnumbered copies
Security classification.....UNCLASSIFIED

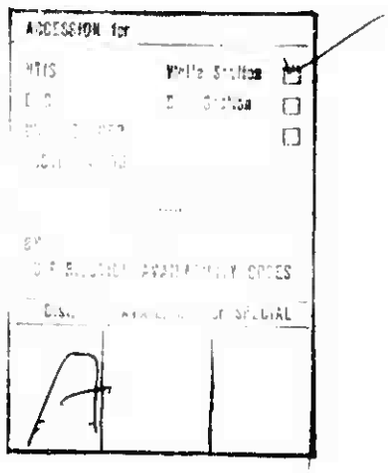

Naval Weapons Center

AN ACTIVITY OF THE NAVAL MATERIAL COMMAND

Paul L. Pugh, RADM, USN . . . . . Commander

Walter B. LaBerge, Ph.D. . . . . Technical Director

FOREWORD

Since the early phases of World War II the solid propellant rocket motor has continued to grow in importance as a propulsion system for various kinds of ordnance developed by the Navy and used by the Fleet. From small ordnance-type rockets for aircraft firing, such as the 2.75-inch folding-fin aircraft rocket, to the Polaris and Poseidon missiles for projecting strategic nuclear warheads from submerged submarines, the solid propellant rocket motor or engine has been an important component of the weapon system.

In the past, propellant development and rocket motor design have been empirical processes because of limited understanding of the complex combustion processes that take place within the rocket combustion chamber during propellant burning. The objective of the studies reported herein has been to elucidate the mechanisms of combustion of composite solid propellants and to apply this understanding to the development of solid propellants having superior burning characteristics.

The program was sponsored by the Naval Air Systems Command under NAVAIR TASK A310310C/008A/3R02402002 to the Naval Weapons Center. The work described in this final report was performed at the Naval Weapons Center and at the Georgia Institute of Technology under contract N00123-72-C-0242.

This report has been prepared for timely presentation of information. Because of the continuing nature of research in this area, refinements and modifications may be made in the future.

Released by
E. W. PRICE, *Head*
Aerothermochemistry Division
15 June 1973

Under authority of
HUGH W. HUNTER, *Head*
Research Department

CONTENTS

UNCLASSIFIED

Security Classification

DOCUMENT CONTROL DATA · R & D

Security classification of title, body of abstract and indexing annotation must be entered when the overall report is classified)

1 ORIGINATING ACTIVITY (Corporate author) Naval Weapons Center China Lake, California 93555	2a. REPORT SECURITY CLASSIFICATION UNCLASSIFIED 2b. GROUP

3 REPORT TITLE

MECHANISMS OF COMBUSTION, FINAL REPORT

4 DESCRIPTIVE NOTES (Type of report and inclusive dates)

Final research report

5 AUTHOR(S) (First name, middle initial, last name)

T. L. Boggs and D. E. Zurn, Nsval Weapons Center
and
W. C. Strshle, J. C. Handley, and T. T. Milkie, Georgia Institute of Technology

6 REPORT DATE	7a. TOTAL NO OF PAGES	7b NO OF REFS
July 1973	122 126	63

8a CONTRACT OR GRANT NO	9a. ORIGINATOR'S REPORT NUMBER(S)
b PROJECT NO NAVAIR TASK A3103IOC/008A/3R02402002	NWC TP 5514
c d	9b OTHER REPORT NO(S) (Any other numbers that may be assigned this report)

10 DISTRIBUTION STATEMENT

Approved for public release; distribution unlimited.

11 SUPPLEMENTARY NOTES	12 SPONSORING MILITARY ACTIVITY
	Naval Air Systems Command Naval Material Command Washington, D. C. 20360

13 ABSTRACT

This report summarizes studies of the combustion of smmonium perchlorate-polymeric binder-ammonium perchlorate sandwiches. The first section describes the combustion of sandwiches utilizing polyurethane, carboxyl-terminated polybutadiene, hyroxyl-terminated polybutadiene, or polybutadiene acrylic acid binders. The second section deals with the deflagration of sandwiches with Fe_2O_3 or Harshaw Cu0202 catalysts incorporated in the ammonium perchlorate, the HTPB binder, or at the AP-HTPB interface. The third section is concerned with the combustion of sandwiches incorporating as-received or a special preoxidized sluminum within the HTPB binder. The final section is comprised of an analyticsl mooeling of the sandwich combustion.

DD FORM 1 NOV 65 1473 (PAGE 1)

S/N 0101-807-6801

UNCLASSIFIED

Security Classification

14 KEY WORDS	LINK A		LINK B		LINK C	
	ROLE	WT	ROLE	WT	ROLE	WT
Combustion						
Carboxyl-terminsted polybutadiene						
Polybutadiene scrylic acid						
Composite propellants						
Scanning electron microscopy						
Ammonium perchlorate						
Catalysts						
Deflagration						
Cinephotomicrography						
Polyurethane						
Hydroxyl-terminated polybutadiene						
Aluminum						
Analytical models						

SECTION 1

INTRODUCTION

T. L. Boggs
Naval Weapons Center

The combustion of composite propellants is a complex set of concurrent reactions taking place in the gas, liquid and solid phases of a heterogeneous mixture. The importance of the various possible reaction steps is dependent upon such considerations as propellant composition, how the various ingredients are included in the propellant (e.g., particle size of the oxidizer, degree of mixedness, binder type, degree of cure, etc.), and the environment in which the propellant is burned (pressure, initial sample temperature, environmental gas, etc.). Each of these considerations is important since a change in one parameter causes other changes in the overall combustion behavior. However, at present, the knowledge which would allow one a priori to predict combustion behavior does not exist. Thus we cannot predict, given only the data on a propellant mix sheet, such characteristics as the burning rate, temperature sensitivity and susceptibility to combustion instability of the resultant propellant. Predictive capability is largely dependent upon empirical correlation rather than on analytic models which reflect a fundamental understanding of the combustion processes. This is, of course, a consequence of the complexity of the problem. The physicochemical processes occurring during combustion of composite propellants, even if they were known and understood, are so complex that analytical models which are mathematically tractable would bear little resemblance to the actual combustion. Thus we have propellant combustion models which are based on one-dimensional regression, one-dimensional heat transfer, oversimplified kinetic parameters and reaction rates, and which often don't include physical considerations such as liquid phases and accumulation of species. On the other hand, the experimental observations of burning propellants have shown complicated three-dimensional microstructure of the burning surface, three-dimensional flame structure, liquid binder products, aluminum agglomeration, processes which are both spatially and temporally variant. None of the propellant ingredients dominate the combustion at all times and the relative importance of one reaction may vary with changes such as pressure increase.

In view of these considerations, the subject program was initiated to gain fundamental understanding of the mechanisms of composite solid propellant combustion. The work was accomplished at the Naval Weapons Center (NWC) and at Georgia Institute of Technology under NWC Contract No. N00123-72-C-0242.

Before presenting the work of this program, a general description of solid propellant combustion follows. It is hoped that this characterization may provide a background for the considerations of the present work.

The typical composite propellant is a heterogeneous mixture of ammonium perchlorate (AP), catalysts, metal fuel (usually aluminum (Al)), and enough polymeric binder to bond the granular materials into a solid propellant grain. This heterogeneous mixture burns by propagation of the combustion wave into the body of the unreacted propellant as a consequence of heat transfer from exothermic reactions. These reactions are assumed to occur very near the surface of the propellant but our knowledge as to where is extremely limited--some investigators claim the reactions occur in the condensed phase, others claim the energy release occurs for all practical purposes at the surface, while others argue for the release to occur in a very narrow region in the gas phase. The first analytical attempts to understand propellant combustion assumed the propellant to be homogeneous with an imposed energy balance; the heat supplied from the exothermic reactions to the unreacted propellant is that required to maintain a steady supply of reactants to the reaction zone.

These assumptions allowed an idealized one-dimensional description of the combustion to be formulated. Unfortunately such assumptions are invalid when the dimensions of heterogeneity of the propellant are comparable to or of larger scale than the thickness of the thermal wave, and when the component ingredients have varied behavior. Thus, for the case of the typical composite propellant burning at millimeters/second to several centimeters/second the heterogeneity leads to a three-dimensionally complicated combustion wave with diffusion of mass and energy perpendicular to the regression of the surface.

The Aerothermochemistry Division, NWC, has been studying combustion of composite propellants for several years. At the outset, it was decided that rather than blindly plunging into the full complexity surrounding the combustion of propellants, the course of our investigations would follow a progression from the study of individual ingredient's combustion behavior through several intermediate studies, to finally the study of the propellant itself. We made major contributions to the understanding of AP decomposition and deflagration and Al combustion. Once an understanding of the individual ingredient's behavior was obtained, then additional complexity was added by making pseudo-two-dimensional systems of oxidizer-binder-oxidizer sandwiches. Additional

complexity was then added by including Al and catalysts within the sandwiches. Thus our strategy has been to reduce the problem of propellant combustion first to one of geometrical simplicity and ingredient characterization and step-fashion to include more geometrical complexity and the interaction of ingredients.

The programs have conclusively demonstrated that the oxidizer, binder and metal fuel additives all burn differently from one another, and as a function of pressure and temperature display different combustion properties themselves. It is not the purpose of this work to review all of the individual reactions which are possible, nor to review all the voluminous speculation about these reactions. The purpose of the present work has been to study the interactions of the various ingredients in a combustion situation. To do this one must draw upon and proceed from a knowledge of how the ingredients react in a combustion situation.

The following is a very brief description and it is not intended to be all-encompassing. Rather the purpose of presenting this sketch has been to provide a background from which to view the work of the present programs. Readers desiring detailed proof of these items which are listed in summary fashion should consult the indicated references.

The combustion of AP, the principal ingredient of most composite propellants, has been extensively studied and is reported in Ref. 1-5 and the references of those reports. Those reports have shown this oxidizer capable of self-deflagration. The major characteristics of this self-deflagration are a low pressure deflagration limit at approximately 300 psi (T_o = 26°C), the existence of four distinct regimes of combustion between 300 and 10,000 psi, the existence of a liquid froth on the surface of the crystal deflagrating between 300-900 psi, a change of energy transfer mechanism with pressure increase (from one occurring predominantly in the froth at low pressure to gas phase controlled at pressures above 2000 psi), a critical dependence on purity of the sample, a flame temperature of about 1200°K, a surface regression rate between 0.3 cm/sec at 26°C and 300 psi to 1.3 cm/sec at 150°C and 2000 psi, and a surface temperature between 700-900°K.

The polymeric binders used in propellants are less well characterized with few studies having been made (Ref. 6-9). The major conclusions show that binders melt and gasify in manners dependent on binder type, heating rate and pressure.

When one considers the number of analytical models purporting to describe the combustion of solid propellants, it is amazing how little is actually known about the combustion. Unfortunately, most experiments which have been performed have lacked the resolution necessary to prove conclusively the existence or absence of certain reaction mechanisms; although that does not seem to deter many from using these

uncertain observations as mathematical singularities when applied as boundary conditions. The argument may appear to be philosophical but it should not be easily dismissed. Inherent is an unsymmetric argument; experimental observation can only disprove the boundary condition, never fully prove it. As an example, consider the burning of oxidizer and fuel slabs burning edgewise to the interface. The question to be considered is whether the leading edge of the reaction occurs at the interface, because if it does the interface can then be used as a boundary and matching can be performed at this point (e.g., at the boundary condition the rate of fuel regression equals the rate of oxidizer regression). If the observations show that maximum regression occurs in the oxidizer or fuel portions then obviously the boundary condition mentioned above is invalid. But should the experimental observation indicate that the maximum regression rate appears to occur at the interface and yet the spatial resolution is ±100 μm, then the condition of maximum regression occurring at the interface has not been proven--a 200 μm zone has been defined--and therefore the use of the above mentioned boundary condition may not be applicable.

The area of greatest uncertainty when discussing propellant combustion is the gas phase. Although one can find references which claim to have information of flame structure and transport mechanisms (laminar, turbulent, etc.), critical examination reveals that the observations are of such poor resolution that the claim cannot be supported. In contrast to the above uncertainty, some agreement has been reached concerning the microstructure of propellant surfaces during combustion (Ref. 10-14). Most of the observations have been made using samples quenched from burning. It is true that no quenching process is without artifacts but as discussed in Ref. 4 the level of credence and advocacy of any one observation has been matched to the extent of agreement with different observations (primarily cinephotomicrography (Ref. 13 and 14) and flame spectra (Ref. 12)). The results have shown that: AP crystals protrude above the binder at low pressures ($p < 450$ psi) and are recessed with respect to the binder at high pressures ($p > 600$ psi); polyurethane (PU) binder melts during burning to the extent that at higher pressures, where the oxidizer particles are recessed, the molten binder is able to flow over the AP crystals causing self-extinguishment of the propellant; interfacial or subsurface reactions between the AP and binder were not apparent for PU and carboxyl-terminated polybutadiene (CTPB) binders, and the AP crystals were observed to form a thin, surface melt and undergo subsurface reactions in the molten phase with in-depth liberation of gas resulting in bubbles and volcano-like fumaroles.

When Al is included within the propellant it is usually of small size (2-40 μm) and reasonably well mixed within the binder. Films of burning aluminized propellant have shown that the Al usually collects into large accumulates which ignite only with great difficulty. The accumulation and subsequent agglomeration of Al lead to low combustion efficiency and also have consequences for the damping of combustion

instability. Once again, the behavior of an ingredient (Al) is dependent upon the dimensions of the heterogeneity of the propellant and the thickness of the combustion wave and the test parameters. At low pressure the flame stands off quite far from the surface and the surface temperature of the propellant is not sufficient to ignite the Al. Thus larger accumulates might be expected at low pressures, other parameters being unchanged, with large agglomerates formed at the propellant surface. These large agglomerates would ignite less readily and burn more slowly and hence at greater distance from the surface. This would result in less energy feedback to the surface. Other cases of how the propellant heterogeneity affect the Al agglomeration and combustion are detailed in Ref. 15, pages 88-95.

The sandwich configuration, a layer of binder laminated between two layers of oxidizer, was chosen as the best method for studying the interaction of ingredients during combustion. Because the ingredients have a precisely definable location immediately prior to reaction when these samples are burned on edge--the direction of regression is along the plane of the lamina--it is possihle to separate cause and effect with greater resolution than possible in the propellant case.

This sandwich method has been used (Ref. 15-24) "as a compromise between the complexity of the three-dimensional 'combustion zone' and the naivety of a one-dimensional approximation" (Ref. 16). The main criticisms of this method are: (1) that the dimensions of the ingredient layers are not the same as encountered in actual propellants nor does the reaction zone encounter heterogeneity in the direction of burning, and (2) that at pressures above 1000 psi the AP is regressing so rapidly compared to the binder that the situation is not typical of propellant combustion; the height of binder projecting above AP is several orders of magnitude greater than the heterogeneity of typical propellants. Although the criticisms are certainly true, the sandwich technique is useful for studying the important events occurring at or near the oxidizer binder interface and the flames occurring above the interface. The sandwich technique is advantageous in that the separation of ingredients into precisely definable regions provides greater resolution of observation, while providing an opportunity to observe interactions arising from the combination of oxidizer and fuel.

Nadaud, who used two 5 mm x 5 mm x 20 mm slabs of fuel sandwiching an equal sized piece of pressed AP, or .4 mm x 5 mm x 10 mm fuel between two 2 mm x 5 mm x 10 mm AP pieces, concluded that for

> the pressure domain 1-20 atm diffusion phenomena are dominant. Fenn's theory (Ref. 25), in which a symmetrical gasification of the fuel and of the oxidizer is assumed, may be utilized. The junction between the fael and oxidizer in the solid phase receives the highest heat fluxes from the reaction zone, and vaporization is faster there. In the domain of pressure

20-80 atm, with AP and most of the solid fuels used (polyurethane, polybutadiene, polyisobutene), the diffusion and decomposition phenomena control the oxidizer regression rate which is modified by the variation of local mixing ratio and by additives such as copper chromite. (Ref. 19.)

The experimental method used by Nadaud (and Powling, Ref. 18) has been compared with later work by Hightower and Price (Ref. 16), and it seems clear that the observations by Nadaud would not be able to resolve the exact location of the leading edge of the burning front, a limitation that was less applicable to the methods of Hightower and Price. These latter observations made with sandwiches using AP sheets cleaved from high purity single crystals showed that in almost all cases tested the maximum regression occurred within the AP portions of the sample. They hypothesized that this was a consequence of the dominance of the AP deflagration with added effect from the diffusion flame and three-dimensional heat loss to the endothermic binder.

Other results obtained by Hightower and Price using pure AP single crystals sandwiching 100-150 μm or some thin (≈25 μm) films of polybutadiene acrylic acid (PBAA), pointed out that interfacial reactions between oxidizer and binder were not significant in determining the regression of the surface. Carboxyl-terminated polybutadiene and PU were also tested in an exploratory manner but the results were not reported. They also concluded that, aside from supplying pyrolysis products to be consumed in the diffusion flame, the binder did little more than act as a heat sink. They reported evidence of molten surface material on both the oxidizer and binder, and in a few cases of binder flow onto the AP surface. In general, the results were not consistent with the phalanx flame model of Fenn (Ref. 25), insofar as the role of the oxidizer-binder flame tip governing a maximum regression rate at the oxidizer-binder interface is concerned.

Varney and Strahle (Ref. 20 and 23) have contributed much to an understanding of sandwich combustion. Their systematic investigation provided thermal decomposition characteristics of polysulfide, PBAA, and CTPB binders, as well as studying the combustion behavior of sandwiches of compacted sheets of AP and these binders at pressures from 300 to 2400 psi. In all cases tested Varney found evidence for "the presence of a binder melt on the oxidizer surface at combustion pressure levels from 300 psig to 2400 psig" (Ref. 20). His results also tended to support the conclusion of Hightower and Price (Ref. 16) that interfacial reactions between binder and oxidizer are insignificant. His final conclusion was that "any analytical combustion models which are based upon dry propellant surfaces and/or dominant interfacial reactions are open to severe question."

Absent in the above studies (and all others preceding the work conducted under this program) has been the observation of flame structure and the correlation of this parameter with microstructure and surface regression. This investigation provides data in this area as well as giving higher resolution observations of quenched samples. This investigation has also, for the first time, provided data on how the additions of Al and catalysts affect the combustion in the sandwich configuration.

Although much mechanistic insight has been gained through interpretation of experimental results, the lack of analytical modeling of the sandwich combustion has continually hampered full understanding. There has only been one previous analytical treatment of sandwich combustion (Ref. 21), but so many of the physics, chemistry and surface structure details were omitted to render the mathematics tractable that the model is useless for interpretation of sandwich combustion. One purpose of the present program was to develop an analytical model to interpret experimental results. Ideally, the processes which should be considered are (a) the two-dimensional condensed and gas-phaae transport phenomena, (b) a full model of AP deflagration, (c) the chemistry of binder pyrolysis, (d) the chemical kinetics of AP deflagration and of reactions between the AP decomposition products and pyrolysis products, (e) the chemistry modifications caused by catalysts or any interfacial reactions, (f) the effects of binder melts, and (g) changes in diffusion flame structures. Obviously, treatment of all of these effects would present a formidable task. An initial attempt at model development is described in this report.

The work to be described was performed at two laboratories; in an effort to fully credit all parties for their efforts, this report is divided into sections with the authors given for each section. This arrangement may result in some redundance but it is believed the advantages of such an arrangement outweigh the disadvantages. The sections include the behavior of AP-binder sandwiches, AP-binder-catalyst sandwiches, and AP-binder-Al sandwiches, and the analytical modeling.

SECTION 2

THE DEFLAGRATION OF AMMONIUM PERCHLORATE-POLYMERIC BINDER SANDWICH

Part 1

T. L. Boggs and D. E. Zurn
Naval Weapons Center

EXPERIMENTAL APPROACH

Sandwiches were made by curing a film of binder between matched, cleaved sections of AP single crystal. The binders used and the formulations are given in Table 2.1. The thickness of the binder layer was controlled by using shim stock, or wire, of the desired thickness or diameter, inserted between the AP sections. After the binder cured, these spacers were cleaved from the sandwich and the sandwiches were cleaved to a suitable sample size. The resulting configuration was a thin layer (25 μm, 127 μm or 250 μm thick) of binder sandwiched between two AP crystals of approximately 1 cm x 0.5 cm x 0.075 cm, giving a sandwich of ≈ 1 cm x 0.5 cm x 0.2 cm.

Cinephotomicrography of the combustion of these sandwiches was conducted using the NWC window bomb (Ref. 2 and 15), a 2500 watt xenon source and a LOCAM camera. A chopper wheel was placed between the xenon light source and the window bomb to allow the alternate observation of the sample surface and then the visible flame structure.

Samples were obtained for scanning electron microscopy by terminating combustion by rapid depressurization using the bomb venting method developed by Varney (Ref. 20). Burst diaphragms consisted of 5 mil thick mylar discs stacked in order to insure the proper burst pressure. Initiation of the venting occurred on command by passing an electrical current through a nichrome wire sandwiched between the last two discs. As the wire was heated it cut the discs, causing the catastrophic bursting of the other layers, thereby venting the bomb. Although depressurization rates were not measured and it has been shown that the rate of depressurization can have some effect on the rapidity of the quench (Ref. 26), we

TABLE 2.1. Binder Formulstions.

Carboxyl terminated polybutadiene (CTPB)	
Butarez CTL II.	97.561 w%
MAPO.	2.439
Cured minimum of four days at 72°C	

Hydroxyl terminated polybutadiene (HTPB)	
R45M HTPB pre-polymer	84.046 w%
CAO-14 Anti-oxidant	1.00
DDI 1410 (diisocyanate) . . .	14.954
Cured seven days at 60°C	

Polyurethane	
Estane.	96.56 w%
TMP	2.32
1,4BD	0.72
TEA	0.40
Cured minimum four days at 72°C	

PBAA	
PBAA.	84.0 %
EPON 828.	16.0 %
Cured minimum four dsys st 72°C	

feel confident that the structures seen on the quenched ssmples were indicstive of those during combustion, except for s few csses where the rspid depressurizstion was of sufficient "strength" to remove structures, such ss chars, which were only tenuously held to the sample.

This certsinty is based on considering the two types of chsnge which might be associated with depressurization quenches. The first type of change is physical or mechanicsl. Exsmples of this type of change would be disruption, cooling snd solidification of melts, snd the expsnsion of gases during depressurization. The other type of chsnge

might be progressive transient modifications such as continued decomposition or phase shifts during the depressurization. Considering the first class of artifacts: the structures seen on the quenched samples were also seen when cinephotomicrography of the burning samples was used. Those objects seen on the quenched samples but not on the films were not given much credence, except when it was possible to trace their origin (e.g., bubbles caused by expansion of gases and cooling of the froth on AP crystals). The second class of artifacts is not a consideration in the present study because of the large burst orifice used--a 1.0 inch orifice, which gives dp/dt values of greater than 10^5 psi/sec at 400 psi and 10^6 psi/sec at 1000 psi (Ref. 15).

The surfaces of the quenched samples were coated with gold-palladium and then the surface was examined using a scanning electron microscope (SEM). After examination the samples were potted in Dow Corning Sylgard 184 encapsulating resin. This potting facilitated the cleavage of samples in a cross-section to reveal the sandwich profile. Once this cleavage was accomplished the samples were again coated and examined using the SEM. In the following sections the micrographs of the cleaved sandwiches are not shown. Line drawings taken from the micrographs are instead shown. This was done to facilitate communication--there was not much contrast between the sample and the potting compound.

RESULTS

Table 2.2 presents a summary of the various observations of the study.[1] While a bit awkward, this tabular presentation was used because of the large volume of results. The following explains the contents of the table. The columns labeled "AP" and "binder" listed under the cinephotomicrography heading refer to the surface of these ingredients. The terms "bubbles" or "froth" refer to structures on the AP that previously have been described using these terms (Ref. 1 and 2). Figure 2.1 shows micrographs of these structures when quenched. The term "maximum regression" refers to the material which leads in the regression. The sectioned samples were viewed in profile to determine the conditions at the interface (the "interface" column under the "scanning electron microscopy" heading) and the degree of symmetry of the quenched sandwich about its binder center.

"No discontinuity" denotes that the profile was continuous across the AP-binder interface. In most cases there was no abrupt change of slope (nor change in sign of the slope as would be predicted by considering interfacial reactions or the type reaction of Fenn's phalanx flame). Any discussion as to change in slope at the AP-binder interface

[1]The PBAA results are not tabulated here. Although such a tabulation would have made a more complete presentation, the results did not differ significantly from the results presented for HTPB and CTPB. It was therefore decided not to list these results.

TABLE 2.2. Summary of Results From Scanning Electron Microscopy and Cinephotomicrography of Nonmetallized Ammonium Perchlorate-Binder Sandwiches.

CTPB

Pressure, psia	Binder thickness, microns	Scanning electron microscopy			Other
		AP surface	Binder	Interface	
100	25				
	127	Max. regression	Liquid & flows	No discontinuity	Symmetrical regression
	254	Max. regression	Where binder flowed regression retarded	No discontinuity	Unsymmetrical
300	25	Sloped toward binder, bubbles & froth, max. regression	Liquid & flows	Notched in binder	Unsymmetrical
	127	Bubbles, max. regression	Liquid & flows		
	254	Max. regression	Liquid & much flow	No discontinuity	Moderately symmetrical
500	25	Bubbles, max. regression	Some binder flow onto AP, retards regression	Evidence for notch in binder	Moderately symmetrical
	127	Max. regression one AP burns faster than other	Liquid & flow protrudes	No discontinuity	Non-symmetrical
	254	Max. regression	Liquid & much flow, protrudes	No discontinuity	Symmetrical
700	25	Bubbles	Binder flow onto AP retards regression	Evidence for notch in binder	
1,000	25	Bubbles, max. regression	Thick liquid flow	No discontinuity	Moderately symmetrical
	127	Bubbles, max. regression, one AP burns faster than other	Binder protrudes well above AP, liquid	No discontinuity	Unsymmetrical
	254	Fingerprint, bubbles, max. regression	Liquid & flows, projects well above AP	No discontinuity	Unsymmetrical

TABLE 2.2. (Contd.)

CTPB

Pressure, psia	Binder thickness microns	Cinephotomicrography		
		AP surface	Binder	Flame
100	25			
	127	Max. regression	Liquid & flow onto AP	Almost candle (≈375μ high)
	254	Max. regression	Liquid	Almost candle (≈4.3 mm high)
300	25			
	127	Max. regression	Liquid & flows onto AP	Turbulent diffusion (≈2.25 mm)
	254	Max. regression	Liquid & flows onto AP	Two diffusion flames on either side of protruding binder & merge into one (≈4.3 mm high)
500	25	Bubbles, max. regression	Liquid, little flow	Turbulent diffusion
	127	Bubbles, max. regression	Liquid, some char ≈1 mm protrusion	Turbulent diffusion
	254	Bubbles, max. regression	Liquid, some char ≈1 mm protrusion	Large (≈3.3 mm) turbulent diffusion
1,000	25	Max. regression	Liquid (≈325μ protrusion)	Turbulent diffusion
	127	Max. regression	Liquid & some char	Turbulent diffusion
	254	Max. regression	Liquid & ≈1.8 mm char (total protrusion ≈3 mm)	Large (≈6 mm) turbulent diffusion

TABLE 2.2. (Contd.)

HTPB

Pressure, psia	Binder thickness microns	Scenning electron microscopy			Othar
		AP surface	Binder	Oxidizer-binder interface	
100	25	Max. regression		No discontinuity	AP didn't burn well poor, non-plener burn
	127	Mex. regression	Liquid & much flow	No discontinuity	Same as above
	320	Mex. ragression		No discontinuity	Same es ebove
300	25	Mex. regression froth with binder flow	Liquid & flow	No discontinuity	Non-planar symmetrical
	127	Max. regression	Liquid & flow	No discontinuity	Unsymmetrical
	320	Max. regression froth with binder flow	Liquid & flow	No discontinuity	Moderately symmetrical
500	25	Bubbles, max. regression	Thick flow on AP results in decreese rete	Binder "ripped out" leaving apparent depression?	Unsymmetrical
	127	Max. regression	Binder flow	Notch	Moderately symmetricel
	320	Froth, mex. regression	Liquid & flows, protrudas greetly above AP	No discontinuity	Symmetrical
700	25	Bubbles	Liquid, flow onto AP		
1,000	25	Bubbles	Thick liquid flow		
	127	Mex. regression	Protrudes, flows onto AP, retarded rate	No discontinuity	Nonsymmetrical
	320	Froth, inex. regression	Protrudes, flows onto AP, retarded rate	No discontinuity	Nonsymmetrical

TABLE 2.2. (Contd.)

HTPB

Pressure, psie	Binder thickness microns	Cinephotornicrogrephy		
		AP surface	Binder	Flame
100	25			
	127	Sloped toward binder	Some liquid, some char	Candle (≈4 mm high)
	320	Sloped toward binder	Some liquid, some cher	Lerge distended candle (2.5 to 7.5 mm high)
300	25			
	127	Bubbles max. regression	Liquid, no cher	Turbulent diffusion
	320	Bubbles, max. regression	Much liquid, some cher	Turbulent diffusion (flamelets ≈2.3 mm, total flame zone ≈3.5 mm)
500	25	Bubbles, max. regression	Liquid	Turbulent diffusion
	127	Bubbles, max. regression	Protrudes above AP, liquid tip	Turbulent diffusion
	320	Max. regression	Protrudes above AP, liquid tip end char	Turbulent diffusion
1,000	25	Uneven regression	Liquid	Turbulent diffusion
	127	Max. regression	Liquid & much char	Turbulent diffusion
	254	Fingerprint, max. regression	Some liquid, much ettached char	Turbulent diffusion
	320	Mex. regression	Much attached cher (≈2.3 mm)	Turbulent diffusion (≈5 mm fleme zone)

TABLE 2.2. (Contd.)

Polyurethane

Pressure, psia	Binder thickness, microns	Scanning electron microscopy			Other
		AP surface	Binder	Interface	
100	25	Max. ragression sloped toward bindar		No discontinuity	Moderately symetrical regression
	127	Max. regression sloped toward binder, no evidence of bubbles		No discontinuity	Moderately symmatrical regression
	320	Sloped toward binder		No discontinuity	
300	25	Max. regression	Binder flows over AP & mixes	No discontinuity	Moderately symmetrical regression
	127	Max. regression	Binder flows ovar AP & mixes	No discontinuity	Unsymmetrical
	320	Max. regression	Binder flows over AP & mixes	No discontinuity notch	Unsymmetrical
500	25	Max. regression	Much flow & mix with molten AP	No discontinuity	Moderately symmatrical
	127	Bubbles	Much flow	No discontinuity	AP & binder regress at equal rates
	320	Bubbles, max. regression	Much flow	No discontinuity	Unsymmetrical
700	25	Bubbles	Much binder flow	No discontinuity	Symmetrical
1,000	25	Max. regression	Not much protrusion	No discontinuity	Unsymmetrical
	127	Max. regressinn			
	320	Max. regression	Liquid & flows over AP & mixes, protrudes	No discontinuity	

TABLE 2.2. (Contd.)

Polyurethane

Pressure, psia	Binder thickness microns	Cinephotomicrography		
		AP surface	Binder	Flame
100	25			
	127		Liquid	"Flameless"
	320		Liquid (≈750 wide)	Very thin, hardly visible
300	25			
	127	Bubbles	Liquid	Very thin, periodically moves side to side (≈500μ travel)
	320	Bubbles, max. regression	Liquid	Candle (≈3.8 mm high)
500	25	Bubbles, max. regression	Liquid	Very thin, hardly visible
	127	Bubbles	Liquid	Small (≈500μ)
	320		Liquid & char, protrudes ≈2 mm (≈1 mm char)	Two diffusions on either side of char (≈3.6 mm high)
1,000	25	Max. regression	Liquid	Small, hardly visible
	127	Max. regression	Liquid; doesn't protrude as much as did CTPB & HTPB (750μ vs 3 mm)	Small diffusion (≈500μ)
	320	Fingerprint	Liquid & flows (at rate of ≈1.7 cm/sec) over AP	Very slight; mixed due to Pu flow

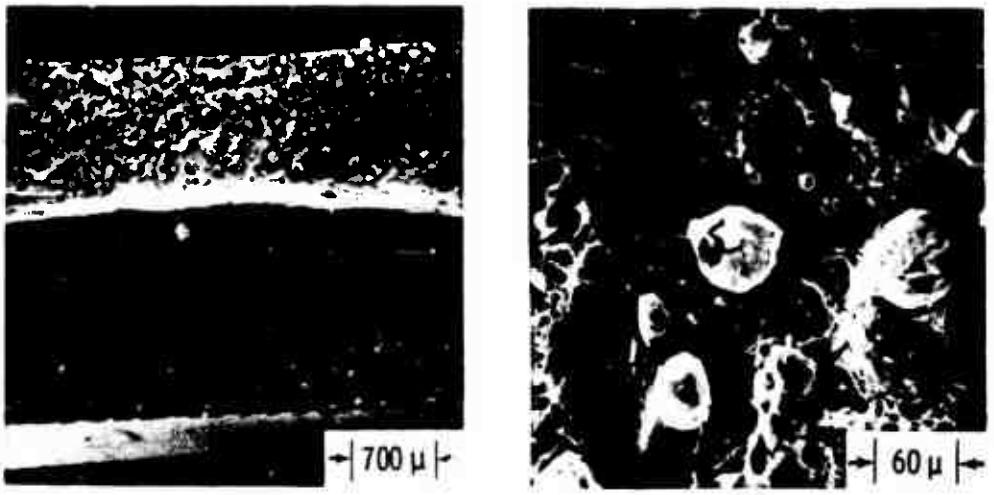

(a) (b)

FIG. 2.1. Surface Structure of Sandwiches Having 25 µm CTPB Binder Quenched at 500 psi.

must also include a discussion of the magnitude of change expected. In Section 5, Strahle presents the "sandwich paradox" (page 98) where he states ". . . a continuous slope [across the interface] is impossible". Professor Strahle discusses why a change is to be expected, but an expected magnitude is not given. The profiles examined by Varney (Ref. 20) show evidence of both what appears to be a smooth continuous interface (see Fig. 47b, 49b, and 43 of Ref. 20) and a change of slope at or very near the interface (see Fig. 42c, 46c and 46d of Ref. 20). Varney (Ref. 20) used an optical microscope to examine the interface of his quenched samples. In this study an SEM with its greater resolution was used. Sample profiles (as noted earlier, these line drawings were taken directly from the SEM) are shown in Fig. 2.2-2.4. A quick glsnce shows the difficulty in trying to discuss the profile at the interface. The profiles shown in Fig. 2.2 all indicate continuous slope <u>across</u> the interface although the majority of the AP and binder surfaces have different slopes. In contrast, the profiles of Fig. 2.3 show distinct changes of slope at or extremely near (< 100 µm) the interface. Adding to the difficulty in discussing slope at or very near the interface, sre profiles such as shown in Fig. 2.4; one case shows a large drop of melted binder on the interface, while the other shows reflex in the binder. This is further complicated because several samples displayed a "notch" effect in the binder as shown in Fig. 2.5. This notch wss common when thin (≈ 25 µm) binder layers were tested. Hightower and Price (Ref. 16) observed this same phenomens when sandwiches containing thin (≈ 30 µm) layers of PBAA were tested as did Varney (Ref. 20) for 30 µm and 50 µm thick PBAA sandwiches. In all of the sbove, although the notch is a curious anomaly and may be relsted to the quench, the maximum regression was <u>always</u> found to be in the AP portions of the sandwiches.

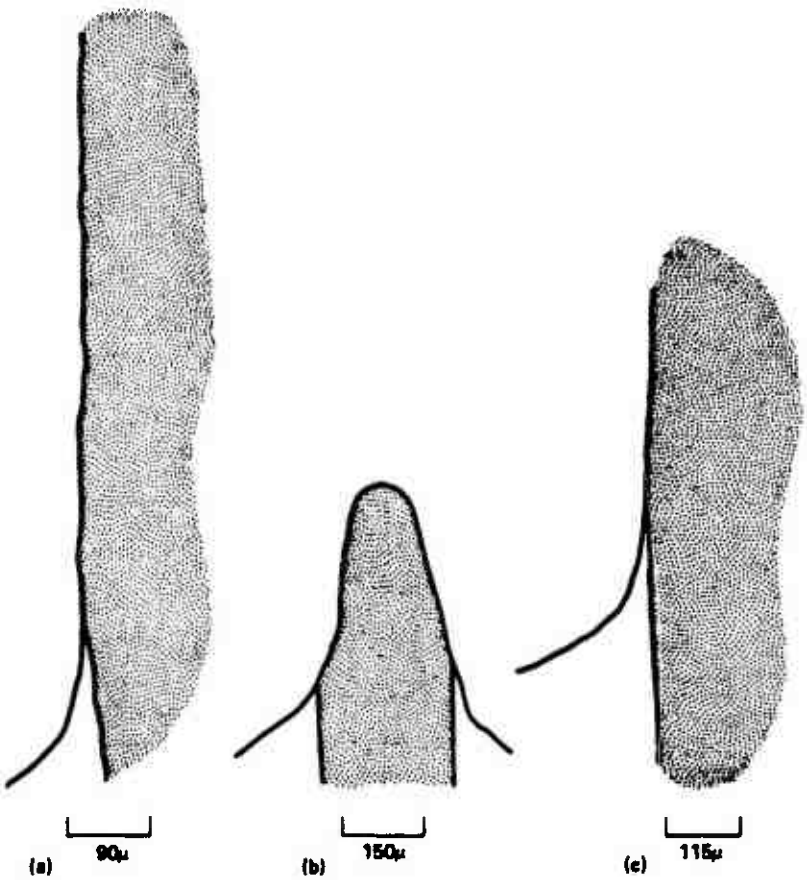

FIG. 2.2. Profiles of Sandwiches Showing Continuous Slope Across the Interface.

A judgement as to the symmetry of the quenched sandwiches is quite subjective; often samples which appeared symmetrical under the optical microscope appeared somewhat asymmetrical when viewed using the SEM. Figure 2.6 shows examples of a relatively symmetrical (Fig. 2.6a) and an asymmetrical (Fig. 2.6b) profile, as inferred using the SEM.

The term "candle" flame refers to the classic diffusion flame structure as exhibited by a candle (Fig. 2.7a). Several of the sandwiches burned in this fashion at low pressure. The term "turbulent diffusion" flame is somewhat of a misnomer. First, it is not a single flame but many flamelets, unsteady both spatially and temporally. This unsteadiness indicates a turbulence--not the high Reynolds number turbulence of fluid mechanics but rather an intrinsically turbulent flow field csused by the nonsteady inhomogeneous nature of the combustion. When sandwiches displaying this "turbulent diffusion" flame are viewed transversely the rapidly moving flamelets are seen (Fig. 2.7b). When it is viewed on edge, what appears to be a single turbulent diffusion flame is seen--as illustrated in Fig. 2.7c. Recent work by Brown, Kennedy and Netzer

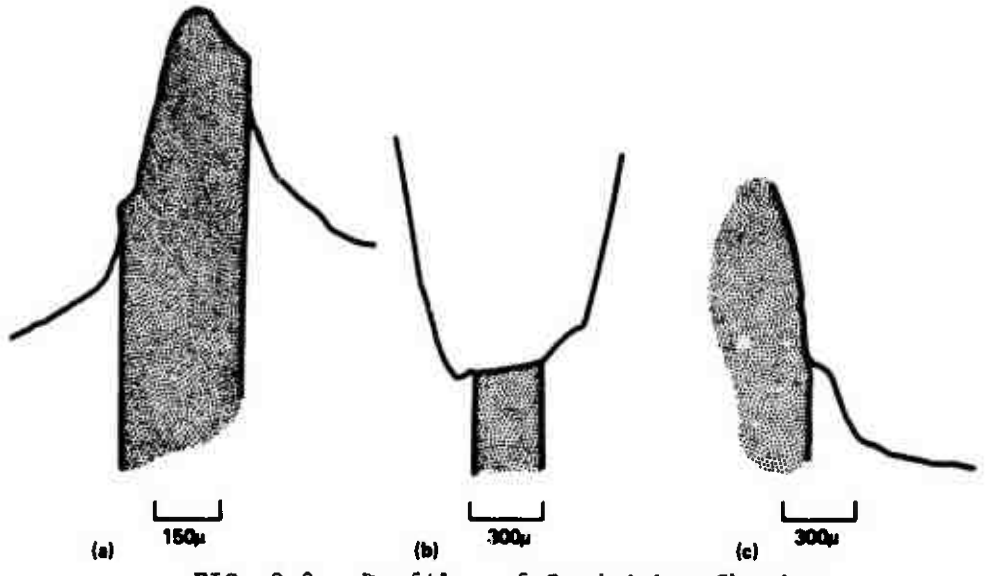

FIG. 2.3. Profiles of Sandwiches Showing Change of Slope at the Interface.

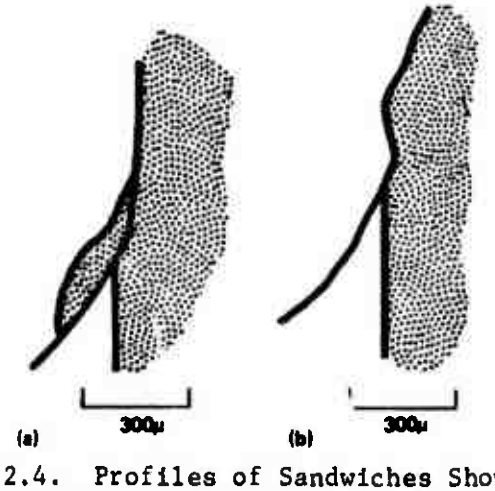

FIG. 2.4. Profiles of Sandwiches Showing Anomalous Structures Near the Interface.

(Ref. 27-29) was performed at the Naval Postgraduate School using a color Schlieren system and cinephotomacrography of burning sandwiches. The results show different flame structures depending on whether the sample was burned above or below the low pressure self-deflagration limit of the AP.

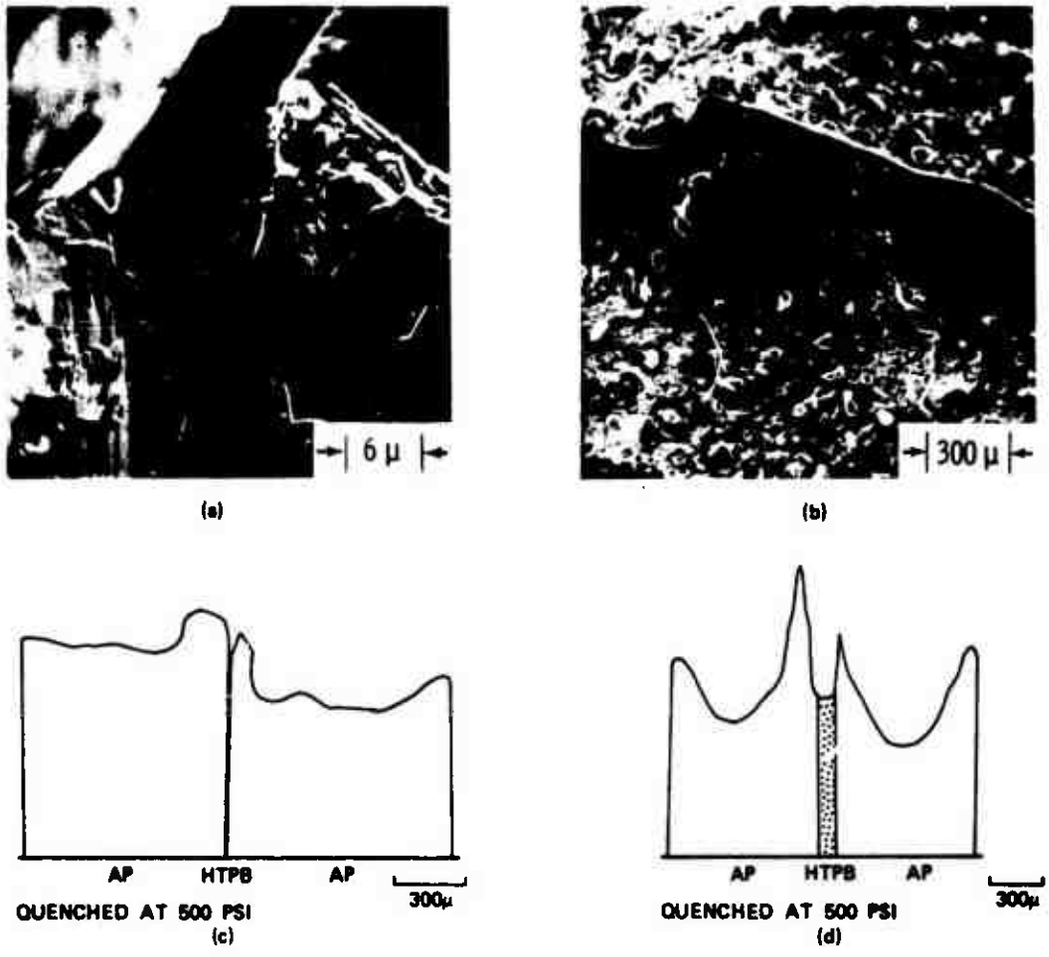

FIG. 2.5. Sandwiches Showing a Notch in the Binder. (a) HTPB 25 μm 500 psi· (b) CTPB 25 μm 700 psi· (c) HTPB 25 μm 500 psi· (d) HTPB 125 μm.

The following quotes are from Ref. 27:

> Flame structure appears to be different for pressures above and below the low pressure deflagration of AP.
>
> Sandwich burner flames below the P_{dl} of AP are lsminsr. Above the P_{dl} the flames sppear to be turbulent but further tests will be required to verify this result.
>
> Two distinct flame regions were observed, one sbove the binder (or binder post) and one near the binder/AP interface. Both flames were nonsteady snd consisted of many small "flamelets".

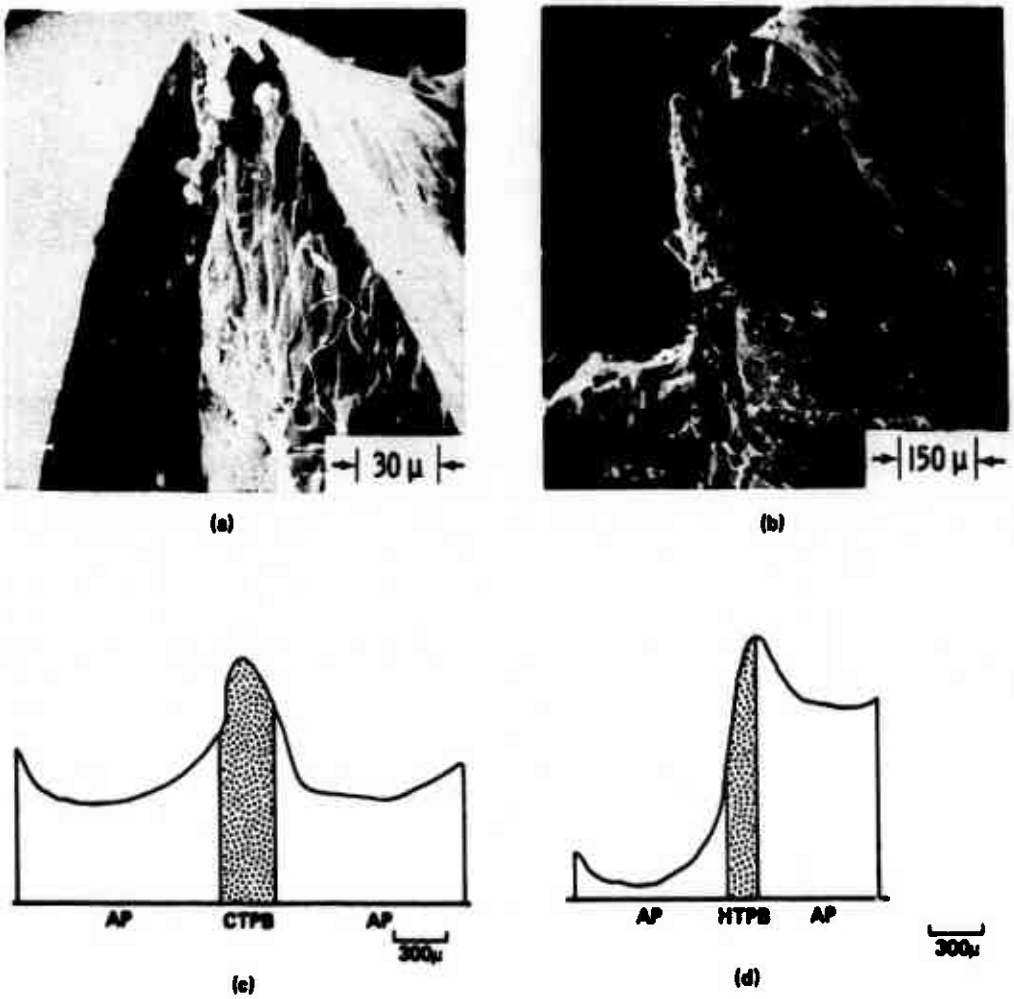

FIG. 2.6. Sandwich Profiles: (a,c) Symmetrical; (b,d) Asymmetrical.

The effact of bindar thickness on the overall sandwich profile is shown in Fig. 2.8 and 2.9. Thin bindars aeem to heve little effect on the profile naar the interfaca while tha thick binder layers cauae a lower regresaion rate of the AP adjacant to the binder. The abova observations confirm thoaa of Hightower and Price (Ref. 16):

> Second, the AP appeared to be ragrassing at a lesaer rate adjacent to the binder, producing a "trailing edga" effact with the aurfaca of tha AP blanding smoothly into tha binder surface forming a continuoua ragressing surface at the interface. At highar burning pressures (above the deflagration limit of AP) the AP will burn as a monopropellent and that part of the burning surface that was well

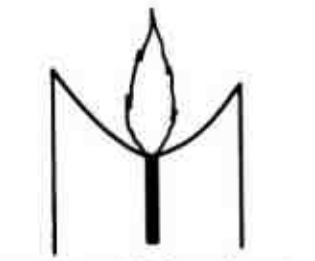

CANDLE DIFFUSION FLAME.

(a)

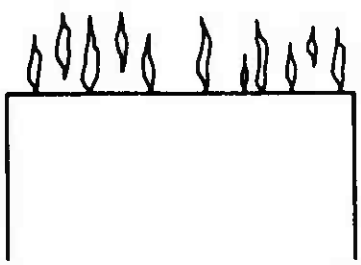

TURBULENT DIFFUSION FLAME VIEWED TRANSVERSELY.

(b)

TURBULENT DIFFUSION FLAME VIEWED ON EDGE.

(c)

FIG. 2.7. Flame Structure.

removed from the binder layer was observed to regress as a plane wave. This surface was usually inclined at a slight angle. presumably to allow the regressing surface to maintain a steady-state configuration with the point of maximum regression rate. At lower pressures (below the deflagration limit of AP) the AP will not undergo sustained steady deflagration unless some additional energy is supplied to the burning surface. Under these conditions it was observed that regression of the AP occurred only in close proximity to the binder layer where the presence of an oxidizer-fuel flame (apparently a diffusion flame) could assist the AP deflagration process. This produced a burned sandwich with the outside crystal faces virtually undisturbed and a deep groove burned into the sample centered around the binder layer. Even under these conditions, however, the maximum regression of the surface was still observed to occur a short distance from the binder interface. Although the addition of lithium fluoride to the binder produced a

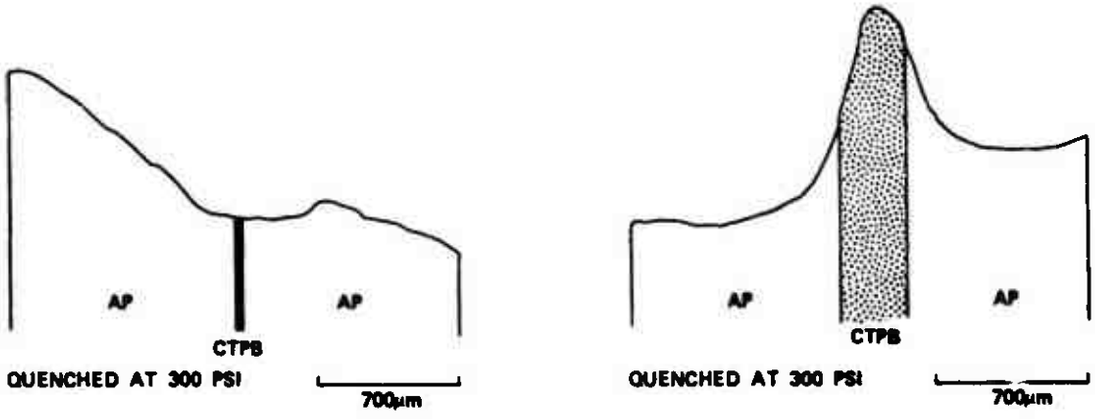

FIG. 2.8. The Effect of Binder Thickness on Sandwich Profile at 300 psi.

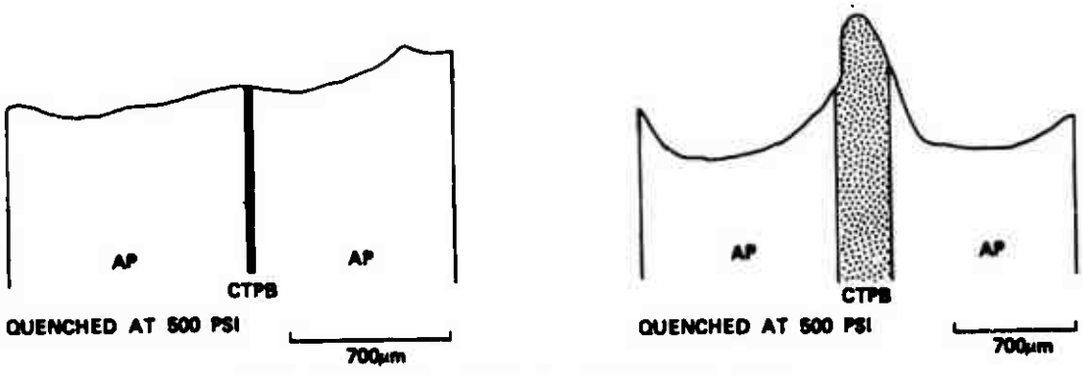

FIG. 2.9. The Effect of Binder Thickness on Sandwich Profile at 500 psi.

distinct change in burned surface pattern of the ssnd-wiches it did not slter the features of the burned profile near the oxidizer-binder interface region.

The profiles of sandwiches burned with s thinner binder layer (on the order of 30 μ) were observed to be significsntly different from those with thick binder layers. Figure 10 [not shown in this report, is simjlsr to Fig. 2.5c] shows the profile of s ssnd-wich with an uncatalyzed PBAA binder layer spproximate-ly 30 μ thick that was burned st 500 psis snd quenched. There is sn asymmetry about the binder layer thst wss not observed in the sandwiches with thicker binder layers. Examination of this sample wi:h higher magni-fication revealed a curious dip in the binder, but

> with the contour of the burned surface remaining very smooth across the interface. The large hump of AP to the right of the binder layer was observed to have a very thin binder layer on its surface. High-speed motion pictures have shown this hump to be present during burning with a visible flame distributed above this region. The general nature of the flame structure can best be described as unstable and was observed to move bsck and forth across the binder layer. The unstable nature of the flame may be the cause of the asymmetry observed in the thin binder sandwiches. With sandwiches containing thicker binder layers the flame zone appeared to be of a much more stable nature although it was observed to consist of a series of "fingerlike" flamelets instead of a continuous flame sheet.

Hightower and Price also observed:

> The phase transition layer was also observed in the sandwich profile sections. For samples burning above the low pressure deflagration limit of AP the phase change thickness was observed to be approximately constant from the region near the point of maximum regression to the outer crystal edge. In this region for a crystal burning at 1000 psig typical dimensions of the phase change thickness would be on the order of 10 to 12 μ. Near the binder layer, where the AP exhibits the "trailing edge" effect, the phase change layer is observed to vary in thickness, being thinnest at the bottom of the dip, or maximum regression point, and becoming noticeably thicker at the interface. This thickening near the interface indicates that the heat flow is two-dimensional in the vicinity of the interfsce, with heat from the flame region being transferred through the AP into the binder.

In the same publication a figure showing the relation of cubic phase thickness (from which the surface temperature can be cslculated) and the surface profile was presented (Fig. 2.10).

A gsthering of data from Table 2.2 indicates that all of the sandwiches tested had the following characteristics:

1. The binder became liquid as the combustion front approsched.
2. The maximum regression occurred in the AP portions of the sample.
3. Evidence for interfacial reactions between AP and binder was not found.

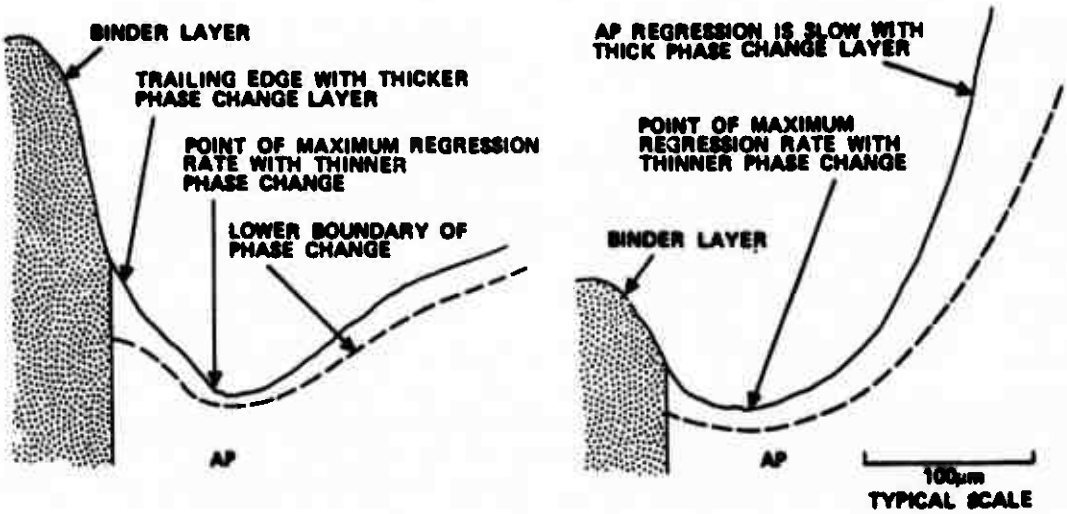

FIG. 2.10. The Relation of Surface Profile and Cubic Phase for (a) Sandwiches Burned at Pressures Above the P_{dl} of AP (300 psi) and (b) Sandwiches Burned at Pressures Below the P_{dl} of AP. Figure from Ref. 11 and 12.

4. The surface structure of the AP was identical to that reported for the case of self-deflagration (Ref. 1-4) except when p < 300 psia and in certain cases where liquid binder (or its products) flowed over the crystal surfaces.

The CTPB, HTPB and PBAA sandwiches displayed many common characteristics which were different from those of polyurethane. The characteristics common to the polybutadienes include:

1. The liquid resulting from the binder was quite viscous and flow was limited to the proximity of the original binder interface (Fig. 2.11). There did not seem to be appreciable mixture of binder liquid and the liquid due to AP deflagration.

2. A char was observed to be formed from the binder liquid, especially at pressures $\gtrsim$ 500 psi and for thick (> 130 μm) binder layers. The particular HTPB formulation tested formed this char more readily than did the CTPB.

3. Below the low pressure deflagration limit of the AP ($P_{dl} \approx$ 300 psi) the sample regressed as shown in Fig. 2.7a with a classic laminar diffusion flame. At pressures grsater than the AP P_{dl}, the samples regresssd as shown in Fig. 2.7b and with a "turbulent diffusion flame".

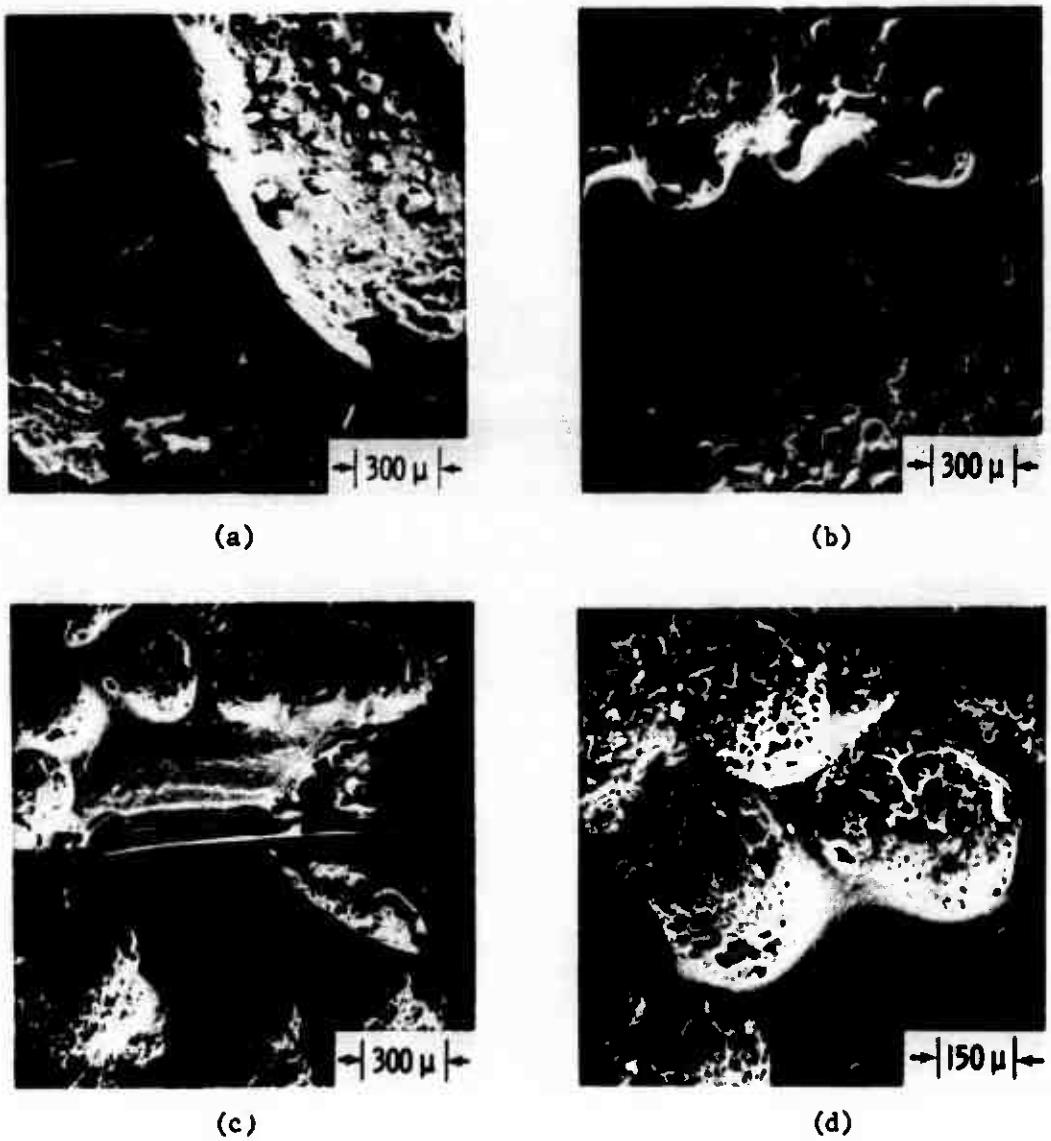

FIG. 2.11. Sandwiches Showing Binder Flow: (a) CTPB 25 μm 700 psi, (b) HTPB 50 μm 500 psi, (c) HTPB 75 μm 300 psi, (d) HTPB 75 μm 300 psi.

4. The effects of pressure on the profile are shown in Fig. 2.12. As pressure was increased the AP regressed much more rapidly than did the binder, leaving the binder protruded above the AP.

In contrast to the polybutadienes, polyurethane displayed different combustion properties:

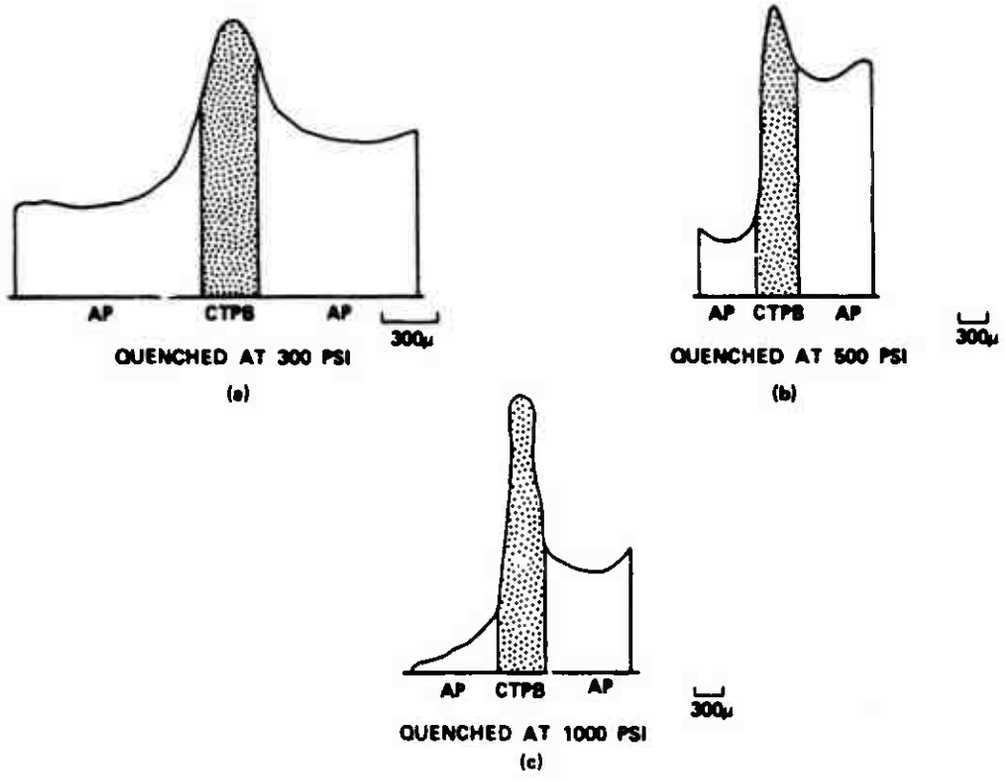

FIG. 2.12. Profile of CTPB Sandwiches Showing the Effects of Ambient Pressure.

1. The liquid resulting from the binder was of much lower viscosity, copious in quantity, and flowed readily over the AP (Fig. 2.13). In one motion picture the surface was regressing at 0.4 in/sec and the liquid was flowing scross the surface at 0.7 in/sec. It also appeared that mixing between the AP and binder liquids occurred, although this observation was not adequately verified.

2. Because the binder liquified so easily, the large projections of binder above the AP, seen for the polybutadiene samples as the pressure was increased, were not seen for polyurethane, except for the tests using thick binder layers.

3. The flames for these sandwiches were hardly, if st all, visible, especially for the 25 μm thick binder case snd were otherwise extremely small in size, compared to those of the CTPB and HTPB sandwiches.

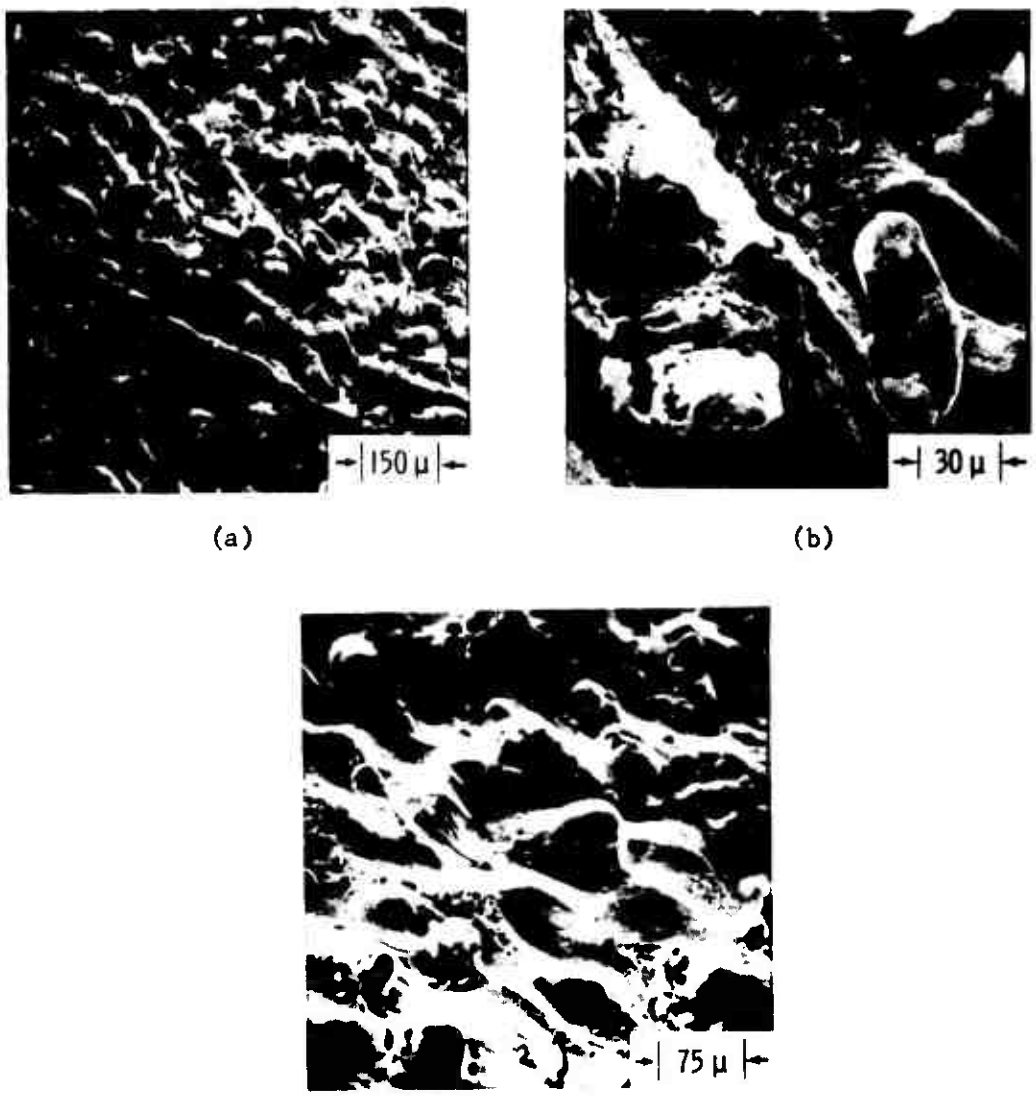

(a) (b)

(c)

FIG. 2.13. Surface of Polyurethane Sandwiches Quenched at 1000 psi: (a) and (b) ≈ 25 μm; (c) ≈ 250 μm Thick Binder.

4. The self-extinguishment of several samples occurred when the wstery binder products precipitously flowed over the AP thereby "smothering" the reaction.

Becsuse of the large differences when the combustion of the polybutadiene sandwiches was compared to that of the polyurethane sandwiches, and because of the gross ignorance surrounding the combustion/pyrolysis of binders, s few ancillary experiments were performed. In the first of these, thin binder samples were simply subjected to a match flame

in 1 atm of air and viewed using a binocular microscope. The CTPB, PBAA and HTPB samples ignited and slowly burned with a vigorously bubbling liquid surface. The bubbles were of approximately 100 μm diameter and smaller. In contrast the polyurethane would not ignite in this atmosphere. A liquid of less viscosity than observed for the polybutadiene samples was formed but there was very little bubbling within the liquid. Those bubbles which were formed were relatively large (> 400 μm).

In other experiments, various degrees of cross-linking of the HTPB binders were studied. The preliminary results of this work show that the amount of liquid formed from the binder and the extent of the flow is inversely related to the value of the CNO/OH ratio. In addition, it appears that the type of isocyanate used in the formulation of the HTPB affects the amount of carbonaceous char formed.

Although these ancillary experiments were simply conceived and executed, and hence do not provide results of a quantitative nature, they point out that much additional work must be done in an effort to understand how binders react in the combustion wave.

Although the measurement of burning rate of the sandwiches was not a primary consideration of this work, burning rates were measured from the films. The data, ranging from ≈ 0.09 in/sec at 100 psia to ≈ 0.35 in/sec at 1000 psia, were not complete (often a film showed the burning behavior in lucid detail but in such a manner that an accurate burning rate could not be obtained), but several generalizations could be drawn. In general the burning rate data for the sandwiches were clustered about the deflagration rate curve for pure AP. In all cases tested, increased binder thickness, from ≈ 25-300 μm, caused slightly increased burning rate. The inverse burning rate-binder thickness effect of PU sandwiches which Varney reported (Ref. 16) was not observed.

DISCUSSION

The observations of this work lead to the conclusion that even in this two-dimensional model configuration, past thinking has been entirely too simplistic. Even though we may attempt to force the results, if not our thinking, into less restrictive one-dimensional, or pseudo-multidimensional models, the observations of this study serve to remind us that combustion is a three-dimensional nonsteady phenomena. This, of course, does not completely negate the value of the more restrictive models, both mathematical and experimental, because these simpler, more tractable forms often provide the level of understanding prerequisite to undertaking the study of more complex phenomena. Indeed a modeling is included in this project. Observations from the pseudo two-dimensional sandwich combustion can tell us what to look for in the three-dimensional studies.

Taking the most obvious results of this study we find that the combustion of the sandwiches is dependent on binder type. Although this isn't surprising it does point out our gross ignorance in this area. For instance, mathematical models commonly treat the binder simply as an endothermic source of pyrolysis products. Those models which do differentiate between binders seem to do so only in an effort to classify as "abnormal"--i.e., doesn't fit their burning rate "law"--a set of propellants giving anomalous results. Instead, what we must do is recognize the many possible reactions the binder can undergo during the combustion and find under which conditions or what reactions may be dominant. We need to ask ourselves:

1. Does the binder liquify?

2. If so, is it a highly viscous material or can it flow over other ingredients?

3. What are the wetting problems of liquid binders on AP? Can the liquid binder hold aluminum particles at the regressing surface?

4. What is the miscibility/solubility of the liquid resulting from AP deflagration and the binder liquid?

5. When and how does it vaporize?

6. How do the answers to these questions affect the flame structure and other sources of energy feedback necessary to sustain combustion?

In the case of the sandwich configuration, it appears that the interpretation of Hightower and Price (that the binder, aside from supplying pyrolysis products and serving as a heat sink, plays little part in the combustion) is only partially valid for the polybutadiene samples and probably less valid for the polyurethane sandwiches. The burning rate curves and a qualitative energy balance seem to indicate that the effect of added fuel is balanced, in the sandwich configuration, by the energy required to liquify and vaporize the binder. Thus their hypothesis would appear substantiated. But it has also been observed in this study and in the work of Varney that the binders become liquid and can flow. The results of this study have shown that this flow, when it covers the AP, slows the regression of the AP and affects the location and stability of the individual flames. The binder flow can also be important in the case of the polyurethane propellant strands as a self-extinguishment agent as had been proposed by Derr and Boggs (Ref. 23 and 24). It will also be shown in Section 4 that the liquid binder is important for the accumulation of Al during combustion. Thus it has been shown that the binder does more than just supply products and serve as a heat sink.

Evidence of the binder being liquid snd capable of flow might be cited by some in arguing for interfacial reactions; they might argue that the liquid binder could flow over such reaction sites during quench snd so obscure them. If such sites were present during combustion, snd sssuming thst the binder could not flow into such aites during combustion (which would make the process self-limiting), these binder-filled crevices should be revesled when sectioned profiles were examined. No such evidence was found when the ssmples were viewed using optical microscopy (Ref. 7 and 16) and scanning electron microscopy (Ref. 22).

Even for sandwiches incorporating the ssme binder type we need to recognize the changes caused by varying such parameters ss pressure. For example, we have seen markedly different behsvior depending on whether the pressure was above or below the P_{dl} of the AP. Similarly, pressure also influences the relative regression rates of the binder and AP. Therefore under some conditions an sccumulstion of one species at the surface and/or severe mixture fluctuations in the gss phase ss s consequence of the shedding of the materisl might be expected. This accumulation of species, coupled with the liquid nature of binder, poses a possible criticism of those mathematical models based on the propellsnt geometry prior to burning--is the surface geometry during combustion directly relatable to the precombustion geometry?

Similarly, we have seen that our concept of flame structure and the consequences have been extremely naive. To illustrate this point the following excerpt from s JANNAF Workshop on Steady-Stste Combustion snd Modeling of Composite Solid Propellant Combustion, recently sttended by individusls sctive in this field, is presented from Ref. 30:

> The possibility that turbulent transport exists between the binder/oxidizer flame and the burning surface was neither established nor denied. Arguments against the presence of turbulent transport were bssed on results of Schlieren and high-speed cinematogrsphy studies of burning propellants and the low Reynolds number (1 to 10 based on the oxidizer diameter) sssociated with the flow of gas from the propellant surfsce. Arguments for the presence of turbulent transport were based on the premise that the products of binder pyrolysis snd AP decomposition products issue from the surfsce at different speeds and directions, thus negsting the significance of low Reynolds number.

As shown in this study, and more recently confirmed by the outstsnding color Schlieren photographs of Netzer (Ref. 29), the lstter choice is the most nesrly correct for the ssndwich burning st p > 300 psi. Not only do the products issue st different directions snd speed, but the resulting flsme is spatially snd temporally unstesdy. If this intrinsic

nonsteady nature carries over to the case of composite propellants it is of importance, since the dimensions of ths instability ara of the same order as the heterogeneity of the propellant, the thermal profila within the solid, and the thickness of the "flame zone". In addition the change in flams structure from the classic diffusion flame to the "turbulent" flame at the pressure (and rate) of the lower deflagration limit of ths AP, coupled with the lack of structure indicative of a liquid (bubbles and froth) on the AP of the sandwiches quenched from $p < 300$ psi, may indicate that a $p < 300$ the AP sublimes and these products and those of the binder decomposition burn in a laminar diffusion flame. This is the case most commonly treated in mathematical models--AP sublimation (or decomposition) and binder pyrolysis followed by a laminar diffusion flame--but it should be notsd that this is probably only true at pressures less than approximately 300 psia. Abovs this pressure the AP can self-deflagrate and the flama structure changes to the "turbulent diffusion flame".

SUMMARY AND RECOMMENDED FUTURE WORK

An investigation of this type often poses more questions than it answers and it is certainly true in this case. Before delineating soma areas for future work, let us review some of the questions answered.

1. There was no evidence found for interfacial reactions and the leading point of the regression was always in the AP. This is contrary to the interpretation of Nadaud (Ref. 19) and Powling (Ref. 18) and is directly opposite to the assumptions made in the models by Fenn (Ref. 25) and Hermance (Ref. 31). However, it is consistent with the observations of Hightower and Price (Ref. 16) using single crystal AP sandwiches, and Varney and Strahle (Ref. 7, 20, and 23) using pressed AP sheets in their sandwiches.

2. All of the binders tested displayed a liquid, in agreement with the study by Varney and Strahle. This is in contrast to the assumption used by Steinz, et al (Ref. 32), to explain why some propellants weren't correlated by tha granular diffusion flame (GDF) modsl. Thsy ssem to hava classed propellants having liquid binders as "abnormal" and excludad them from consideration. Ths liquid also flowed over ths AP, the extent being dependent on binder typs and pressura.

3. The flame structure was not the simple diffusion flame, except at pressures lower than ≈ 300 psi. At $p > 300$ psi polybutadiene sandwiches burnsd with many spatially and temporally unsteady flamelets whoss motion indicates ths "turbulent" naturs of the combustion. Tha polyurethane samples often burned with a barely visible flams.

Much work needs to be done. We need to know the temperatures at which the various binders become liquid, the viscosity of the resulting liquid, the wetting characteristics of the liquid, and the temperature at which the binder gasifies. We need to know the correlation between the AP-binder interactions and the flame characteristics, including the processes causing flame instability. And finally, we must determine the importance of discontinuities that are present in propellants having a heterogeneous mixture of ingredients, and the relative importance of situations associated therewith but not applicable to study using the sandwich model.

Part 2

W. C. Strahle, J. C. Handley, and T. T. Milkie
Georgia Institute of Technology

INTRODUCTION

The investigations of Georgia Institute of Technology, like those conducted at NWC, were initiated prior to the subject AIRTASK. Much work was performed by Varney, Jones and Strahle under institutionsl funding. Varney (Ref. 20) investigated samples quenched by rapid depressurization using a unique silicone replica technique and photomicroscopy. The binders polysulfide (PS), polyurethane (PU), polybutadiene acrylic acid (PBAA), and carboxy terminated polybutadiene (CTPB) were used. The pressure range 300-2400 psig was spanned. Compacted polycrystalline AP was used. Boggs (Ref. 4) found that the deflagration rates of samples prepared at Georgia Institute of Technology matched single crystal deflagration rates, and that the pressed sam; e results showed no sppsrent difference in quenched surface profile b :ween pressed AP sandwiches and samples made with single crystal AP. Significsnt conclusions were:

1. There was no evidence of interfacial reactions between the binder and oxidizer at any pressure or with any binder.

2. All four of the binders exhibited a melt regardless of the pressure.

Because of uncertainties in the flame structure and location, in the sandwich regression history and in the potential ejection of the binder in the quench process, Varney concluded that it was imperative that high-speed motion pictures be taken of the sandwich combustion process.

Jones (Ref. 33) has carried out cinephotomacrography studies of the ssme sandwich configurations studied by Varney with the addition of copper chromite (CC) and iron (III) oxide (IO) runs at 600 and 2000 psi. These results are discussed in Section 3.

Jones' motion picture work was also valuable in removing some of the uncertainties introduced by quench testing such as:

1. The relevance to steady state
2. The role of the binder melt
3. The flame location
4. The origin of asymmetric profiles
5. The possible ejection of sandwich material during the quench process

Jones found that, indeed, part of the binder, protruding above the mean surface, was being ejected during quench. Jones confirmed the results of Boggs and Zurn (Ref. 22) that the flow of the flow of the binder melt does change the flame structure for PBAA, CTPB and PU binders by moving the mean flame surface above the AP. In the case of PS, however, the melt does not appear to flow onto the AP. Jones found that a steady state is indeed attained and that asymmetries develop from asymmetric ignition, local unsteadiness, or sandwich flaws.

APPARATUS AND TECHNIQUE

Cinephotomacrography was accomplished using a stainless steel window bomb, capable of being pressurized to 6000 psi, a Hycam 16 mm high speed motion picture camera, and a 2500 watt xenon light source. Ignition of the samples was accomplished using a drop of Goodyear pliobond rubber cement applied to the top of the sample and an ignition wire. Quenched samples were obtained in the manner of Varney (Ref. 20) and were viewed using an optical microscope capable of 2000X magnification.

The AP was a certified grade granular material which was compacted, using 22,000 psi for 8-24 hours, into pellets 0.050 inch thick. The HTPB binder was prepared as follows:

Ingredient	w %
R-45M	90.428
IPDI.	6.450
A02246 antioxidant. .	0.980
MT-4 bonding agent. .	2.142

The PU, PBAA and CTPB were prepared as reported by Jones (Ref. 33).

SANDWICH MECHANICS AND DISCUSSION

Figure 2.14 shows the scheme for describing the sample profile, and the mechanics of data analysis used in this program. This matter of

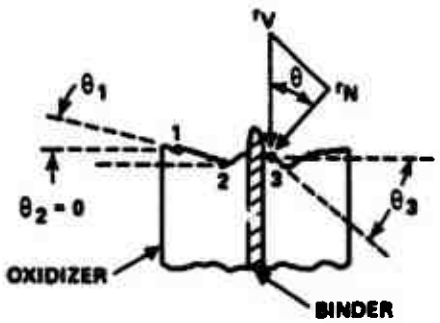

$$r_V = \frac{r_N}{\cos\theta} \qquad r_{V1} = r_{V2} = r_{V3} = \text{CONSTANT}$$

$$\theta_3 > \theta_1 > \theta_2 \rightarrow r_{N2} > r_{N1} > r_{N3}$$

(a) REGRESSION ANALYSIS MODEL

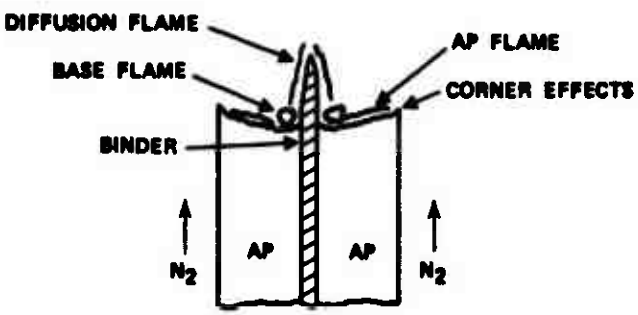

(b) COMBUSTION MODEL

FIG. 2.14. Sandwich Mechanics.

definition is included in this section for emphasis when discussing sample profiles. The main difficulty in once having presented such a scheme is that it is possible to become dogmatic and try to interpret all results within the framework of the simple situation presented. Therefore it must be emphasized that the figure is primarily a matter of definition (indeed there are many obaervations which do not "fit" within this framework) and applicable only under the specified conditions (and should not be boldly extrapolated to other conditions with any degree of credence). Thus, although in Fig. 2.14, θ_1 is shown above the horizonal, results obtained with no nitrogen purge (hence, little if any convective cooling along the sample edge) and at pressures between 500 and 1000 psi showed the opposite effect; the angle was below the horizontal. Similarly, with no purge and at pressures below 300 psi, θ_1 was in the direction shown and of quite large magnitude, but the majority of the AP was not self-deflagrating. Thus, it must be remembered that the figure is a conceptual framework only. Results obtained using the scheme must still be interpreted considering the actual physical details.

It must also be cautioned that the results reported in this section are based solely on motion picture photography of samples burning in a nitrogen purged bomb. Recalling the contradiction between observations of Nadaud and of Powling and those of Hightower and Price, some reservation must be made regarding microscopic accuracy of determination of the location of the leading edge of the regression front when combustion photography is used alone. This is especially true when nitrogen purge is used. Just as there is convective cooling along the sides of the sample, one would expect such cooling up along the front and rear faces of the sandwiches, giving rise to an artifact not typical of the bulk of the sample. Thus the appearance of a leading edge at the interface will be reported with some catalyzed samples, but this interfacial location is not established with the same level of accuracy as with the quenched samples of the NWC section, and in Hightower and Price, and Varney.

Within the above limitations some cause and effect arguments can be made. The results of Hightower and Price, Varney, Boggs and Zurn, and Jones have all shown that when sandwiches are burned at pressures greater than 300 psi, the AP regresses independently of the binder (i.e., self-deflagration) when it is observed at distances greater than a few hundred micrometers from the binder-oxidizer interface (but away from edge effects if a nitrogen purge were used). For such sandwiches, the normal regression rate at point 1 of Fig. 2.14a is that of pure AP. If the AP regresses much more rapidly than does the binder, a "Christmss tree" profile, with no point of zero slope on thin samples, or no change in sign of slope on thick samples and a zero slope occurring for the AP solely regressing by self-deflagration, is seen.

Results

Figures 2.15-2.20 show PU behavior over the pressure range of 300-3200 psia with omission at 1000 psia and 2400 psia, due to the work of Jones.

FIG. 2.15. AP-PU-AP; 300 psia.

FIG. 2.16. AP-PBAA-AP-PU-AP; 600 psia.

FIG. 2.17. AP-PU-AP; 1500 psia.

FIG. 2.18. AP-PBAA-AP-PU-AP; 2000 psia.

The PU behavior produces a quite flat AP surface over the entire pressure range, resulting in little separation of the AP burning rate ($\dot{r}\cos\theta$) and the sandwich burning rate ($\dot{r}$), as seen in Fig. 2.21. There always appears at some point in the run a leading edge binder melt as shown in Fig. 2.17. In the case of Fig. 2.16 the glossy substance on the right-hand sandwich face is a binder melt flow. The orange part of the

FIG. 2.19. AP-PBAA-AP-PU-AP; 2800 psia.

FIG. 2.20. AP-PBAA-AP-PU-AP; 3200 psia.

flame is on average displaced from the interface onto the AP surface which strongly indicates that the effective location of the binder-oxidizer (BO) interface is displaced outward by a melt.

The flatness of the AP profile is, of course, the reason for very little separation of the open and blackened points on Fig. 2.21. But this figure points out a difficulty which was encountered in the program.

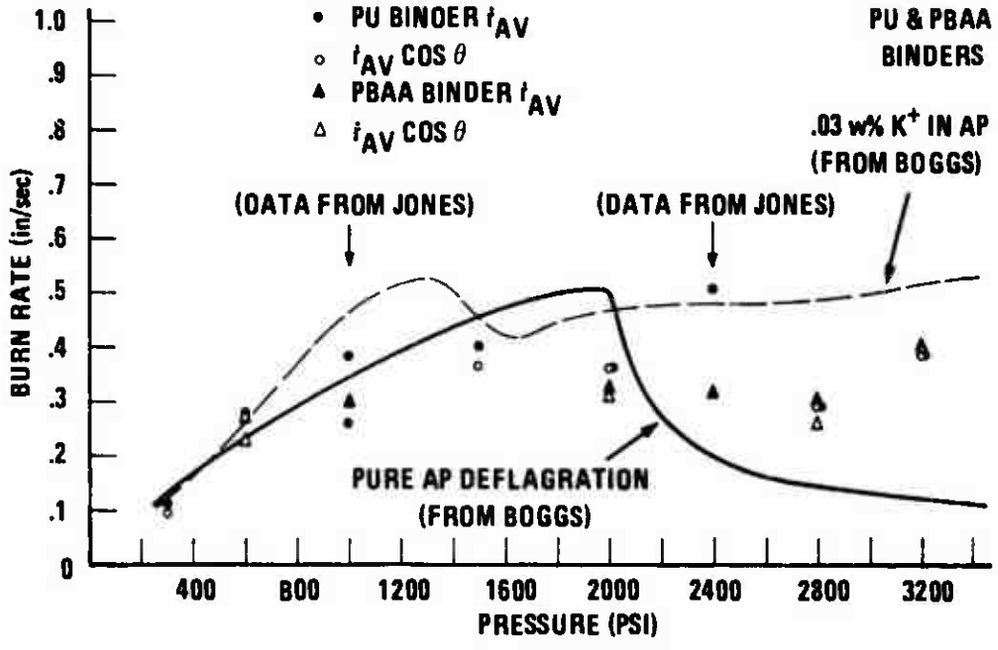

FIG. 2.21. Burn Rate for PU and PBAA-AP Sandwiches

Ideally, the open points should follow the pure AP burn rate curve, as was found to be the case by Jones. Viewing Fig. 2.21 and 2.22, however, while the open points are consistent, regardless of the binder, the pure AP curve is not followed.

One possible explanation for disagreement with the pure AP curve may be the presence of impurities. This is illustrated by the effect of 0.03 wt % K^+ on the deflagration rate as reported by Boggs (Ref. 4 and 34) and shown as a broken line on Fig. 2.21 and 2.22. An analysis of the Georgia Institute of Technology materisl was madeat NWC and showed s K^+ content of 0.03 wt %. It is not clear where or when this impurity originated, and it is notable that the burning rate results obtained by Jones for the same material did not show the above anomaly. However, use of the material was continued in the program to avoid introduction of a change midway in the program.

The PBAA results are shown in Fig. 2.16-2.20. Pressures excluded are 1000, 1500, and 2400 psia which were performed by Jones. The flame for PBAA is brighter and visibly more extensive thsn for PU. The majority of the time during runs is spent with a reasonably flat AP profile. The "Christmas tree" profile does appear sporadically at 2000 psia as shown in Fig. 2.18. Jones found flat profiles at 1000 and 1500 with a "Christmas tree" profile at 2400 psia. An exception to the flst profile is found at 2800 psia, but this is due to an ignition transient effect in Fig. 2.19. [Editors note: The discussion of the profile here

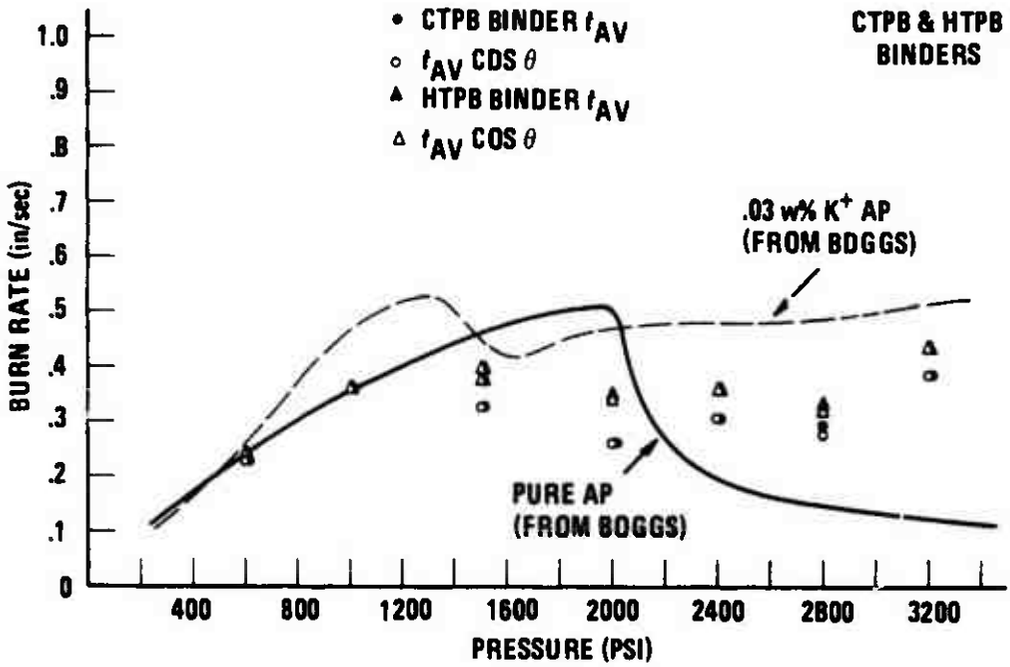

FIG. 2.22. Burn Rate for CTPB and HTPB-AP Sandwiches.

utilizes a different scale resolution than the discussion of the NWC Section 2]. From the burn rate data of Fig. 2.21 it may be seen that after a steady state was reached the AP was parallel with the horizontal. Coupled with the work of Jones, the melt behavior of PBAA is that the melts are as extensive but more viscous than with PU.

Figures 2.23-2.30 show the behavior of HTPB and CTPB ssndwiches. With one exception the behavior of these two binders is almost identical. The flames are visibly more extensive than with PBAA; the visible flames are definitely displaced over the AP, away from the binder; and the AP profiles are flat with the exception of "Christmas tree" profile development at 2400 psia (Fig. 2.28). The main exception appears to be s systematic increase in the AP burn rate if HTPB is used. The effect is mild (≈ 20%) as seen in Fig. 2.22 but appears systematic and outside of experimental error in burn rate determination (≈ 10%). The only reasonsble explanation for this phenomenon appears to be a mild radistion contribution from the BO flame to the AP heat input. This is plausible since the HTPB flame is slightly hotter than the CTPB flame.

With the exceptions of operation near the low pressure deflagration limit of AP and operation with binders producing a "Christmas tree" profile at 2400 and 2800 psig, these results, coupled with Ref. 7 and 33, indicate that the binder plays only a smsll role in the deflsgration rste of sandwiches. With pure binder-AP sandwiches, if exothermic effects sre

FIG. 2.23. AP-HTPB-AP-CTPB-AP; 600 psia.

FIG. 2.24. AP-HTPB-AP; 1000 psia.

greater than endothermic effecta, and if the chemical kinetica of the binder-AP flames were sufficiently fast, there ahould be a diatinct leading edge of regression near the interface and there ia not. There should be a distinct separation of vertical burn rate and AP burn rate producing s sharp upslope of the AP away from the interface and this is not observed.

FIG. 2.25. AP-HTPB-AP; 1500 psia.

FIG. 2.26. AP-HTPB-AP-CTPB-AP; 1500 psia.

The inescapsble conclusions are that either the kinetics are too slow, even st 3200 psia, to augment the sandwich rate, the binder melt flows inhibit regression near the interface, or that endothermic effects plsy s large role. This is not inconsistent with previous remarks about inhibition csusing a "Christmas tree" profile. The question is one of size

FIG. 2.27. AP-HTPB-AP-CTPB-AP; 2000 psia.

FIG. 2.28. AP-HTPB-AP-CTPB-AP; 2400 psia.

scale. Varney's photographs show at p > 1000 the "Christmas tree" in all cases within a limited distance of the binder. It is, in fact, difficult to imagine a process which would cause the extensive inhibition responsible for the "Christmas tree" profile of Fig. 2.28. Since these always occur in a pressure regime characterized by an extensive

FIG. 2.29. AP-HTPB-AP-CTPB-AP; 2800 psia.

FIG. 2.30. AP-HTPB-AP-CTPB-AP; 3200 psia.

needlelike surface structure on AP samples quenched from these pressures, one wonders whether or not the AP itself is taking a major role in the formation of the profile of Fig. 2.28, except that it is a logical progression of the difference of relative regression rates between oxidizer and binder discussed in Section 2 by NWC. In Fig. 2.18 and 2.28 it might

be noted that the binder chars are more extensive than in the other photographs. Whether or not this is significant is unknown.

With these motion picture results an extensive catalog of behavior with PS, PU, PBAA, CTPB, and HTPB binders with compacted polycrystalline and pure crystal AP has been completed. The conclusions appear to be as mentioned above. With the exception of certain anomalous results and operation near the low pressure deflagration limit, the binder is a clear inhibitor to regression near the interface. Whether this is due to melt flows, slow chemical kinetics, or losses due to heating or pyrolyzing the binder, is unclear. Certainly an analytical model might be used to give an idea of the size scales involved with each kind of inhibition and the detailed effects on surface shape.

SECTION 3

THE DEFLAGRATION OF AMMONIUM PERCHLORATE-POLYMERIC BINDER CATALYST SANDWICHES

W. C. Strahle, J. C. Handley, and T. T. Milkie
Georgia Institute of Technology

INTRODUCTION

The details of catalyst effects in composite solid propellant combustion are largely unknown. Proposed mechanisms usually are based upon the presumption that catalysts increase the heat feedback to the propelland and/or raise the surface temperature by:

1. Accelerating the gas phase reactions (Ref. 35-37)
2. Promoting exothermic reactions of gases on the surface of catalyst particles embedded in the propellant (Ref. 32 and 37)
3. Promoting heterogeneous reactions of gases with the solid or molten fuel (Ref. 37 and 38)
4. Modifying the pyrolysis mechanism of the fuel (Ref. 37)
5. Promoting crevice reactions in the gas phase or between gases and solids at the oxidizer-binder interface in the presence of catalyst particles (Ref. 32).

As in the previous sections, the sandwich technique was used here also. The sandwich also offers a unique vehicle for the study of catalyst effects, because of the variety of ways in which the catalyst may be added to the sandwich, especially with compacted AP.

Nadaud (Ref. 19) performed experiments using AP as the oxidizer and polyisobutene and polybutadiene binders with 1% copper chromite catalyst present in the AP, the fuel, or both. The experiments were conducted over the pressure range 0-80 atm. The other major work in the area of catalyzed AP-binder sandwiches was that performed by Jones (Ref. 33).

This study was concerned with the combustion of AP-CTPB sandwiches with 2 w% Harshaw Cu0202 catalyst in the AP, in the binder, or painted at the interface, burning over the pressure range 600 to 2000 psi. Unfortunately the two sets of data cannot be readily compared. The pressure ranges of the two studies were obviously different and only slightly overlapping; but perhaps of more consequence Nadaud reported a "flame flashback velocity" rather than a sandwich burning rate as reported by Jones.

The present work is an extension of that performed by Jones. An HTPB binder was used, and the pressure range was extended to encompass 600-3200 psi.

EXPERIMENTAL

Three types of catalyst additions were employed:

1. Two percent by weight pressed in with the AP alone[2]
2. The same volumetric loading mixed in the binder alone
3. A methyl alcohol paint of catalyst on the AP disc which was dried before applying the binder.

These will be referred to as Types 1, 2, and 3, respectively.

Because of the large number of tests required (four catalyst configurations consisting of no catalyst, Type 1, Type 2, and Type 3; seven pressures; and two catalysts, giving a total of 56 different conditions), it was decided to economize by investigating two or three conditions per test run. Sandwiches made of disparate materials can be used if the regression rates of the various components are not greatly different. Indeed, Jones confirmed the earlier hypothesis of Hightower and Price that for thick binders (Jones used ≈ 125 μm thick binders) the two sides of the sandwich burned independently. Using this independent behavior as a guide, double and triple sandwiches (three AP layers and two layers of binder) were constructed with the binder 125 μm thick. The double sandwiches were constructed with Type 1 on one side and Type 3 catalyst addition on the other side. The triple sandwiches were primarily used with IO in one layer of HTPB and CC in the other.

Burning rates and profiles were determined by detailed observations of the movie film. The interpretation of catalyzed sandwiches presents a more interesting problem than with binder-AP sandwiches, because in the case of Type 1 sandwiches the pure AP rate is altered. It is imperative to recognize that data are only taken after a steady state

[2]The deflagration rates of these materials are presented for various pressures and initial sample temperatures in Appendix A.

profile has been achieved during a run. As a consequence the vertical regression rate of a point anywhere on the surface is a constant. That is, the vertical regression rate at the interface is the same as that on the AP or catalyzed AP. A surface which has an angle of inclination to the horizontal must therefore be regrassing slower in a direction normal to the surface than the vertical regression rata. In Type 1 sandwiches the regression rate normal to the catalyzed AP is representative of pure catalyzed AP behavior. The vertical regression rate maasures the effects of the fastest physico-chemical processes in the system. In the catalyzed cases these always occur in the vicinity of the binder oxidizer interface.

It should be cautioned that observations were made on the sandwich edge facing the camera; these observations are tharefore subject to some edge effects. However, the camera angle and depth of field were sufficient in many runs to determine that no large errors are incurred by taking data from the leading edga. One other difficulty, the affects of which will become apparent later, was that of accurately assessing the surface inclination of AP when running Type 3 sandwiches at high pressure.

RESULTS

Figure 3.1-3.14 show the results of HTPB-Harshaw catalyst Cu0202(CC)-AP sandwich studies, and Fig. 3.8-3.21 show the corresponding results for iron oxide (IO) catalyzed sandwiches. It should be noted that the original observations were made from color motion pictures. The figuras presented here are to document the results. Obviously much detail is sacrificed by single frama, black and white, reproduced pictures as opposed to the actual motion pictures. To fully appreciate the actual footage it is suggested that the reader borrow the color films from Dr. Strahle. It is emphasized, however, that data were taken only after a steady profile had bean achieved, and the surface was clearly visible over a substantial portion of the run. In the Type 1 casas a whita line has been drawn on tha photographs to outline the aurface shape.

While the photographs are for documentation purposes the primary interpretation tools arc the burning rate data of Fig. 3.22 and 3.23. In these figures two burning rates are given; one is the vertical regrassion rate which is the same regardless of the position of measurement and the second, $r_{AV} \cos \theta$, is the rate normal to tha AP surfaca away from the binder where the AP has achieved a definable, constant slope. If these two rates are nearly the same, it indicates that the inclination angle is small and that there is little intaraction between the binder and oxidizer, just as in the uncatalyzed cases of the pravious saction. In such a casa, it would be expectad that the vartical regression rate would follow the pure AP-bindar burning rate curve quita closely. As saan in Fig. 3.22 and 3.23 tha Typa 2 catalyst addition with either IO or CC producas this affect. Surprisingly, catalyst

FIG. 3.1. AP-CC at Interface-HTPB-AP-HTPB-CC in AP; 600 psia.

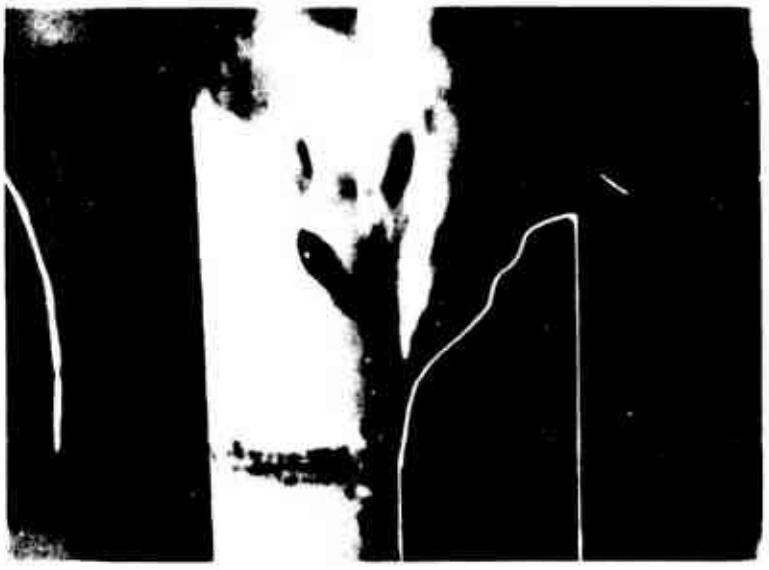

FIG. 3.2. AP-CC at Interface-HTPB-CC in AP; 1000 psia.

addition to the binder produces very little catalytic effect. Viewing Fig. 3.11, as an example, there is virtually no change in profile shape from the uncatalyzed case. While there does appear a mild effect on soms other figures, Fig. 3.8 and 3.9, for example, the inclination angles are so small that cos $\theta \simeq 1$ and virtually no burning rats

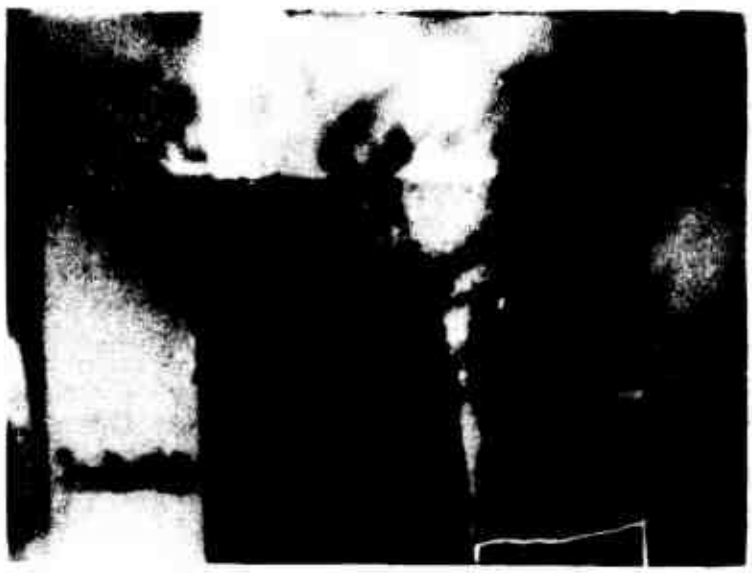

FIG. 3.3. AP-CC at Interface-HTPB-AP-HTPB-CC in AP; 1500 psia.

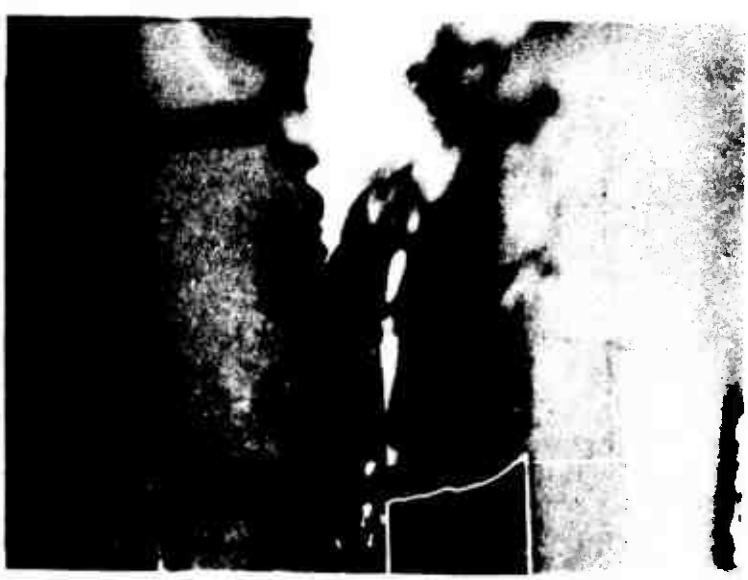

FIG. 3.4. AP-CC at Interface-HTPB-CC in AP; 2000 psia.

difference between the vertical and normal rates is apparent. It is furthermore interesting that no "Christmas tree" profiles occur at high pressure when catalyst is added to the binder alone. Finally, from detailed motion picture review there is no evidence that the binder char is any less extensive than in the uncatalyzed cases.

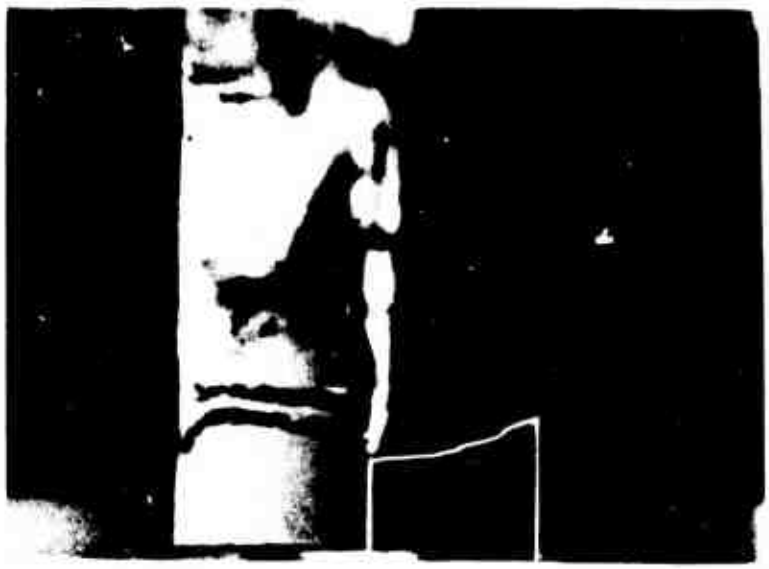

FIG. 3.5. AP-CC at Interface-HTPB-CC in AP; 2400 psia.

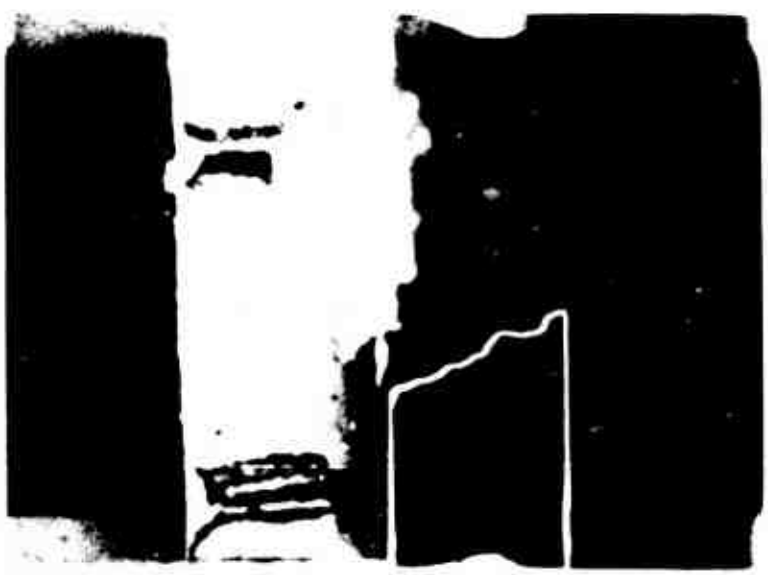

FIG. 3.6. AP-CC at Interface-HTPB-CC in AP; 2800 psia.

The conclusions for Type 2 addition appear to be that:

1. Any oxidative attack upon the condensed binder is not enhanced, if it exists at all.

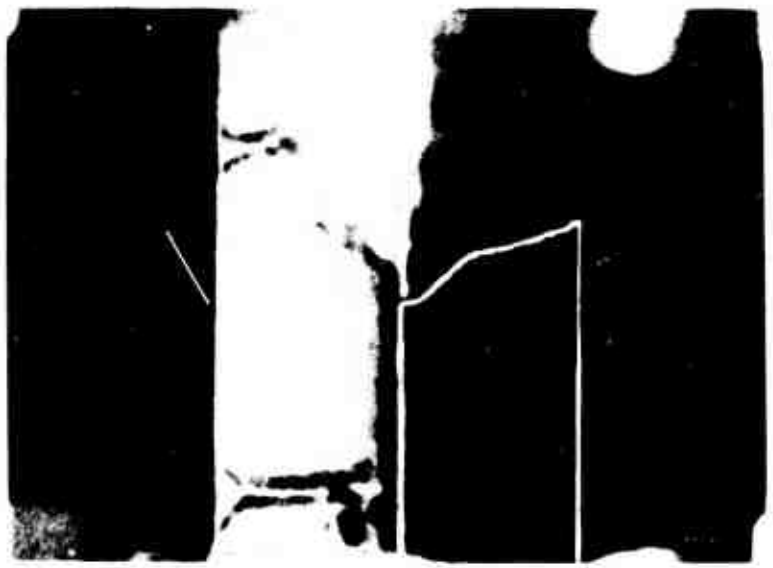

FIG. 3.7. AP-CC at Interface-HTPB-CC in AP; 3200 psia.

FIG. 3.8. AP-IO in HTPB-AP-CC in HTPB-AP; 600 psia.

2. Addition of catalyst to the gas phase from the "cold" fuel side is ineffective.

3. The pyrolysis rate of the fuel is not enhanced.

If any of these conclusions were violated, there would have to exist an augmented vertical regression rate over the uncatalyzed cases, which

FIG. 3.9. AP-IO in HTPB-AP-CC in HTPB-AP; 1000 psia.

FIG. 3.10. AP-IO in HTPB-AP-CC in HTPB-AP; 1500 psia.

does not occur, and for conclusion (3) a decrease in the amount of binder char would have to occur, which does not.

The Type 1 and 3 cases, however, produce strong catalytic effects. Consider the CC results. In particular the Type 1 results will be discussed first. In Fig. 3.22 the vertical regression rate (dark circles)

FIG. 3.11. AP-IO in HTPB-AP-CC in HTPB-AP; 2000 psia.

FIG. 3.12. AP-IO in HTPB-AP-CC in HTPB-AP; 2400 psia.

is lifted above the uncatalyzed case significantly over the entire pressure range, with the effect becoming stronger the higher the pressure. While not an exceedingly strong effect, it may also be seen that the normal regression rate (open circles) on the CC-loaded AP is distinctly lower than the vertical rate. In Fig. 3.1-3.7 this result is a consequence of a definite inclination of the black surface to the horizontal.

FIG. 3.13. AP-IO in HTPB-AP-CC in HTPB-AP; 2800 psia.

FIG. 3.14. AP-IO in HTPB-AP-CC in HTPB-AP; 3200 paia.

These results indicate that, (1) the pure AP rate is enhanced by CC addition, which is well-known, and (2) some rate process ia being enhanced in the vicinity of the BO interface. The second conclusion ia inescapable; if there were nc effect taking place in the vicinity of the BO interface the CC loaded AP surface would be flat, just aa with the uncatalyzed binder-AP cases.

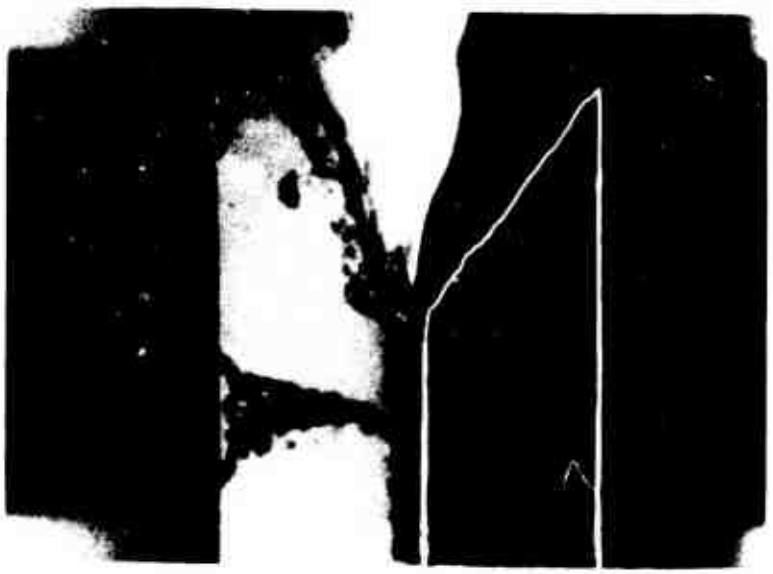

FIG. 3.15. AP-IO at Interface-HTPB-IO in AP; 600 psia.

FIG. 3.16. AP-IO at Interface-HTPB-AP-HTPB-IO in AP; 1000 psia.

The type 3 experiments must be recognized as somewhat uncontrolled because the catalyst loading may be variable. Nevertheless, this experiment can give information on catalyst behavior in the vicinity of the interface, when the catalyst is not intimately dispersed in either the binder or the oxidizer. Consider the vertical burn rate curve (solid triangles) on Fig. 3.22. The vertical burn rate is always higher

FIG. 3.17. AP-IO at Interface-HTPB-IO in AP; 1500 psia.

FIG. 3.18. AP-IO at Interface-HTPB-IO in AP; 2000 psia.

thsn the uncatalyzed burn rate, is somewhat lower than the Type 2 burn rate, but appears to increase in catalytic activity as the pressure spproscheo the high end of the tested range. First of all, it sppesrs in this csse, because the CC is not mixed with the AP or binder, thst the cstalytic activity must be taking place in the gas phase (whether or

FIG. 3.19. AP-IO at Interface-HTPB-IO in AP; 2400 psia.

FIG. 3.20. AP-IO at Interface-HTPB-IO in AP; 2800 psia.

not heterogeneous catalysis on the catalyst particle is occurring). The different pressure sensitivity from the Type 1 results suggests that the primary catalytic mechanism is different from the Type 1 results. Although some catalysis of the AP deflagration rate could be occurring in the interface vicinity, the different pressure sensitivity

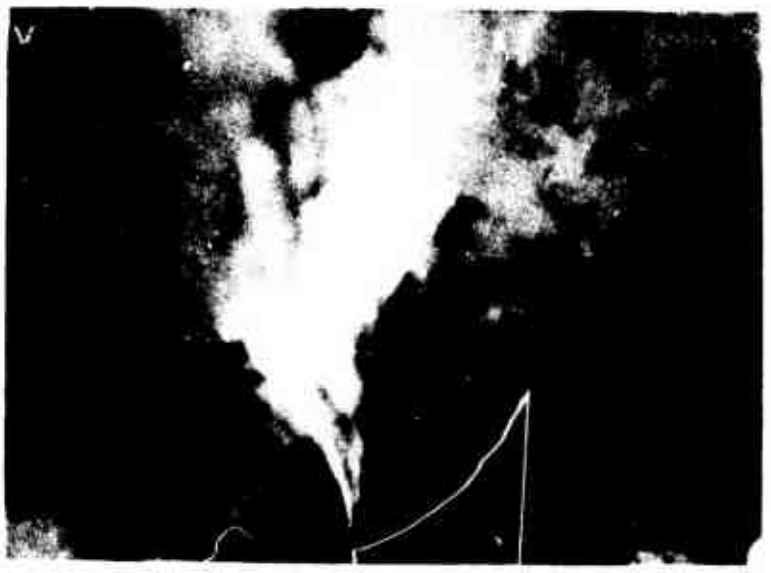

FIG. 3.21. AP-IO at Interface-HTPB-IO in AP; 3200 psia.

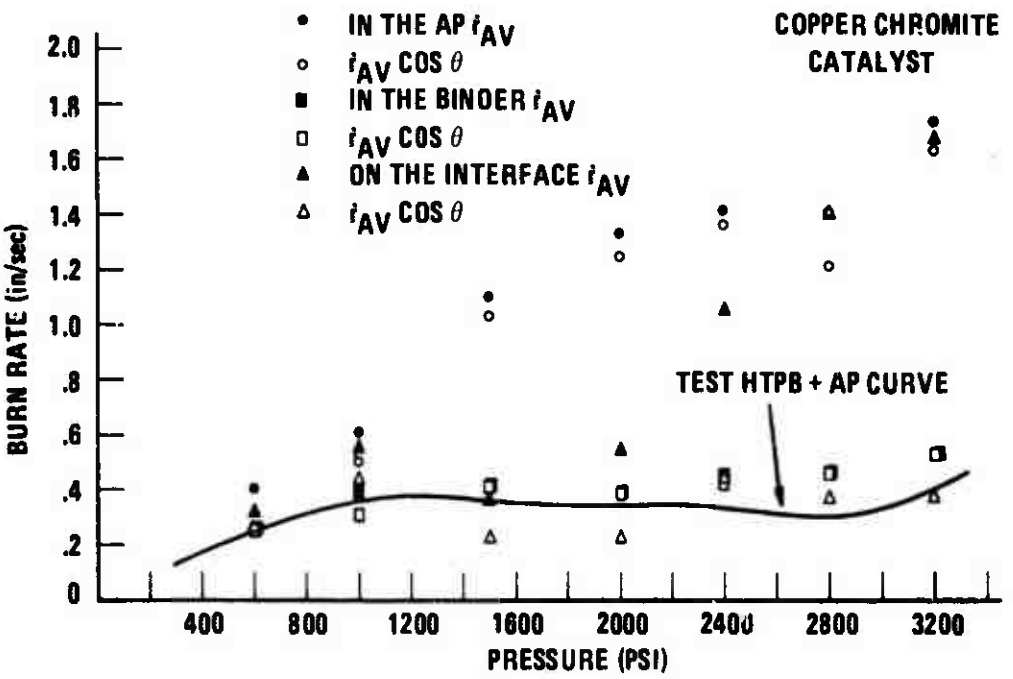

FIG. 3.22. Burn Rate for CC-Catalyzed AP-HTPB Sandwiches.

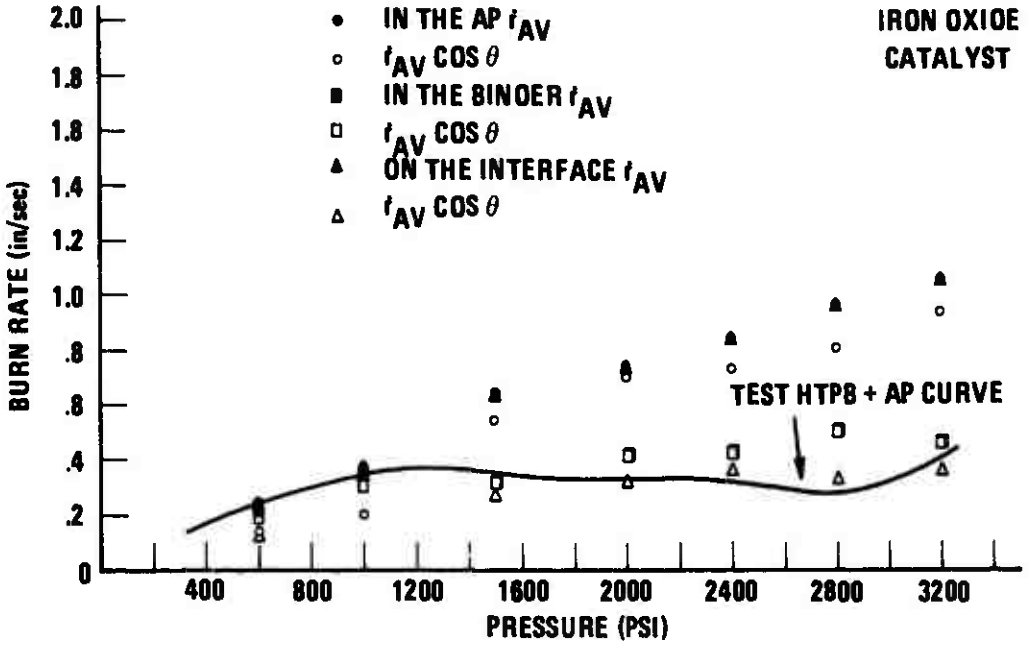

FIG. 3.23. Burn Rate for IO-Catalyzed AP-HTPB Sandwiches.

from the Type 1 results suggests a catalysis of the BO reactions. Since the catalyst concentration in the interface vicinity is much higher than that in the Type 1 result, the evidence is that what one is seeing is an augmentation of the effect producing the separation of the open and black circles on Fig. 3.22; i.e., a catalysis of the BO reactions.

The open triangles on Fig. 3.22 represent the pure AP burn rate and they are seen to follow the uncatalyzed burn rate curve. Thus, there appears no outward transfer of the catalyst from the interface region. While this was expected to be the case, it is mentioned here because of the curious IO results to follow.

In a private communications with Mr. T. L. Boggs it has been learned that CC-loaded AP is highly radiation sensitive and it is possible that the sensitivity could be part of an effective catalytic mechanism for the Type 1 results. It might also explain why the Type 3 results are only mildly catalytic until a sufficiently high pressure is reached.

The IO results are shown in Fig. 3.23. As previously mentioned, there is virtually no effect when the catalyst is loaded into the binder (Type 2). The Type 1 and Type 3 effects are somewhat different as compared with the CC results. Viewing first the Type 1 results for the vertical burn rate (solid circles), there is a depression of the rate until about 1000 psi but a uniform increase with pressure. The open circles are uniformly depressed from the solid circles, indicating that

there is a surface inclination to the horizontal, which in turn indicates catalytic activity near the BO interface. However, the open circles remain below the pure AP curve until roughly 1500 psi, confirming the known fact that IO is an AP burn rate depressant at low pressure. However, the surface slant and the consequent separation of the solid and open circles indicate that the binder and oxidizer reactions are augmented at all pressures.

Viewing now the Type 3 results, the solid circles and solid triangles have identical rates. Consequently, it is impossible to tell whether the IO is primarily acting on the AP near the interface or acting on the BO reactions. Here the indication is not clear as it was with CC. The open triangles follow the normal burn rate curve, with one important exception to be noted, showing that Type 3 addition has little effect away from the interface on the AP processes. The exception is an apparent depression of the AP burn rate at 600 psi. On Fig. 3.15, however, note the black residue on the AP surface on the side with Type 3 addition. This curious effect, whereby a residue appears far away from the catalyst loading site, may be related to the burn rate depression. In any event the Type 3 results show that at sufficiently high pressure, where the residue disappears, the primary catalytic activity is in the gas phase, because the Type 3 addition does not intimately mix the catalyst and oxidizer. Whether or not the primary mechanism is with the AP or BO reactions cannot be determined, however.

DISCUSSION

These results, coupled with the previous results of Jones (Ref. 33), indicate opposite trends than those proposed by other investigators. The most startling result is that inclusion of both catalysts within the binder had little effect on the deflagration rate or the sample profile. The conclusions may be reached that neither CC nor IO modify the pyrolysis mechanism of the fuel, promote heterogeneous attack of the oxidizer upon the binder or are effective when introduced into the gas from the "cold" fuel side.

The conclusions with CC catalyst are that at all pressures it is an effective AP catalyst and it has a mild effect upon processes in the vicinity of the interface, especially above 1600 psia. In order that this interface process be effective it is necessary that the catalyst be accessible to the gas phase from the "hot" oxidizer side. In future work, quenched combustion studies with scanning electron microscopy will be made to better determine the nature of the interface processes. Of extreme interest will be the precise location of the leading edge of regression and the effect on binder melts.

At all pressures, IO is catalyzing some process in the vicinity of the BO interface; snd this is the dominant catalysis process, until about 1000 psia. Above 1000 psia it is impossible to tell whether AP catalysis or BO reaction catalysis is the dominant mechanism. Again, higher resolution experiments must be performed to isolate the nature of the BO interface processes.

Comparing IO with CC it appears that IO is at least as effective in catalyzing the interface processes as CC to 1500 psia. However, CC is more effective in catalyzing AP itself. The effects upon AP itself are consistent with previous work (Ref. 35). The effects noted are consistent with those of Jones using CTPB. It may be concluded that even under catalysis there is little difference in the behavior of CTPB as compared with HTPB.

CONCLUDING REMARKS

The present sandwich results have several implications toward the behavior of propellants, using AP, CC, or IO over the pressure range studied, but for either HTPB or CTPB binders. First, since the conventional method of catalyst addition is through a binder mix, it is imperative that a large surface area of AP be presented. That is, the smaller the oxidizer grind the more effective the catalyst should be. Second, since the AP is not conventionally loaded with catalyst, it is the interface processes which must be catalyzed, implying IO would be as effective as CC up to 2000 psia, with CC becoming more effective thereafter. Third, it would be worthwhile to investigate methods of loading the AP with catalyst or coating the AP particles with catalyst.

There is also a correspondence between the uncatalyzed sandwich and propellant behavior. Above the low pressure deflagration limit, the binder in the sandwich does not alter the deflagration rate over that of pure AP, also restricting this comment to below 2000 psia. That is, for sufficiently large particle size the binder is along for the ride, although it does alter the microstructure in the vicinity of binder-oxidizer interfacas. This conclusion is in accord with that of Ref. 13 and 39.

In order that further information be gained concerning the mechanism of catalytic activity in the interface vicinity, high resolution study of quenched samples should be undertaken. Whether or not heterogeneous sttack is taking place upon the bindar may be determinad and further suggestions concerning propellant behavior with catalyst addition may be made. Complementary use of cinephotomacrography and quenched combustion results with the simple sandwich configuration is expected to yield a simple, inexpensive, effective method of catalyst screaning for propellant application, as has been initially shown in this report from the cinaphotomacrography work.

SECTION 4

THE DEFLAGRATION OF AMMONIUM PERCHLORATE POLYMERIC BINDER-ALUMINUM SANDWICH MODELS

T. L. Boggs and D. E. Zurn
Naval Weapons Center

INTRODUCTION

Powdered aluminum (Al) is often used in composite propellants to improve performance and to suppress combustion instability. Unfortunately the actual combustion behavior of Al does not always fulfill the theoretical potential; instead of the performance predicted assuming complete reaction of Al to aluminum oxide (Al_2O_3), a lesser performance is actually obtained and a portion of the Al is unburned. In movies taken of propellants burning in a window bomb many complex phenomena involving the Al were seen (Ref. 40). It is beyond the scope of the present effort to review all the phenomena and would be unnecessarily repetitious since an excellent review article describing Al combustion is forthcoming (Ref. 41). Although a detailed review will not be given here a brief introduction is included to familiarize the reader with the "setting and magnitude of the problem". For more detailed information please consult Ref. 42-46.

The first studies (Ref. 40) showing the behavior of Al in propellants revealed:

> . . . not only that the original aluminum particles in the propellant accumulate at the burning surface but that subsequently they form large agglomerates of molten aluminum which burn in the gas phase above the propellant surface with a vigorous detached flame. The entire sequence of events occurring with the aluminum can be described, in general, as follows. During the steady state combustion of aluminized solid propellants, the AP and the binder pyrolyze and the original aluminum, protected from ignition by its own oxide coating, is left behind and accumulates on the surface of the propellant. After the accumulation period, the aluminum behaves in one of two ways:

(1) If conditions are favorable for aluminum combustion, e.g., sufficient oxidizer available, sufficiently high pressure and/or temperature, etc., a small portion of the accumulated aluminum, perhaps only one or two of the original particles, ignites. This event is most likely to occur at a time when the accumulate is most effectively exposed to the oxidizer-binder diffusion flame and/or the decomposition products of the oxidizer. The heat from this small zone of burning aluminum generates a thermal wave which passes through the remaining portion of the accumulated aluminum and melts the rest of the accumulate. The entire mass then draws up into a spherical ball of molten aluminum and leaves the surface of the propellant burning vigorously.

(2) If conditions are unfavorable for aluminum combustion, the accumulated aluminum will not ignite locally; instead, it will remain on the surface of the propellant until it is undermined sufficiently by the regression of the AP and binder so that it is released (unignited) into the gas phase. Under some conditions, the accumulate is heated enough to "sinter" the accumulate into an irregularly shaped mass which exhibits a red glow and apparently undergoes surface oxidation without complete melting of Al_2O_3 present.

In addition to the large spherical agglomerate and the large irregular accumulated mass of aluminum, a third type of aluminum behavior has been observed. The third type is the ignition and combustion of a single original aluminum particle. This type of aluminum combustion has been observed to a greater or lesser extent in all the propellants that have been photographed. It is obvious that this is the most efficient way to burn aluminum in solid propellants and efforts should be expended to eliminate the aluminum accumulation and agglomeration processes and produce only single particle ignition and combustion.

Since the above was written, much additional work has been done and is summarized in Ref. 41. Briefly, it has been shown that the behavior of the Al in question can be explained in terms of these known properties of Al and Al_2O_3, and demonstrated most unambiguously by certain controlled laboratory experiments at the relevant temperatures.

First, one cannot stress too often the role of the oxide skin on the aluminum, which is known to inhibit aluminum from reaction because of its low chemical reactivity, low permeability [and high melting point]. Second, the vapor

pressure of the aluminum is negligible at temperatures near those of the propellant burning surface (425-900°K). These first two points explain the "reluctance" of the aluminum to ignite as noted above. However, third, there are some properties conducive to slow reaction of the aluminum under these conditions, processes that also can lead eventually to adhesion or coalescence of aluminum particles prior to their ignition. Fourth, there is not much known about the state or status of the oxide skin as it goes through the temperature rise, and it is easily possible that phase change or dehydration offer an opportunity for adhesion as yet unknown to us. These processes, insofar as they are currently known, will be described in some detail.

The coefficient of thermal expansion of solid aluminum is greater than that of aluminum oxide, so some cracking, porosity or deformation of the oxide may occur in the range below the aluminum melting point of 933°K. If cracking or porosity do occur, the exposed aluminum no doubt oxidizes quickly in those locations where oxidizing species are plentiful, thus continuously "healing" the surface defects as they form. The exact behavior would be expected to depend on the condition of the oxide skin, shape of the aluminum particle, local temperature, and oxidizer concentration [and kind of oxidizing species]. Whatever the response of the aluminum, it may be greatly exaggerated or changed when its melting point is reached.

When aluminum melts, it expands by 6.6% volumetrically, implying a sudden increase in circumference of 1.9%. This expansion is easily visible with particles heated in a hot stage microscope. As noted before, the condition of the oxide (mechanical properties or structures of the material) is not well-known at these temperatures and heating rates, except that the oxide is far from the alpha oxide melting point (2323°K) and is presumably fairly rigid unless it is exceedingly thin. Thus it seems reasonable that the oxide skin will in some way become flawed, cracked, or made porous locally by the sudden expansion of the interior aluminum when it melts. Accompanying this would be some leakage of the molten aluminum. Alternately, if the particle is initially far from spherical, it may be made more spherical by stress redistribution [in the skin] to accommodate for the aluminum expansion (with or without cracking), provided the properties of the particular oxide skin permit the distortion. This would obviously depend on original shape of the particle, original quality of the oxide skin (e.g., thickness or crystal phase), on the temperature-time history

during the distortion, and the local state at various locations on the particle. However, the moment of melting of the aluminum is necessarily in all cases a moment of high physical activity of the oxide skin, and of high potential for leakage of aluminum through the oxide skin.

Once the aluminum particles melt, the accumulated aluminum responds to two concurrent processes that tend to establish interconnected "accumulates" of particles. One process, which is most effective in regions of low oxidizer concentration, is by "wetting" of adjoining particles by molten aluminum, which may sometimes lead to complete coalescence of particles. The second process, which is most effective when oxidizer concentration is appreciable, is the oxidation of leaking aluminum to form oxidized "bridges" between particles, but with complete coalescence impeded by oxidation of leaking aluminum. In terms of propellant microstructure, one might expect the "coalescence" process to be more likely in surface regions overlaying binder areas, and the oxidative welding process to be more prevalent in surface regions overlaying or adjoining oxidizer material. In either case, a means is provided for the aluminum particles to form and preserve the "accumulate" state even at temperatures where the binder and oxidizer have largely gasified and lost the capacity to "wet" the whole aluminum accumulate. Even under these conditions the accumulate may be temporarily held loosely to the surface by local contact with molten binder and/or oxidizer on the underside, and ignition may still be delayed by the continuing formation of protective oxide on all "leaking" aluminum. . .

The laboratory tests give good support to the more speculative interpretation of Al behavior as inferred above on the basis of propellant combustion photography. Obviously the Al behavior on the propellant burning surface is rather varied in nature, depending on nature and spatial disposition of other ingredients and on the combustion zone structure and chemistry, as a whole. But the principal features of the Al behavior are from Ref. 41:

1. Reluctance to leave the surface because the Al remains in condensed phase and is restrained by a wet surface of other ingredients, predominantly binder.

2. Reluctance to ignite at the surface because [illegible]e protective oxide coating, and sometimes protective [illegible]ure of a fuel environment.

3. A resulting tendency for Al to accumulate on the surface as the surface recedes.

4. Presence of processes by which varying degrees of adhesion or coalescence of accumulated Al can occur, setting the stage for formation of relatively large Al "agglomerate" droplets.

The previous Al combustion research performed at NWC (Ref. 40-51) has provided information as to how single Al particles burn (Ref. 43 and 46-51) and how Al in propellant accumulates, agglomerates and burns (Ref. 40-43 and 45). From this multifaceted effort many of the processes responsible for the behavior of Al in propellants were described. The purpose of the present work was to bridge the gap existing between the single particle studies and the propellant combustion studies. The sandwich technique was used because the partition of ingredients into defined regions provided much greater resolution than was possible for the propellant case; the sandwich as a tool offers the opportunity to obtain more definitive (and more publishable) evidence. It should be strongly emphasized that the present work is dependent upon and extends the excellent studies previously performed.

EXPERIMENTAL APPROACH

The Al used in these studies had a nominal diameter of 5 μm. The parameters which were altered were: the pressure (100 psi < p < 1000 psi), the binder thickness (25, 125 and 300 μm), the Al loading in the HTPB binder (50% HTPB/50% Al, 65% HTPB/35% Al, 80% HTPB/20% Al, 90% HTPB/10% Al, and 95% HTPB/5% Al), and the Al type (as-received and an Al whose oxide thickness was carefully controlled (Ref. 51) which will be called preoxidized Al in the ensuing discussion).

This special preoxidized Al was made under a separate task and is more fully described in Ref. 52. The main differences between the as-received and preoxidized Al are the thickness, porosity, and strength of the oxide (Al_2O_3) coating on the original Al particles; the oxide on the preoxidized material is approximately five times thicker than that on the as-received material. It was anticipated that this thicker oxide would reduce the degree of agglomeration as compared to the as-received and that the differences in behavior would be highlighted using the sandwich technique.

RESULTS FROM SCANNING ELECTRON MICROSCOPY (SEM)

Although it certainly would be possible to simply present micrographs taken of samples quenched at the various conditions studied, that is not done here because such a presentation would necessarily be redundant (with the description of the movies and sample to sample). Rather micrographs are presented only to illustrate specific mechanisms and terminology.

As defined in Ref. 41 and as used in this text, the terms "accumulate" and "agglomerate" are taken to mean:

Accumulate (noun) - an irregular combination of interconnected ingredient particles (each somewhat distinguishable from other particles in the matrix) sometimes extending to a cohesive layer over the burning surface.

Agglomerate (noun) - the collection of ingredient particles in one usually spheroidal body. Although many hundreds of particles may form an agglomerate, after formation the particles have no individual identity. They form an indistinguishable part of the whole. An agglomerate is usually caused by the melting of an accumulate and is usually ignited or in the process of igniting if oxidizing species are plentiful.

Figure 4.1 shows several accumulates. The one shown in micrograph (a) is an accumulate of fine particles showing no agglomerates while the other micrographs show a few very small agglomerates within the accumulate. The micrographs (c-f) show the "bridges" joining adjacent particles within the accumulate.

Figure 4.2 shows a small agglomerate, micrograph (a), and several shots of an oxide shell, bound to an accumulate matrix having several agglomerates within it. No effort was made to quench and capture the truly large agglomerates (several hundred microns diameter) produced by the ignition of accumulates.

The Flow of Binders. In Section 2 it was shown that flow of molten binder often occurs onto the AP. This same phenomena occurred with the binders having incorporated Al. Figure 4.3 shows some of the effects of binder flow. In Fig. 4.3a, looking down on the surface, the dashed line shows the binder-AP interface; above the line is aluminized binder (labeled B in the figure), below the line, the AP (labeled AP in the figure). The arrows labeled BF show a few areas of binder flow extended greater than 300 μm onto the AP. The arrows labeled A point to a few of the many accumulates existing on the AP. Figure 4.3b shows the binder flow labeled BF) out onto the AP. The white lines bracket the binder layer (labeled B). Figure 4.3c is an increased magnification of the center portion of Fig. 4.3b. The size and extent of Al accumulates (arrows labeled A point to these structures) on the binder can be seen. The binder flow is also shown. The binder flow as shown in these micrographs helps explain why, as the movies show later, Al ignition often occurred several hundred micrometers from the original AP-binder interface.

The Relative Lack of Agglomerates Formed by the Preoxidized Al. The micrographs taken of the samples containing preoxidized Al show very little agglomeration at the surface (and the movies showed evidence of only a moderate agglomeration after ignition) although accumulates are readily apparent. Figure 4.4 presents a few micrographs of quenched samples of sandwiches which had the preoxidized Al incorporated within the binder.

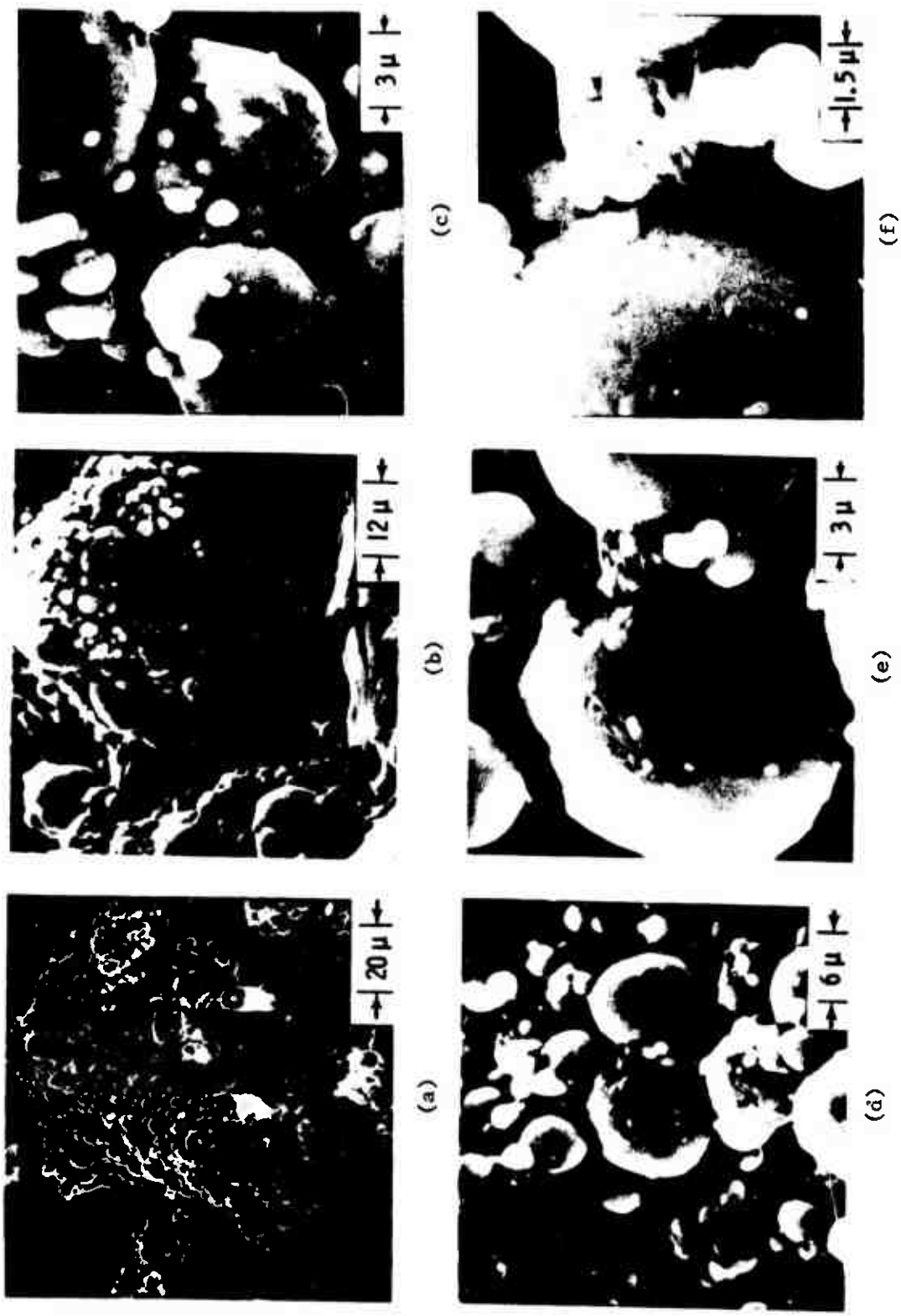

FIG. 4.1. Accumulates of As-Received Al From a Sandwich Which Incorporated 50% Al/50% HTPB Binder 25 μm Thick, Quenched at 1000 psi.

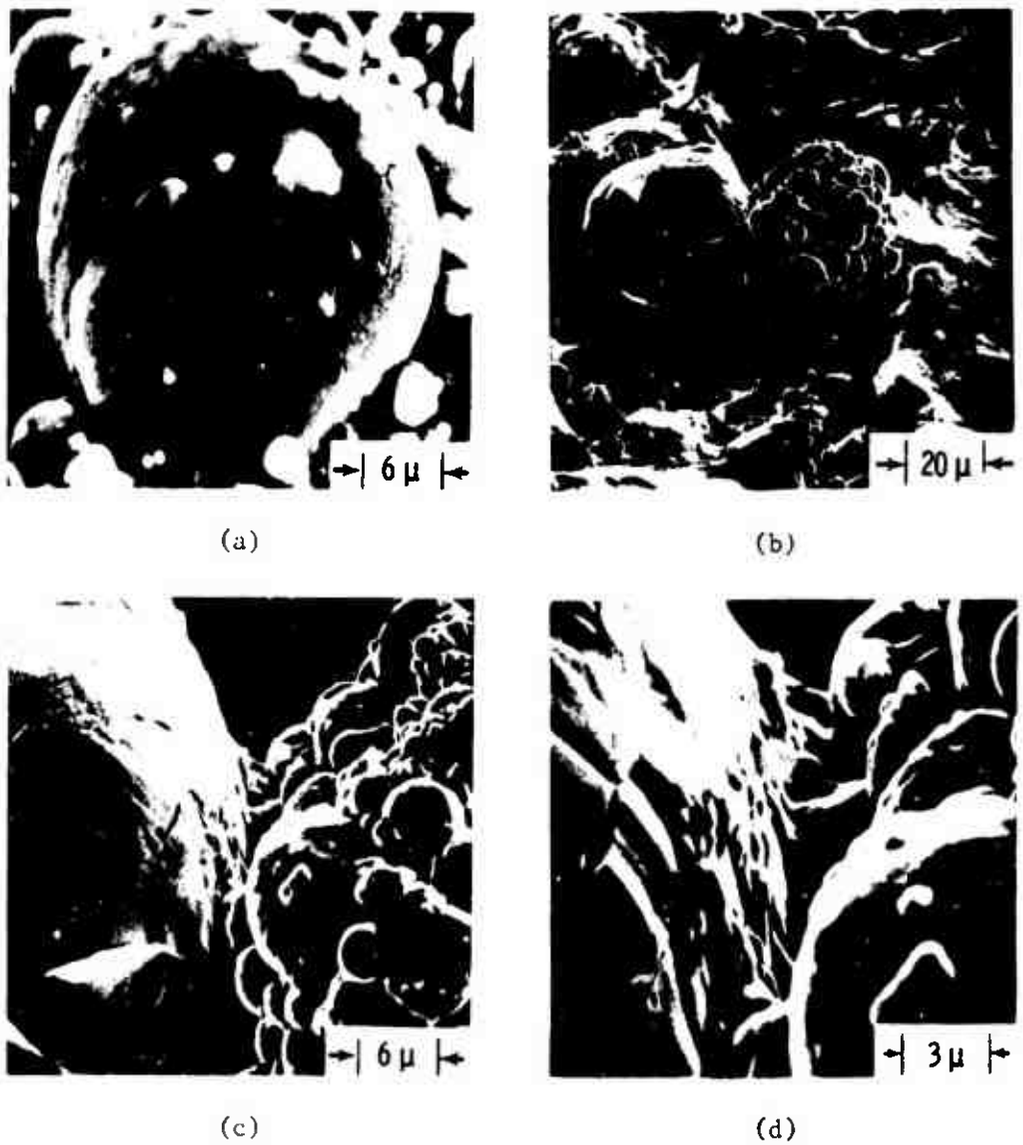

FIG. 4.2. Quenched Samples of Sandwiches Which Incorporated (a) 50% Al/50% HTPB 25 μm Thick, Quenched at 1000 psi, (b)-(d) 50% Al/50% HTPB 320 μm Thick, Quenched at 500 psi.

RESULTS FROM CINEPHOTOGRAPHY

Many of the data obtained in the program were in the form of motion pictures and are available upon request from the authors. The following is a description of events seen in the movies, but to fully appreciate the complexity of the behavior the movies must be viewed. The descriptions follow in outline form. The effects of pressure and binder thickness of a given loading of as-received Al are discussed for each of the

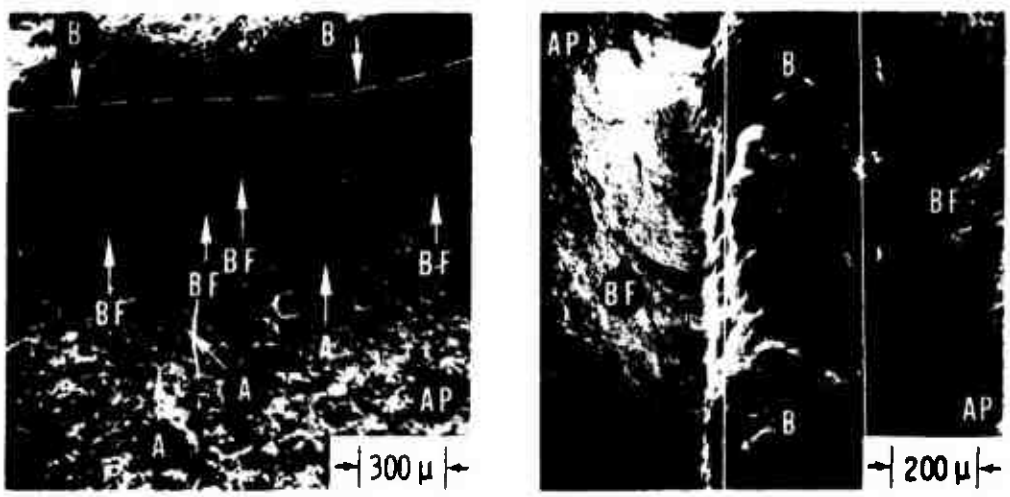

(a) (b)

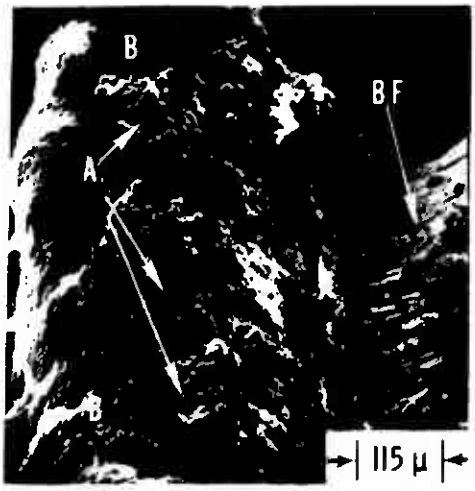

(c)

FIG. 4.3. Quenched Samples Showing Binder Flow: (a) 50% Al/50% HTPB Binder, 25 μm Thick, Quenched at 1000 psi, (b) and (c) 50% Preoxidized Al/50% HTPB 320 μm Thick, Quenched at 100 psi.

various loadings and then the behavior of the sandwiches incorporating the two types of Al are compared.

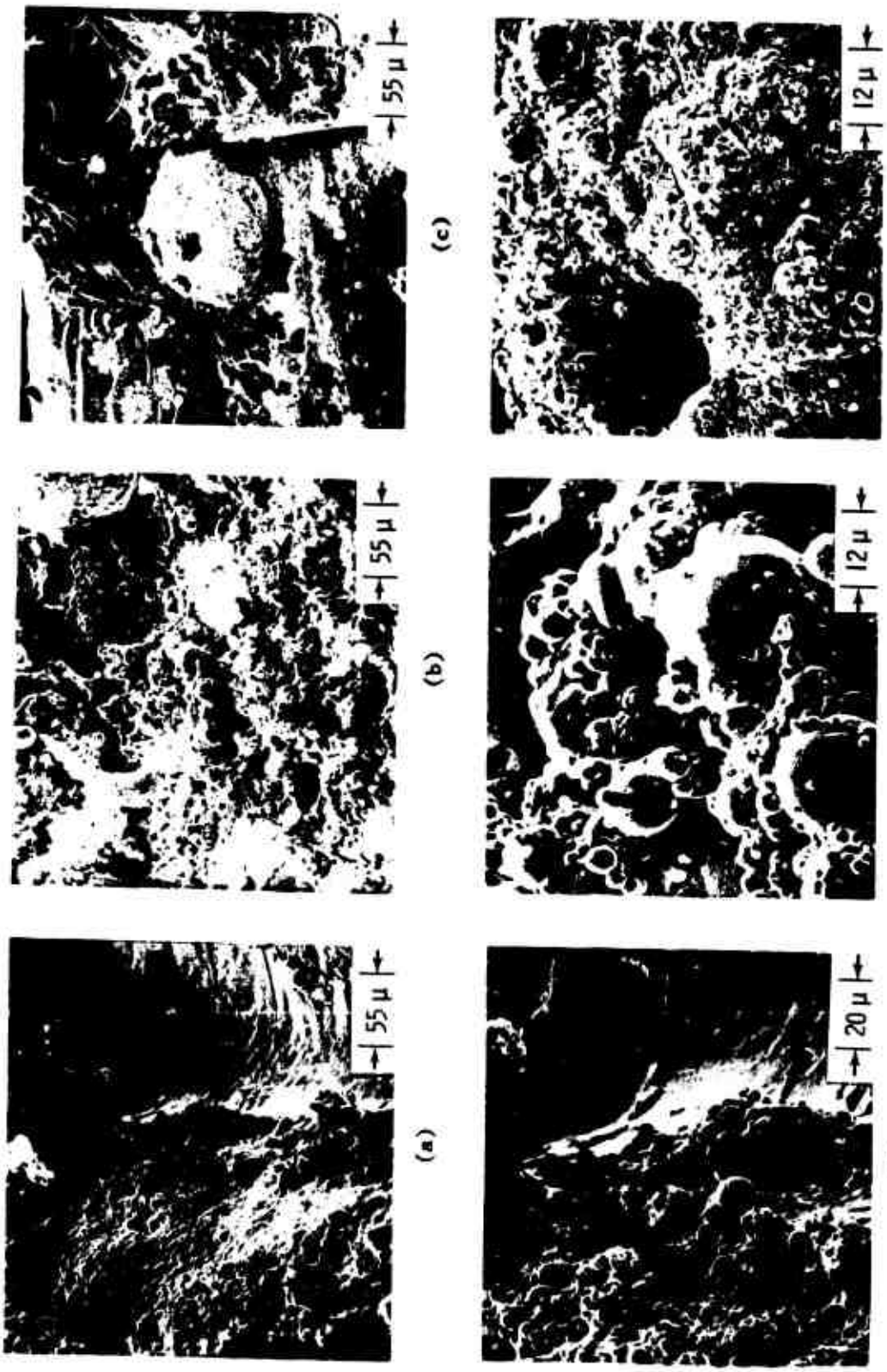

FIG. 4.4. Quenched Samples of Sandwiches With 50% Preoxidized Al/50% HTPB: (a) and (d) 320 μm Thick Quenched at 100 psi, (b) and (e) 25 μm Thick, 800 psi, (c) and (f) 25 μm, 500 psi.

I. 50% HTPB/50% 5 μm AS-RECEIVED Al

A. Thin Binder (25 μm)

1. p = 1000 psi. At this pressure and binder thickness the AP regressed slightly faster than did the binder. As the binder pyrolyzed, the Al accumulated but few of the accumulates were seen to leave the surface. Rather they ignited and agglomerated on (or extremely close to) the surface. The size of the agglomerates, which then left the surface, were about 520 μm in diameter, which indicates that approximately 10^6 particles (originally 5 μm) formed these agglomerates. When one of the agglomerates ignited there was a brilliant flash, which was followed by several frames of no Al combustion, then another flash, etc.

2. 800 psi. As above, except the agglomerates were mobile on the surface before igniting. The agglomerates seemed to be smaller (400-500 μm), and some of moderate size (< 300 μm) were evident.

3. 500 psi. As above, except smaller agglomerates (≈ 300 μm) were evident and more fine particle (≈ 75 μm) combustion occurred. The time to repopulate the surface with Al (the period of no Al combustion between flashes) increased.

4. 300 psi. At this pressure (the low pressure deflagration limit of the AP) the majority of the AP didn't regress as fast as did the binder. The result was the shape seen in Fig. 4.5, with the binder flowing as indicated (and as seen in Fig. 4.3). The ignition of the Al occurred very near the interface between the binder flow and the AP, about 500 μm from the original binder-AP interface.

5. 100 psi. The thin binder samples ignited at this pressure did not sustain combustion.

B. Thick Binder (300 μm)

1. 1000 psi. At this pressure and binder thickness very little combustion of Al occurred. After the AP burned an aluminized char was left from what had been the aluminized binder. All of the Al combustion which occurred (an extremely limited amount) occurred extremely near the AP interface.

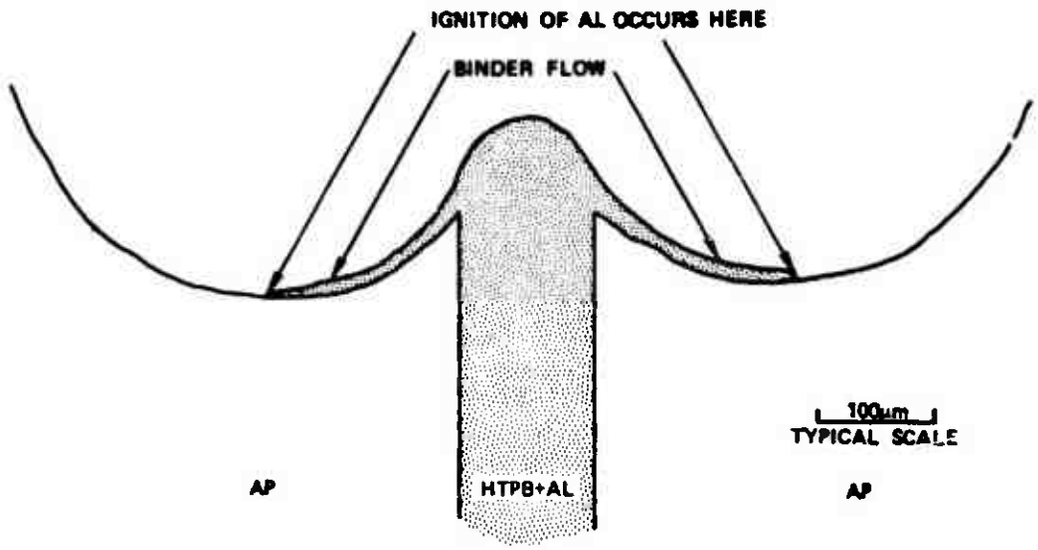

FIG. 4.5. Profile of Sandwich With 50% HTPB/50% 5 μm As-Received Al Burned at 300 psi Showing Binder Flow and Ignition Sites.

2. 800 psi. The behavior for the sample burned at this pressure was similar to that of the 1000 psi case.

3. 500 psi. Large agglomerates (> 1000 μm) formed on the binder and glowed orange. When one of the agglomerates projected into the oxidizer rich areas adjacent to one of the flamelets ignition occurred, resulting in burning agglomerates of approximately 700 μm diameter.

4. 300 psi. As with the thinner binder layer, the binder flowed 100 to 300 μm onto the AP. Aluminum ignition occurred very close to this interface.

II. 65% HTPB/35% 5 μm AS-RECEIVED Al

A. Thin Binder (25 μm)

1. p = 1000 psi. The AP regressed more rapidly than did the binder, leaving a tip of binder exposed. Large accumulates (up to 1500 μm) formed on the binder and resided on the surface up to 0.02 seconds. When some of the flamelets "washed over" this accumulate (with the thin binders the flamelets are unsteady and often appear to move across the binder region) the Al would glow white, indicating rapid oxidation, and draw up into an agglomerate and detach from the binder. In one sequence an accumulate of 1100 μm and a few hundred

micrometers thick drew up into a 500 μm agglomerate within 0.01 sec with the ignition complete within 0.05 sec. Often the accumulate would ignite before fully agglomerating causing several agglomerates to be formed. In one sequence a large accumulate ignited and formed three agglomerates of 190, 420 and 690 μm diameters. This occurred within 330 μm from the binder surface and 0.0025 sec after ignition.

While accumulation and agglomeration, causing large Al spheroids, characterized the Al behavior on the binder, the combustion of fine particles of Al was also discernible. The ignition of these fine particles occurred near the AP-binder flow interface before the particles had a chance to significantly accumulate/agglomerate. Thus two modes were apparent as evidenced by the fine particles coming from the AP-binder interface and the large particles resulting from accumulation/agglomeration on the binder.

2. 800 psi. The behavior at this pressure was like that for 1000 psi. There was accumulation (residence time of up to 0.030 sec) of Al on the binder which ignited as the flamelets (and oxidizer products) washed over the binder, causing agglomerates in the 300 μm range. There appeared to be more fine particles (50-70 μm) burning which gave the overall appearance of more metal burning at 800 than at 1000 psi.

3. 500 psi. At this pressure there was less accumulation and consequently smaller agglomerates (≈ 200 μm diameter) than at the higher pressures. Also, there was more combustion of small (≈ 40 μm) particles. At this pressure evidence of binder flow onto the AP was also seen with ignition of the fine Al occurring at the interface between AP and liquid binder.

4. 300 psi. Almost total lack of accumulation was characteristic at this pressure. Thus there were very few agglomerates seen. The dominant combustion was that of fine particles with ignition occurring at the AP-molten binder flow interface. The combustion of the Al was not uniform. An intrinsic instability was observed with a violent white flash followed by several frames of no Al combustion followed by bright flashing, etc.

3. Thick Binder (125 μm)

1. 1000 psi. At this pressure and binder thickness very little of the Al burned. At the conclusion of the test an aluminized char remained.

2. 800 psi. The sample burned at this pressure behaved much as did the 1000 psi, except there was less projection of the binder above the AP.

3. 500 psi. Much accumulation of Al on the binder was apparent, but these large (≈ 1400 μm) accumulates did not readily ignite.

4. 300 psi. Many of the Al accumulates ignited producing agglomerates in the 500-900 μm diameter range. There was little evidence of the fines burning.

5. 100 psi. More combustion, less agglomeration characterized the burning at this pressure. Once again the Al ignited near the AP-molten binder interface, which was up to 300 μm from the original AP-binder interface. The intrinsic instability noted above (flashing, no Al burning, flashing, etc.) was apparent on these runs too.

III. 80% HTPB/20% 5 μm AS-RECEIVED Al

A. Thin Binder (25 μm)

1. 1000 psi. These samples behaved in much the same manner as did the other thin binder sandwiches at 1000 psi. Accumulates (≈ 800 μm) formed on the binder upon which continued heating formed agglomerates of ≈ 400 μm diameter. Also many fine particles (≈ 45 μm) ignited near the AP-binder interface.

2. 800 psi. Little accumulation/agglomeration occurred and what agglomerates formed were small (≈ 200 μm). Combustion of small (≈ 30 μm) particles were evident with ignition occurring at the AP-binder flow interface.

3. 500 psi. The sample burned in the same manner as did the one at 800 psi.

4. 300 psi. The sample did not sustain combustion.

B. Thick Binder (125 μm)

1. 1000 psi. Very little of the Al in the binder burned and an aluminized char was left at the end of the test.

2. 800 psi. Much accumulation was seen; the accumulates were large (up to 2000 μm). Occasionally parts of these accumulates would ignite and form agglomerates (≈ 300 μm) but usually the large accumulate would simply "slough off" from the surface without igniting.

3. 500 psi. This sample burned in the same manner as did the 800 psi sample.

4. 300 psi. Accumulates formed and were sloughed off. Some fine (≈ 50 μm) particles ignited at the AP-binder flow interface (up to 500 μm from the original AP-binder interface).

5. 100 psi. Very few agglomerates were formed, otherwise the sample burned the same way as did the 300 psi sample.

IV. 90% HTPB/10% 5 μm AS-RECEIVED Al

A. Thin Binder (25 μm)

1. 1000 psi. Very little accumulation/agglomeration occurred. Ignition of Al occurred near the AP-binder.

2. 800 psi. Accumulation occurred which then caused a spectacular form of instability with the flamelets moving from side-to-side of the binder layer (Fig. 4.6). First, Al accumulated on one side (the right side in Fig. 4.6), then flashed. The combustion drew the diffusion flamelets, entraining oxidizing species, to that side. Oxidizer species then contacted the accumulate exposed on the opposite (left) side causing it to ignite. The ignition and violent combustion caused the flamelets to be drawn to that (left) side, thereby causing the accumulate on the right side to be exposed to oxidizing species.

3. 500 psi. The combustion was similar to the 800 psi case, except the oscillations of flamelets from side to side were more pronounced.

4. 300 psi. The combustion was similar to the above two cases except there was less Al combustion.

B. Thick Binder (300 μm)

1. 1000 psi. Little combustion of Al was seen; aluminized char was left at the end of the test.

2. 800 psi. At this pressure there was little evidence of Al combustion.

3. 500 psi. At this pressure there was little evidence of Al combustion.

4. 300 psi. Oscillating flame as described for the thin binder case was apparent.

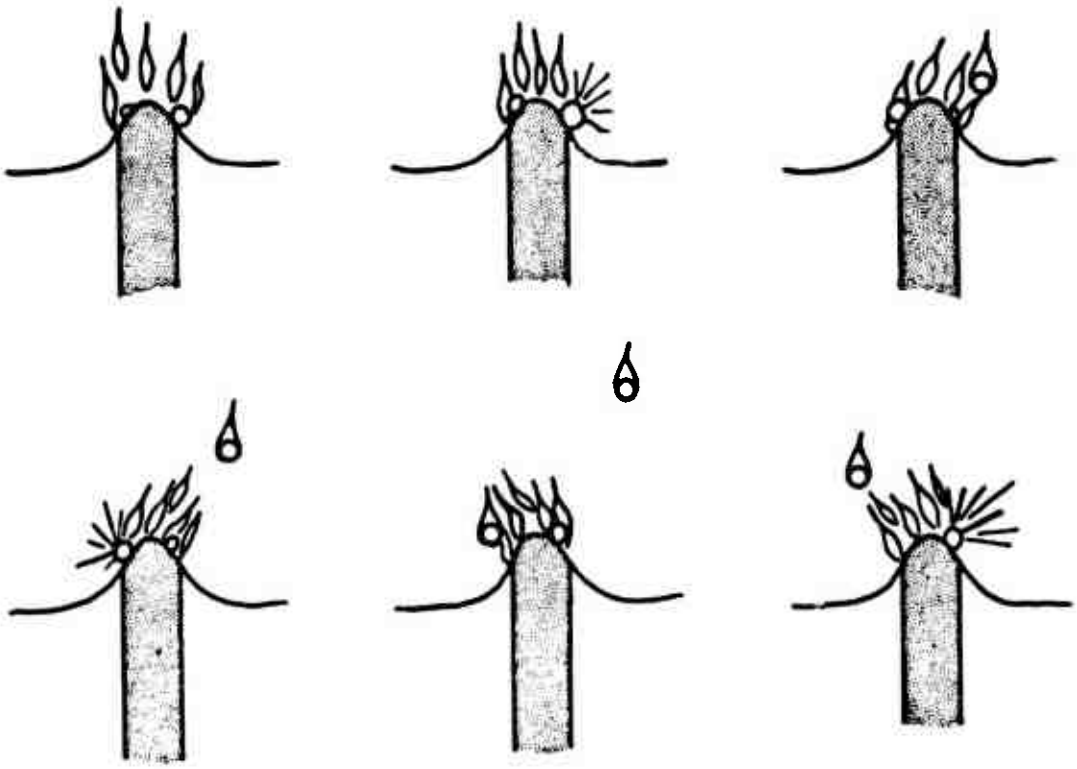

FIG. 4.6. Profile of Sandwich With 50% HTPB/50% 5 μm As-Received Al Burning at 800 psi.

V. 95% HTPB/5% 5 μm AS-RECEIVED Al

A. Thin Binder (25 μm)

1. 1000 psi. Slight accumulation of Al occurred on binder. When accumulates were formed near AP-binder interface they ignited and burned.

2. 800 psi. So little Al burned that the impression was that the binder was unaluminized. What Al did burn ignited on the AP side of the diffusion flamelets.

3. 500 psi. Very little Al combustion was evident.

4. 300 psi. Very little Al combustion was evident.

B. Thick Binder (300 μm)

1. 1000 psi. Accumulation of Al took place on binder. Aluminum ignited near AP interface. Accumulates also ignited when they protruded into the oxidizer rich area adjacent to the flamelets.

2. 800 psi. Aluminum accumulated on binder and caused the oscillating flame as described for the 10% Al/thin binder cases.

3. 500 psi. The combustion was similar to the 800 psi case.

4. 300 psi. The combustion was similar to that above but with the fluctuations less pronounced.

The above data describe the combustion behavior of the sandwiches incorporating as-received Al with changes in ambient pressure, binder thickness and Al loading. The material which follows describes how changing the type of Al affects the behavior; the following descriptions are for the combustion of sandwiches incorporating preoxidized Al.

VI. 50% HTPB/50% 5 μm PREOXIDIZED Al

A. Thin Binder (25 μm)

1. 1000 psi. Some accumulation occurred but by the violence and amount of combustion it appeared that the accumulates ignited, but did not agglomerate. Rather the accumulates (< 200 μm diameter) appeared to be blown apart at ignition to many finer particles. Another noticeable difference, when compared to the as-received material, was the location and intensity of ignition. Contrary to the ignition of the as-received Al, the ignition of the preoxidized material occurred in the flame, not on the surface, and the combustion became fully developed, as evidenced by the white oxide tail, well within the field of view. The flames were all white, not white flashes in otherwise orange hydrocarbon-AP flames seen for the as-received Al cases.

2. 800 psi. At this pressure the combustion was similar to the 1000 psi case but with more accumulation of Al on the binder. Upon ignition many fine particles (≈ 35 μm) were formed.

3. 500 psi. The most noticeable feature was an alteration in flame color between the orange hydrocarbon-AP diffusion flame and the white flame characteristic of hot Al_2O_3. From the violence and rapidity of ignition it

appears that the accumulates did not always agglomerate at ignition but instead often fragmented into smaller, faster burning particles. In one sequence an extremely large (3600 μm) accumulate ignited with a big flash resulting in many small (≈ 70 μm) burning particles. The scene was reminiscent of fireworks on the Fourth of July holiday. The agglomerates which were formed from the preoxidized Al were smaller (the largest agglomerate seen was approximately 250 μm in diameter) than for the as-received Al.

4. 300 psi. The main characteristic at these conditions was an increase of the instability described above. There were blinding flashes of Al, as accumulates ignited and were rended apart, followed by frames showing no Al combustion, just the orange hydrocarbon-AP flame.

5. 100 psi. The flashing indicative of Al combustion followed by no Al combustion for approximately 0.045-0.15 seconds, then flashing, etc., was again apparent. The principle difference here was that at this pressure it appeared that the Al was igniting out on the AP (up to 400 μm from the original AP-binder interface).

B. Thick Binder (300 μm)

1. 1000 psi. There was very little combustion of Al. In fact, the preoxidized material seemed to act as a heat sink as evidenced by the sharp increase in slope at the interface in going from the AP surface to the binder.

2. 800-, 500-, 300 psi. The behavior for these tests was identical to the 1000 psi behavior.

COMBUSTION OF PROPELLANTS INCORPORATING AS-RECEIVED AND PREOXIDIZED Al

The differences seen in the sandwich combustion also were seen when a 12.3% HTPB, 17.5% Al (5 μm) and 65% AP (200 and 400 μm) propellant was burned. At 100 psi agglomeration occurred for the propellant containing the as-received Al (agglomerate size ≈ 200-500 μm) while the agglomerates coming from the propellant containing preoxidized Al (many fewer) were smaller (≤ 150 μm) and more fines were burned in the latter case. The as-received Al agglomerated to larger size and resided on the surface longer, continuing to grow in size. In one sequence, which was not atypical, a small agglomerate grew on the surface from about 70 μm to about 220 μm diameter in approximately 0.012 seconds.

At 350 psi more Al combustion occurred with the combustion of more fine particles for both propellants; the agglomerates were roughly the size found at 100 psi--200 to 500 μm for the as-received material.

At 800 psi there is again increased Al combustion for both propellants. Once again the as-received material agglomerates (to the same size but not to the degree seen at lower pressures) much more than did the preoxidized material. The combustion zone above the propellant containing preoxidized Al had the appearance of a sheet of oxide flame, making measurement of agglomerate size (which was approximately the same as at lower pressure) difficult.

DISCUSSION

The behavior of Al has been shown to be strongly affected by: (1) the environment in which the Al finds itself--on the AP, in a binder region or in the gas phase, (2) the quality and quantity of the oxide surrounding the Al, (3) the number of Al particles present, and (4) the prevailing flame structure.

Considering first the environment, this study conclusively shows the importance of the surroundings on the Al behavior, especially for the cases using as-received Al. The binder used in this study, HTPB, has a viscous melt at the regressing surface (as do the other binders described in Section 2). The liquid phase allows Al powder to accumulate on this sticky surface. What happens to the accumulate is then a function of its location on this molten material relative to the AP and the many spatially and temporally variant flamelets. If the accumulate is near the binder-AP interface several events are possible.

1. The accumulate can, if of sufficient size, project into the oxidizer-rich area adjacent to a flamelet. Should this occur, the accumulate will ignite, forming an agglomerate. If the ignition can be sustained the burning agglomerate will detach from the binder and burn as a large (compared to the original Al particles) particle.

2. Accumulates which are able to leave the binder surface quickly encounter one of the many temporally and spatially variant flamelets (see Section 2). The accumulates ignite on the oxidizer rich side of the flamelets. Concomitant with the ignition, agglomeration occurs and once again the burning of a large particle is seen.

3. With the unsteady nature of the flamelets, it is possible that an attached accumulate be "washed" by a flamelet. When the oxidizer rich area of the flamelet contacts the accumulate both prerequisites for ignition--oxidizing species and high temperature--are met. With the ignition, agglomeration occurs and a large burning particle is formed.

4. Yet another mechanism is possible. This involves flow of the molten binder carrying Al out onto the AP. When the binder pyrolyzes, the Al is left on the AP. This possibility will be further discussed in the section dealing with the existence of Al on AP.

Should the Al be located in a binder area not in the proximity of AP, nor the diffusion flamelets, the possibilities for reaction are not as numerous. The accumulate keeps growing in size until it is either sloughed off and burns remote from the surface (if it burns at all), or until flamelets finally wash over the accumulate and cause ignition (or in the case of a propellant, the binder is "fried" through so that an oxidizer particle is exposed). In both cases the accumulates formed in this manner are order of magnitude larger than those formed near the AP-binder interface. If the particles have a long residence time on the binder and if they are sufficiently heated, another possibility is that the particles will coalesce to form an agglomerate on the binder surface rather than the accumulates discussed above.

From the above discussion it is clear that one of the prime causes of Al accumulation/agglomeration is the molten nature of binder. Since all of the binders tested in Section 2 displayed a molten layer, for propellants using these binders the way to decrease the agglomeration caused by the binder is to reduce the size of binder "patches" available to serve as accumulation sites. To do this one would have to change the AP particle size thereby disturbing the "pocket size of the binder" (Ref. 15) and also the distribution and size of the flamelets.

The sandwich results indicate that Al can exist on the surface of the AP without igniting. This happens because the temperature at the AP surface is not high enough ($T_{SAP} < 600°C$) to rupture the protective oxide coating on the AP. In the case mentioned earlier, where the molten binder flow carried Al out onto the AP, the binder pyrolyzed leaving the Al on the AP. Ignition did not occur while the Al was on the AP. It was not until the Al left the AP surface and encountered one of the diffusion flamelets that the accumulate ignited. Upon ignition, the accumulate formed an agglomerate. In the propellant case Al can exist on the AP if the oxidizer particle size is large because of its isolation from a high temperature source. Indeed samples of propellant quenched from burning often show Al particles on AP particles (Ref. 43 and 44). Thus large diameter AP particles provide another accumulation site. Again the degree of accumulation/agglomeration can be reduced by simply going to a smaller AP particle size.

The relative amount and size of ingredients and the concomitant flame size and structure are also determining factors, as was shown in the sandwich work. The sandwich work shows a more pronounced agglomeration at high pressure (800 and 1000 psi) than at 500 psi. This appears to be contrary to the propellant results where as the pressure was increased, the amount of agglomeration decreased. Although not immediately obvious, the anomaly is self-consistent with our understanding. At the higher pressure and the sandwich configuration, the AP regresses more rapidly than the

binder leaving a protruding binder. More area for agglomeration is provided and this area is further from the diffusion flamelets (especially for the thick binder cases): both conditions are ideal for increased accumulation/agglomeration. In the propellant case the amount of binder exposed and the number and location of flames are controlled by propellant heterogeneity; there is no chance for large protrusions of binder to be formed, and for the Al to be very far from a flamelet. Also, in the propellant configuration as the pressure is increased the propellant burns faster providing less residence time for Al on the binder, and since the accumulation/agglomeration is a slow process we might expect to find less agglomeration and more combustion as the pressure increased. Yet another consequence of pressure increase would be the existence of the flamelets closer to the propellant surface, providing better energy transfer to the solid.

Just as pressure can alter the relative position and amounts of ingredients and flames, the same can be achieved by changing the oxidizer particle size (as has previously been discussed in Ref. 15). Small sized oxidizer particles would decrease the size of binder patches, increase the number of flamelets (thereby increasing the proximity of any Al to a flamelet) and increase the burning rate. All of these changes would contribute to decreasing the amount of accumulation/agglomeration. Thus it can be seen that changes in propellant formulation can not only change ballistic determinants such as burning rates, but also change the accumulation/agglomeration of Al.

The importance of the quantity and quality of oxide coating was amply demonstrated in this program with the comparison of as-received and preoxidized Al. Although both types of Al agglomerated, the extra thickness of oxide coating on the preoxidized material was more protective and resulted in smaller diameter agglomerates than did the as-received material. But it should also be noted that the tests with preoxidized Al and sandwiches having thick binder layers indicated that preoxidized Al, in and of itself, is harder to ignite than the as-received material. This was amply demonstrated by the preoxidized Al not igniting on the sandwich surface as did the as-received material. This disadvantage is somewhat offset by forming smaller, therefore easier to ignite, agglomerates.

Based on the success in reducing agglomerate size by changing the characteristic of the oxide coating, other efforts to change the oxide should be explored. Reference 42 has briefly explored the changes caused by using dichromated Al and found this treated Al to decrease the size of agglomerates and to ignite closer to the propellant surface.

Another consideration affecting the amount of agglomeration is simply the loading level. If less Al is available less accumulation/agglomeration occurs although it is interesting to note that in the sandwich cases the samples having low Al loading displayed severe instabilities in the gas phase. Price has presented other such phenomena under the general label of "phase correlation" (Ref. 53-57).

SUMMARY AND RECOMMENDED FUTURE WORK

1. The accumulation/agglomeration behavior of Al during combustion is strongly influenced by:

A. The environment--binder, AP, and presumably the decomposition products--surrounding the Al.

(1) Aluminum residing on areas of AP will not readily ignite. Particles of as-received Al will sinter together in this environment while particles of preoxidized Al do not readily bond together.

(2) The behavior of Al existing on areas of binder is characterized by accumulation/agglomeration. If as-received Al is on an area of binder subject to high heating (but not oxidizing species) agglomeration will occur via a coalescence. If the as-received Al is on a binder area subject to low energy flux, accumulation (not agglomeration) will occur. The resultant accumulates must be subject to higher heating rates to agglomerate and to both high energy flux and oxidizing species to ignite (often ignition and agglomeration of an accumulate are concomitant). Since the binder provides the "stickiness" prerequisite for the long residence times of the Al, it is anticipated that the "drier" the binder, the less accumulation/agglomeration would result.

B. The quality and quantity of oxide coating. The as-received and preoxidized Al behaved differently. The difference between the two powders is that the preoxidized Al has an oxide layer approximately five times thicker than does the as-received material.

C. The loading level and particle size of the Al. High loading level and small particle size means that there are many adjoining Al particles, and that accumulation/agglomeration would be increased.

D. The prevailing flame structure. The behavior of the accumulation/agglomeration was markedly different depending on whether the pressure was above or below the low pressure deflagration limit of the AP. This was due to the differences between the candle-like diffusion flame seen at low pressures and the turbulent diffusion flamelets seen at high pressures.

2. The findings of this investigation can be used to guide the propellant manufacturer if agglomeration is to be reduced. The findings are listed below in chart form.

Change	Manifestation	Al Behavior
Increase oxidizer particle size	Decrease burning rate, increase size of binder patches	Increase agglomeration
Increase pressure	Increase burning rate, decrease flame stand-off	Decrease agglomeration, more ignition
Increase Al loading	Provide more adjoining Al particles	Increase agglomeration
Increase oxide coating thickness		Decrease agglomeration slightly harder to ignite
Increase oxidizer content	Decrease binder, increase burning rate	Decrease agglomeration
Change binder	All binders liquid, only change viscosity	Not much change

3. Attempts to change the Al particle coating should be made. Processes which would alter the strength, chemical reactivity, permeability and melting point of the oxide should be studied.

4. The preoxidized Al can significantly suppress agglomeration. The mechanism for the reduction seems to be linked with the increased strength of the oxide layer. Agglomerates do not readily form at the propellant surface, presumably because the oxide skin is not as easily rended as is that for the as-received Al--the oxide is more protective for the preoxidized Al case.

Acknowledgement

The authors would like to acknowledge the efforts of Dr. Karl Kraeutle, NWC, who was responsible for manufacturing the preoxidized Al and who made the propellants whose combustion behavior is described in Section 4.5. Dr. Kraeutle and Mr. Zurn, using cinephotomicrography, observed the combustion of these propellants at 350 psi. These same propellants were examined under the present program at 100, 350 and 800 psi.

SECTION 5

ANALYTICAL MODELING OF SANDWICH COMBUSTION

W. C. Strahle
Georgia Institute of Technology

NOMENCLATURE

b	Pyrolysis constant
c_p	Heat capacity of gas phase (at constant pressure)
c_s	Heat capacity of solid phase
E	Activation energy
f	Distribution of gas phase temperature of Eq. (22)
g	Dimensionless temperature
n, s	Coordinates
p	Pressure
q	Dimensionless phase transition (+ if endothermic) or gas phase heat release, $\frac{q^*}{c_p T_o}$ (+ if exothermic)
$\dot{q}$	Dimensional heat release rate per unit volume
R	Universal gas constant
Re	Reynolds number
r	Burn rate
$\dot{r}_{AV}$	Experimental average vertical regression rate
$r_{AV} \cos \theta$	Experimental average regression rate normal to the surface on the AP surface from the binder

T	Temperature
v	Vertical velocity of gas phase
Y	Mass fraction
x, y	Cartesian coordinates
z	$\sqrt{1 + (dy_s/dx)^2}$
α	Thermal diffusivity (or see below)
α, β	Constants due to f distribution
δ	Thickness
ϵ	Dimensionless activation energy, E/RT_o
η	c_s/c_p
θ	Angle between the surface parallel and the horizontal
κ	Curvature, $(d^2y_s/dx^2)/[1 + (dy_s/dx)^2]^{3/2}$
λ	Thermal conductivity
ξ	$\lambda_s c_p/\lambda_g c_s$
ρ	Density
τ_r	Reaction time

Subscripts

AP	Ammonium perchlorate
F	Fuel or NH_3 in the case of AP deflagration
f	Flame
g	Gas
s	Solid phase or gas-solid interface
o	Cold "soak" temperature
v	Vertical

Superscripts

*	Dimensional quantity
'	Differentiation with respect to x
→	Vector quantity

MODEL CONSTRUCTION AND ASSUMPTIONS

Although a rudimentary picture of aandwich deflagration wa. presented in Section 2, it would be desirable to have a reasonably complete analytical model to aid in interpreting results from experiments and to quantitatively establish the magnitudes of physicochemical parameters required to produce observed effecta. Even in the apparently benign two-dimensional configuration, however, the problem is highly complex due to (1) an initially unknown surface shape coupled with inability to precisely determine the position of the leading edge of the regreasion, (2) nonlinearities in the equations due to chemical reaction and the unknown surface, (3) two phase heat transfer, (4) multiple chemical reactions, and (5) a mathematically elliptic problem which reverts to a parabolic problem asymptotically away from the binder-oxidizer (BO) interface (as will become apparent later).

The maximum use of experimental information in the conatruction of the model is sought which still does not restrict the uaefulness of the model in understanding experimental results. Accordingly, there have been several observations which have been used:

1. Far from the BO interface the AP regresses as pure AP. Consequently, the initial model development ia concerned with a semi-infinite slab of AP against a semi-infinite alab of binder.

2. A steady state is achieved experimentally with AP oxidizer. Consequently, time dependence is assumed absent.

3. Viewed from the gas phase toward the solid phase, any curvature of the surface is concave on average. This will influence the choice of coordinate system.

4. The experimental results indicate very little effect of the gas phase binder-oxidizer reactiona upon the aurface profile unless catalyats are employed. Consequently, the initial model concerns itself with alow reactiona (although the neceaaary magnitudes for these reactions to be important is investigated). Catalyst behavior is not inveatigated here.

Since (1) above implies that a boundary condition far out on the oxidizer surface is a pure AP deflagration process, but the main purpose is to investigate the effects of the BO interface phenomena, a very simple AP model is employed. The Guirao-Williams (Ref. 58) model is basically accepted which will limit the pressure range from 20-100 atm. This model will be slightly modified as outlined below. The concern is not with AP itself, and, in any event, there is no model accepted as yet above 100 atm. Actually the 100 atm upper limit is perhaps too severe and for qualitative sandwich analysis purposes the model is adequate to 2000 psia, where a distinctly different deflagration mechanism for AP appears. One of the major modifications is that a pyrolysis law will be used for the AP surface; whereas, it is generally accepted that the AP liquid-gas interface is in equilibrium (Ref. 58). The reason for the present assumption is that it is computationally easier to treat and it more readily yields certain BO interface relationships. While it is not believed that these will be strongly modified by an equilibrium assumption, there is as yet no proof; and a later investigation will treat the equilibrium case.

For the lack of any better information a simple pyrolysis law will be used for the binder solid (or liquid)-gas transition which is pressure independent. Furthermore, no effects of binder melts are considered in this initial treatment.

Other assumptions are made to simplify the analysis which, while they lead to numerical errors of order unity, do not alter significantly the scaling rules developed with respect to other variables. These assumptions are:

1. The thermal and transport processes of the solid AP and binder are identical.

2. The thermal and transport properties of all gas phase species are idential.

3. The Lewis number is everywhere unity in the gas phase.

4. The deflagration process is a constant pressure process.

5. Heat conduction and mass transfer take place by temperature and concentration gradients only, respectively, and the transport coefficients are independent of temperature in both the solid and gas phases.

A final major assumption is that on any vertical line parallel with the sandwich axis the ρv product in the gas phase is as determined at the gas solid interface and all lateral velocities are zero. This is in the spirit of the Burke-Schumann approximation as expounded in Ref. 59. This does yield error in convection effects upon heat transfer and in

actual location of flames, but is too complex to treat here. The assumption may be relaxed by future analysis.

The configuration is shown in Fig. 5.1, in which the coordinate system is rendered stationary by a translation of the interface in the y direction at the rate r. Under the stated assumptions the equations for solution and the boundary conditions are:

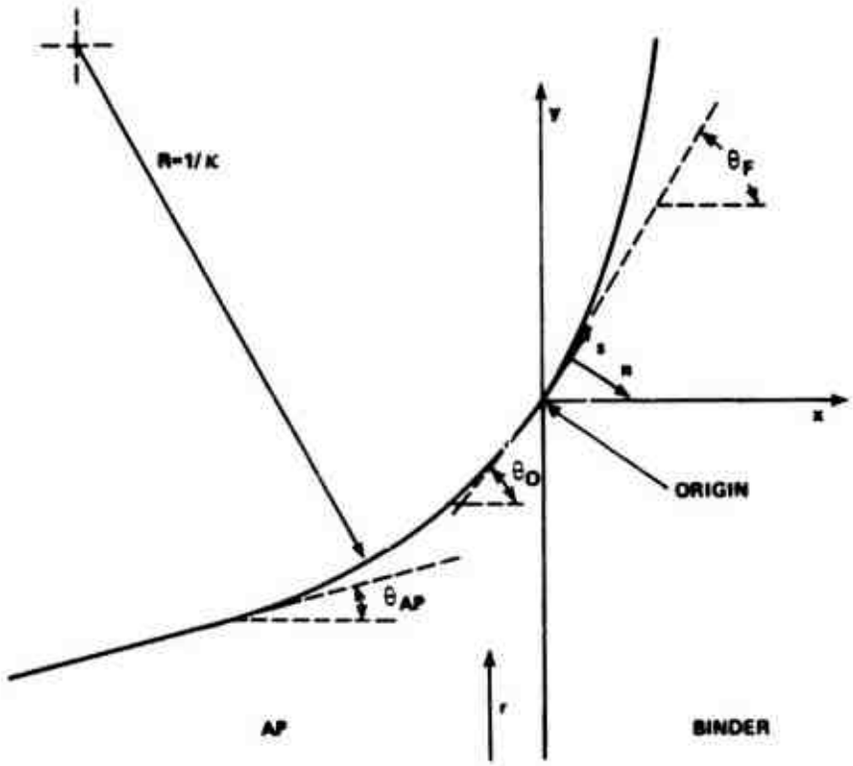

FIG. 5.1. Sandwich Schematic.

Gas Phase

$$\lambda_g\left(\frac{\partial^2 T}{\partial x^{*2}} + \frac{\partial^2 T}{\partial y^{*2}}\right) = \rho v c_p \frac{\partial T}{\partial y^*} - \dot{q}^* \qquad (1)$$

Solid Phase

$$\lambda_s\left(\frac{\partial^2 T}{\partial x^{*2}} + \frac{\partial^2 T}{\partial y^{*2}}\right) = \rho_s r c_s \frac{\partial T}{\partial y^*} \qquad (2)$$

Boundary Conditions

$$T(y^* \to -\infty,\ x^* \text{ fixed}) = T_o$$

$$T(y^* \to \infty,\ x^* \to -\infty) = T_{AP_f}$$

$$T(y^* \text{ fixed},\ x^* \to \infty) = T_o$$

$$T(y^* \text{ fixed},\ x^* \to -\infty) = T_o \text{ if } \theta_{AP} < 0 \text{ or } = T_{AP_f} \text{ if } \theta_{AP} > 0$$

$$\vec{r}\cdot\vec{n})_F = b_F e^{-E_{sF}/RT_s(x^*)}$$

$$\vec{r}\cdot\vec{n})_{AP} = b_{AP} e^{-E_{sAP}/RT_s(x^*)}$$

$$\rho_s r = \rho(y^* = y_s^*(x^*),\ x^*)\ v(y^* = y_s^*(x^*),\ x^*)$$

$$-\lambda_g \frac{\partial T}{\partial n^*}\Big) = \rho_s r\ q_s^* - \lambda_s \frac{\partial T}{\partial n^*}\Big)_{s_s} \tag{3}$$

T everywhere continuous
∇T continuous within a given phase

Equations 1-3 are incomplete in that $\dot{q}^*$, which accounts for heat generated by combustion, requires specification of mass fractions of all pertinent species, with attendant differential equations and boundary conditions required. For clarity of presentation and because of future developments these are omitted. The energy conservation conditions of Eq. 3 undergoes a discontinuity at $x = y = 0$ because q_s^* is discontinuous. Typical numbers used are

$T_o = 300°K$	$\lambda_g = 2.0 \times 10^{-4}$ cal/cm°K sec
$\rho_s = 1.95$ gm/cm^3	$\lambda_s = 1.2 \times 10^{-3}$ cal/cm°K sec
$c_s = 0.275$ cal/gm°K	$c_p = 0.3$ cal/gm°K
$q_{s_{AP}}^* = -120$ cal/gm	$q_{s_F}^*$ is [100 - 1000 cal/gm]
$E_{s_{AP}} = 30{,}000$ cal/mole	E_{s_F} is [3 - 6 x 10^5 cal/mole]

All heat of phase transition in the AP and the exothermic heat of transition to a liquid layer are included in $q^*_{s_{AP}}$, as well as the gasification heat. The orders of magnitude of $q^*_{s_F}$ and E_{s_F} are taken from the work of Varney.

NONDIMENSIONALIZATION OF THE EQUATIONS AND THE CHARACTERISTIC SCALES

The most convenient unit for length to take in the analysis is the one natural to Eq. 2. This is $\lambda_s/\rho_s c_s r = \alpha_s/r$, which contains the eigenvalue of the problem, r, the unknown sandwich regression rate. If r is near the regression rate of AP, then this length unit is known to be very close to the thermal wave depth in the solid AP. Taking 800 psia to be representative with $r_{AP} = 1.1$ cm/sec the characteristic length dimension has the magnitude $\alpha_s/r_{AP} = 2 \times 10^{-3}$ cm = 20 μ. Recall, however, that by definition $r \geq r_{AP}$ so that the actual distance scale will be slightly smaller than the one computed using r_{AP}. The characteristic temperature chosen is T_o so that Eq. 1-3 become, using $\rho_s r = \rho v$,

Gas

$$\frac{\partial^2 g}{\partial x^2} + \frac{\partial^2 g}{\partial y^2} = \xi \frac{\partial g}{\partial y} - \xi^2 \left(\frac{\dot{q}^*/\rho_g}{c_p T_o v}\right) \frac{\lambda_g}{\rho_g v c_p} \tag{4}$$

Solid

$$\frac{\partial^2 g}{\partial x^2} + \frac{\partial^2 g}{\partial y^2} = \frac{\partial g}{\partial y} \tag{5}$$

Boundary Conditions

$$g(y \to -\infty, x \text{ fixed}) = 1 \qquad g(y \to \infty, x \to -\infty) = g_{AP_f}$$

$$g(y \text{ fixed}, x \to \infty) = 1 \qquad g(y \text{ fixed}, x \to -\infty) = 1 \text{ if } \theta_{AP} < 0$$

$$= g_{AP_f} \text{ if } \theta_{AP} > 0$$

$$\left(\frac{1}{z}\right)_F = \frac{b_F}{r} e^{-\varepsilon_{s_F}/g_s} \qquad \left(\frac{1}{z}\right)_{AP} = \frac{b_{AP}}{r} e^{-\varepsilon_{s_{AP}}/g_s} \tag{6}$$

$$-\left(\frac{\partial g}{\partial n}\right)_{s_g} = \xi \left[q_s - \eta \left(\frac{\partial g}{\partial n}\right)_s\right]$$

g everywhere continuous; ∇g continuous within a phase

The parameter ξ in Eq. 4 is nothing more than the ratio of the characteristic solid phase dimension, α_s/r, to the characteristic gas phase dimension, α_g/v. Numerically $\xi = 6.55$, which indicates the first rather large disparity of characteristic dimensions which will be encountered. ξ would disappear everywhere from Eq. 4 if α_g/v were being used as the basic dimension rather than α_s/r. The significance of ξ is that, if other influences were absent, all important phenomena of heat transfer would take place in the gas phase in a region which has a characteristic (dimensionless) dimension of the order of $1/\xi$.

Now in Eq. 5 $\dot{q}^*/\rho_g$ is a heat release rate per unit mass in the gas phase and behaves like a heat release per unit mass divided by a reaction time. Thus,

$$\frac{\dot{q}^*/\rho_g}{c_p T_o v} = \left(\frac{q^*}{c_p T_o}\right) \frac{1}{\tau_r v}$$

which is a dimensionless heat release divided by a characteristic reaction distance in the gas phase. Consequently, the last term of Eq. 4 is of the same order of magnitude as the other terms only if

$$\frac{q^*}{c_p T_o} \left(\frac{1}{\tau_r v}\right) \text{ is } \left(\frac{\xi}{\alpha_s/r}\right)$$

that is, if the ratio of the characteristic heat transfer dimension is of the same order as the dimension required for chemical reaction. Consider, then, reactions between the binder and oxidizer, for which $q^*/c_pT_o \approx 11$. At 800 psi, $v \approx 165$ cm/sec so that unless

$$\tau_r \leq \frac{\alpha_s/r}{v\xi} \frac{q^*}{c_p T_o} = 2 \times 10^{-5} \text{ sec}$$

heat release due to reaction will not be important within a distance of the order of $1/\xi$ of the interface, where the dominant heat transfer processes are occurring in the gas phase. As will be seen later, the pure AP flame is not this fast. Viewing the propane-O_2 data of Ref. 60 hydrocarbon oxidation times are only marginally this fast in the temperature environment seen here. Consequently, it appears that, in accord with experiments for uncatalyzed situations, the BO flame may not be important near the interface and only the heat transfer processes from the hot AP gases may be important in determining the details near the interface. Therefore, the initial model attempt will not consider BO reactions.

It will be seen later that the standoff distance of the AP deflagration flame is of the order of $2/\xi$ to $4/\xi$. Now the Reynolds number based upon vertical distance from the BO interface is

$$Re = \frac{\rho_g v y^*}{\mu} \approx \frac{\rho_g v y^*}{\lambda_g / c_p} = \xi y$$

Consequently, when y is θ $(1/\xi)$ there is the start of a transition from low to high Reynolds number flow. It is known from Ref. 61, and is reasonably obvious from experience with boundary layer flows, that Eq. 4 becomes of parabolic type as $Re \to \infty$. If this occurs, there is no influence of what happens at large y on small y events. Consequently, the interface is not influenced by what happens. Equations 4 and 5 are elliptic as they stand and every point in the field influences every other point, but this character will change at large y. The entire sandwich problem is therefore of mixed parabolic-elliptic type with only a region of the order of $1/\xi$ units thick in the gas phase influencing the interface.

Summarizing, the heat transfer processes in the solid phase take place one unit of thickness into the solid phase; the BO interface is influenced primarily by heat transfer from the reacting AP decomposition products; and at vertical distances where the AP deflagration is completed, the gas phase problem has become parabolic in nature. The BO reactions may as a first approximation be neglected in the elliptic region for uncatalyzed cases.

THE AMMONIUM PERCHLORATE FLAME

The pure AP flame forms a boundary condition at $x \to -\infty$ and must be treated. Following Culick's procedure (Ref. 62) of assuming a flame standoff distance determined by a reaction time of the form given by Guirao and Williams (Ref. 58), and using the surface pyrolysis law mentioned in Eq. 3, a solution to Eq. 4 and 5 may easily be constructed. The only difficulty is with the assumption that the gas flow is vertical while the AP surface is inclined at θ_{AP}.

NH_3 and $HClO_4$ are considered as the decomposition products emanating from the liquid AP layer. For convenience they are considered molecules of the same molecular weight. Since the reaction time is first order with respect to each of these species (Ref. 60) a mass fraction equation must be added to Eq. 4. This is

$$\frac{\partial^2 Y_F}{\partial x^2} + \frac{\partial^2 Y_F}{\partial y^2} = \xi \frac{\partial Y_F}{\partial y} \tag{7}$$

with the boundary conditions

$$-\left(\frac{\partial Y_F}{\partial n}\right)_s = \frac{\xi}{z}\left(\frac{1}{2} - Y_{F_s}\right)$$

$$Y_F(n = n_f) = 0 \tag{8}$$

The solution to Eq. 4, 5 and 7 subject to the appropriate boundary conditions is

Gas Phase

$$g - g_s = [q_{s_{AP}} + \eta(g_s - 1)]\, e^{-\xi/z_{AP}n} \qquad n \le n_f$$

$$Y_F = Y_{F_s} e^{-\xi/z_{AP}n} + \tfrac{1}{2}(1 - e^{-\xi/z_{AP}n}) \qquad n \le n_f$$

$$g_{AP_f} = g_s + q_{g_{AP}} - q_{s_{AP}} - \eta(g_s - 1) \tag{9}$$

Solid Phase

$$(g - 1) = (g_s - 1)\, e^{-n/z_{AP}} \tag{10}$$

Flame Standoff and Surface Condition

$$-n_f = \frac{z_{AP}}{\xi} \ln\left[\frac{q_{g_{AP}} - q_{s_{AP}} - \eta(g_s - 1)}{q_{s_{AP}} + \eta(g_s - 1)}\right] \tag{11}$$

$$y_f = -n_f z_{AP} \tag{12}$$

$$\tau_r = \frac{k_{AP}}{pY_{F_s}^2} = \frac{y_f^*}{\nu} = \frac{y_f\, \alpha_s}{r^2}\left(\frac{\rho_g}{\rho_s}\right) \tag{13}$$

$$Y_{F_s} = \tfrac{1}{2}\left[1 - e^{\xi/z_{AP}n_f}\right] \tag{14}$$

$$\frac{1}{z_{AP}} = \frac{b_{AP}}{r} e^{-\epsilon_{s_{AP}}/g_s} \tag{15}$$

This model may now be forced to fit the AP burn rate curve by investigating the case of horizontal gas-solid interface where $z_{AP} = 1$ and $r = r_{AP}$. At 800 psia the surface temperature is assumed to be 800°K. From Eq. 15 b_{AP} is found to be 1.738×10^8 cm/sec. For an overall exothermicity of the AP deflagration of 320 cal/gm and the assumed $q_{s_{AP}}^* = -120$ cal/gm, $q_{g_{AP}} = 200$ cal/gm. Equation 11 then yields $-n_f = y_f = 2.34/\xi$ which forms the basis for the previous remarks about the scale of the AP flame standoff. For $z_{AP} > 1$ the vertical standoff is larger because the vertical velocities are larger to accommodate the larger mass flow for a fixed horizontal area. From Eq. 14 $Y_{F_s} = .451$ and finally k_{AP} is calculated from Eq. 13 as $k_{AP} = 4.87 \times 10^{-5}$ sec atm. For any other surface temperature, r is calculated from Eq. 15, n_f from Eq. 11, Y_{F_s} from Eq. 14 and p from Eq. 13 yielding a unique pressure-burning rate curve which is known to match the experimental curve quite well (Ref. 63), below 2000 psia.

In any sandwich model Eq. 9 and 10 are boundary conditions on the temperature field far from the BO interface.

SURFACE AND INTERFACE CONDITIONS AND A SANDWICH PARADOX

From the pyrolysis conditions of Eq. 6 an interesting set of relations arises. Differentiating, the curvature becomes

$$n = \frac{-g_s' \quad \epsilon_s}{\frac{dy_s}{dx} g_s^2} \tag{16}$$

Equation 16 relates the radius of curvature of the surface to the derivative of the surface temperature along the interface. In this relation the coordinate relation $dx/ds = 1/z$ has been used. Equation 16 requires that for the surface to be concave viewed from the gas that either g_s increases with s when $dy_s/dx < 0$ or g_s decreases with s when the surface slope is positive. All sandwiches viewed by Varney had positive slope and positive or near zero n at the BO interface, and it may be concluded, assuming the pyrolysis law is valid, that the surface heat transfer

along s is from the AP into the binder, as was predicted by Hightower and Price (Ref. 16).

The detailed interface photography by Varney confirmed the Hightower and Price assertion that there was little evidence that the surface slope at the sandwich interface is discontinuous.[3] If, however, the binder and AP are undergoing independent pyrolysis laws, the temperature is continuous at the interface, and, of course, the vertical regression rate is the same for the binder and oxidizer, it may readily be shown that a continuous slope is impossible. This will be referred to as the "sandwich paradox".

The reason for this paradox lies in the behavior of the energy conservation law at the surface. It must be demanded by the Fourier conduction law that a unique, continuous heat transfer vector exists in the gas phase. This is shown in Fig. 5.2. This heat transfer vector provides the heat of gasification of both the AP and binder at the interface. It must also be demanded that a unique heat transfer vector exists in the solid at the interface. Now in the AP the difference between $\vec{q}_g$ and $\vec{q}_s$ in the direction of $\vec{n}_{AP}$ goes toward providing the (negative) heat of gasification. The component parallel to the surface merely represents heat transport in the $\vec{s}$ direction at the surface. Similarly, the difference between $\vec{q}_{gas}$ and $\vec{q}_s$ in the direction of $\vec{n}_s$ must provide the (positive) heat of gasification of the binder. If $\vec{n}_s$ and $\vec{n}_{AP}$ were parallel (a continuous surface slope), an impossible situation would occur because the two heats of gasification are different. Consequently, the analytical model must allow a discontinuous slope.

Possible reasons for this apparent paradox are:

1. It is not possible to tell with the naked eye whether or not there is truly a continuous slope in Varney's photographs.

2. A post quench binder melt run obscures the actual burning configuration.

3. The possibility exists of heterogeneous attack on either the binder or oxidizer (they do not pyrolyze independently).

4. The assumptions used in formulating the analysis such as equilibrium at the AP-gas interface, or the gas phase provides all the heat of vaporization of the AP and binder, may alter the above reasoning. The

[3] Editor's note: It is doubtful whether the optical micrographs of quenched samples by either Hightower or Varney had sufficient resolution to truly resolve this question. In fact some of the traces taken of scanning electron micrographs of the interface show that the above conclusion does not always apply (see Section 2).

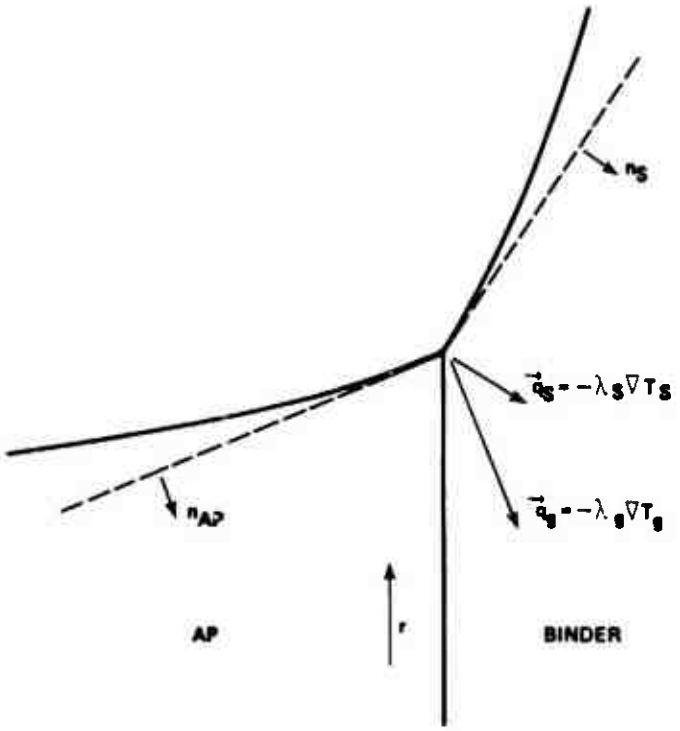

FIG. 5.2. Heat Transfer Conditions at the Binder-Oxidizer Interface.

last reason will be investigated in future work. Presently, however, it will be accepted under the conditions of the analysis that the slope must be discontinuous.

If it is presumed that along the $\vec{n}_{AP}$ line the temperature profile looks like

$$g - 1 = (g_s - 1)\, e^{-n/\delta_{AP}} \tag{17}$$

and along the $\vec{n}_F$ line

$$g - 1 = (g_s - 1)\, e^{-n/\delta_F} \tag{18}$$

then an exact solution to Eq. 5 may be found. Assuming

$$(g - 1) = (g_s - 1)\, e^{-\alpha x} e^{\beta y} \tag{19}$$

in Eq. 5 yields the condition that

$$\alpha^2 + \beta^2 = \beta \; ; \; \alpha \text{ and } \beta \text{ positive} \tag{20}$$

In order that Eq. 19 satisfies Eq. 17 and 18 along the appropriate normal vectors, it is required that

$$\alpha + \beta \left(\frac{dy_s}{dx}\right)_{AP} = \frac{z_{AP}}{\delta_{AP}}$$

$$\alpha + \beta \left(\frac{dy_s}{dx}\right)_{F} = \frac{z_F}{\delta_F} \tag{21}$$

From Eq. 6, if g_s and r are specified, dy_s/dx and consequently the z's are specified. Equations 20 and 21 are three equations in the four unknowns α, β, δ_{AP}, and δ_F. These may be computed uniquely if the heat transfer vector in the gas phase is specified.

If it is presumed that, as will be explained in more detail later, the gas phase temperature profile is represented by

$$g - g_s = (g_1 - g_s)\, f\left(\frac{y - y_s}{\delta_g - y_s}\right) \tag{22}$$

where $g_1 = g_1(s)$ is the temperature along a line $y = \delta_g$ in the gas phase and f is a function with the properties $f(0) = 0$, $f(1) = 1$, the interface heat transfer condition of Eq. 6 may be computed. After some manipulation, an additional equation for α, β, δ_F, and δ_{AP} becomes

$$\frac{g'_{s_{AP}} \left(\frac{dy_s}{dx}\right)_{AP}}{z_{AP}} - \frac{g'_{s_F} \left(\frac{dy_s}{dx}\right)_F}{z_F} =$$

$$\xi\left\{\frac{q_{s_F}}{z_F^2} - \frac{q_{s_{AP}}}{z_{AP}^2} + \eta(g_s - 1)\left(\frac{1}{z_F \delta_F} - \frac{1}{z_{AP}\delta_{AP}}\right)\right\} \tag{23}$$

where

$$g'_s = (g_s - 1)\left(-\frac{\alpha}{z} + \frac{\beta \frac{dy_s}{dx}}{z}\right)$$

is developed from Eq. 19.

A solution to Eq. 20, 21, and 23 has been obtained with g_s and r as parameters at 800 psia and with $q^*_{sF} = 77$ cal/gm. The results are shown in Fig. 5.3. The equations are quadratic in the δ's and above a certain g_s, dependent upon r, no real solutions exist. In the region where real solutions exist, Fig. 5.3 applies. The distressing thing about this figure is that g'_{sF} is never negative which implies from Eq. 16 that the surface is convex.

It is at this point that some trouble may be anticipated in the solution of the sandwich prohlem by approximate methods. The assumed temperature profiles of Eq. 17 and 18 may be highly inaccurate, and/or the assumed profile of Eq. 22, which gives a certain similarity of all temperature profiles in the y direction, may be highly in error.

ATTEMPT AT A SANDWICH SOLUTION

The overriding consideration in the analytical attempt was to avoid a direct numerical integration because of the computer time anticipated with such a method for this complex nonlinear problem. Instead, an integral technique was formulated to simplify the problem while hopefully retaining the relevant physics. While many different approximate techniques were tried during the contract year, the method described below was the one settled upon as the most likely to give success with a minimum of computation.

The solid phase is most conveniently treated in the orthogonal curvilinear n, s coordinate system for which a differential element of length is

$$d\ell^2 = dn^2 + (1 + \kappa n)^2 ds^2$$

The transformation of Eq. 5 yields

$$\frac{\partial^2 g}{\partial n^2} + \frac{\kappa}{1 + \kappa n}\frac{\partial g}{\partial n} + \frac{1}{(1 + \kappa n)^2}\frac{\partial^2 g}{\partial s^2} + \frac{n\kappa'}{(1 + \kappa n)^3}\frac{\partial g}{\partial s}$$

$$= -\frac{1}{z}\frac{\partial g}{\partial n} + \frac{y'_s}{z^2}\frac{\partial g}{\partial s}\frac{1}{1 + \kappa n} \qquad (24)$$

The approach taken was (1) to assume a temperature profile of the form of Eq. 17 with $\delta = \delta(s)$ and $g_s = g_s(s)$ and (2) to use Eq. 24 evaluated at n = 0. This amounts to a collocation at the surface. The result is an ordinary differential equation for g_s.

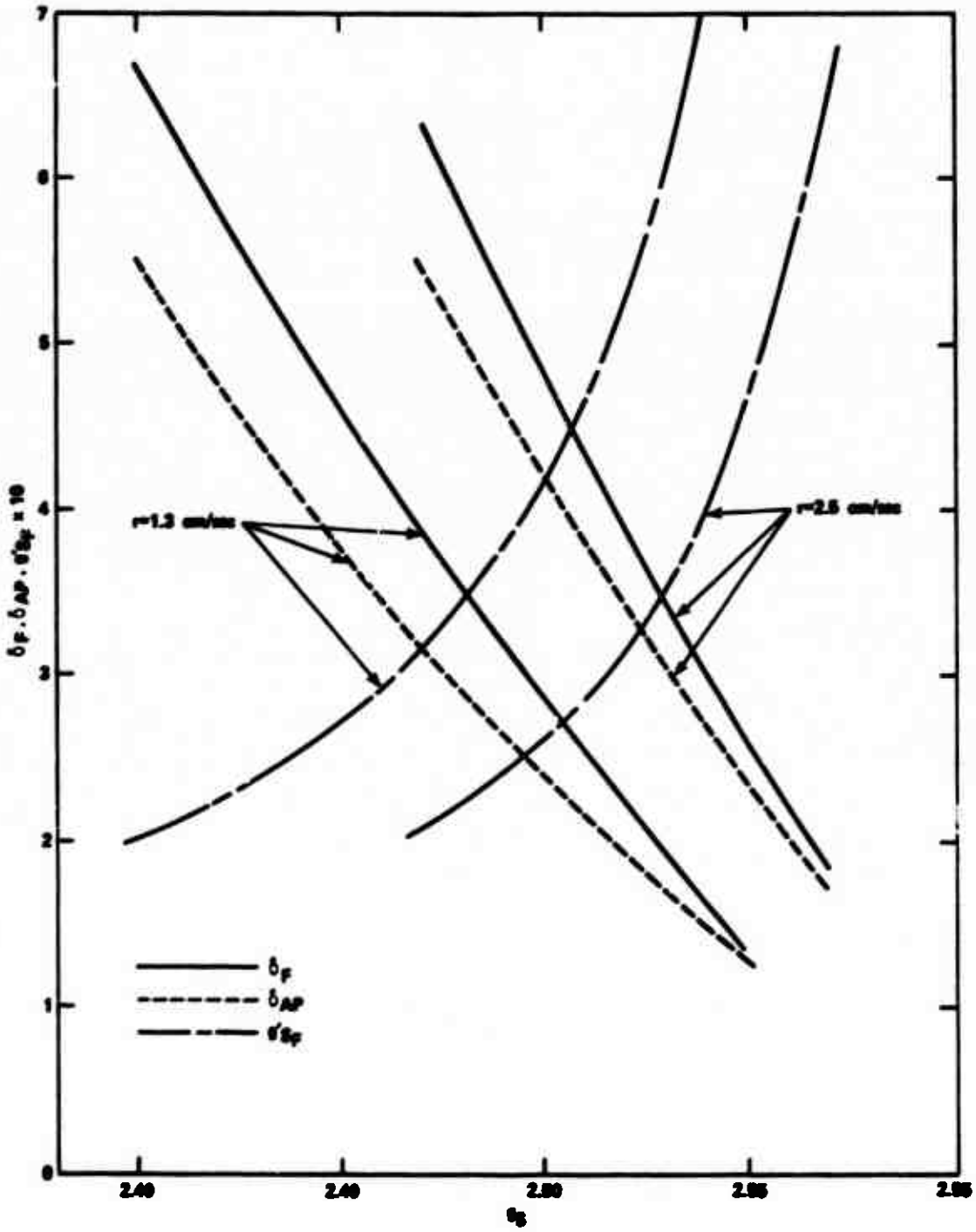

FIG. 5.3. Solution to the Interface Heat Transfer Modal.

$$g_s'' = \frac{(g_s - 1)}{\delta}\left(\frac{1}{z} + n - \frac{1}{\delta}\right) + \frac{y_s' \; g_s'}{z^2} \tag{25}$$

The reasons for this choice are as follows: (1) the thermal profile matches exactly the required pure AP profile as $s \to -\infty$ for $\delta = z_{AP}$, (2) the profile yields the exact interface solution mentioned in the preceding section above, and (3) the collocation at the interface eliminates terms in δ'', δ', and n', which markedly simplifies the calculations. As $s \to -\infty$, the condition required is that $\delta \to z_{AP}$ and $n \to 0$. From Eq. 16 and 25 clearly $g_s'' \to 0$ even though y' is finite (θ_{AP} is nonzero).

The gas phase was treated in a more complex manner. Using the nonorthogonal curvilinear y, a system of coordinates, Eq. 4 becomes

$$\frac{\partial^2 g}{\partial y^2} + z^2 \frac{\partial^2 g}{\partial s^2} + z n y'_s \frac{\partial g}{\partial s} = \xi \frac{\partial g}{\partial y} \tag{26}$$

As mentioned in the previous section, there is good reason for considering an elliptic problem totally embedded within the y-direction scale required for completion of the AP flame. Consequently, a horizontal line located at $y = \delta_g$ which is of the order of $1/\xi$ is selected to bound the elliptic region. At $y = \delta_g$ the parabolic boundary condition is placed on Eq. 26 which says that the first term of Eq. 26 is negligible compared with the rest.

A profile of the form of Eq. 22 is then selected with $g_1 = g_1(s)$ as the temperature value on $y = \delta_g$. Equation 22 is placed in Eq. 26 and integrated over $y = y_s(s)$ to $y = \delta_g$. This amounts to a one-strip integral methed and yields an ordinary differential equation in g_1 and g_s as follows:

$$g_1'' = (1 - 1/\beta)\, g_s'' + \frac{1}{z^2[\beta(\delta_g - y_s) + 1/\xi]}\left\{\left[\xi + \frac{\alpha z^2}{(\delta_g - y_s)} + \beta n z^3\right]x\right.$$

$$[g_1 - g_s] + y_s'\,[1 - nz(\delta_g - y_s)\,]\,[g_s' + \beta(g_1' - g_s')]$$

$$\left. + \beta y_s'(g_1' - g_s') - y_s'\, g_s' - \frac{g_1' z n y_s'}{\xi}\right\} \tag{27}$$

where the parabolic condition has been used in generating Eq. 27 and

$$\alpha = \left.\frac{df(\tilde{y})}{d\tilde{y}}\right]_{\tilde{y} = 0} \qquad \beta = \int_0^1 f(\tilde{y})\, d\tilde{y}$$

Once the profile function f is chosen Eq. 27 is determined. For a linear temperature profile $\alpha = 1$, $\beta = \frac{1}{2}$; for an exponential $\alpha = 0.58$, $\beta = 0.42$.

The basic reason for use of this procedure is that Eq. 27 is already quite complex. The use of more complex temperature profiles to allow dissimilar behavior in y at different s positions would require further generation of more ordinary differential equations since more unknowns than merely g would be introduced. Similarly, the use of more than one strip would introduce more unknowns and require the introduction of more differential equations.

The link between the gas and the solid phases comes about through the interface heat transfer condition of Eq. 6. Using the assumed gas and solid phase thermal profiles

$$\frac{(g_1 - g_s)\alpha z}{\delta_g - y_s} - \frac{y_s'}{z} g_s' = \xi \left[\frac{q_s}{z} + \frac{\eta(g_s - 1)}{\delta}\right] \tag{28}$$

The integration procedure used was the following:

1. Assume values for r, g_s (s = 0), and g_1' (s = 0)
2. At the starting point, s = 0 values are found for z_F and z_{AP} at the interface from Eq. 6, the pyrolysis laws
3. δ_F, δ_{AP}, g'_{s_F}, and $g'_{s_{AP}}$ at the interface are found through the procedure of the previous section.
4. $g_1(0)$ is found from Eq. 28
5. n is found from Eq. 16.
6. Integration of Eq. 25 and 28 may then proceed if at each step n is found from Eq. 16, z from the pyrolysis laws, and δ from Eq. 28.

The boundary conditions are

$$g_1 \to g_s \quad \text{as} \quad y_s \to \delta_g$$

$$\delta \to z_{AP} \quad \text{as} \quad s \to -\infty$$

$$n \to 0 \quad \text{as} \quad s \to -\infty$$

The integration proceeds along positive s until y is within ε of δ_g and then from s = 0 an integration is performed through negative s to some distance greater than $1/\xi$. The errors in the quantities g_1, δ, and n are noted and a systematic variation of the guessed quantities is begun to start a convergence scheme.

This scheme requires that the pure AP deflagration is reached at negative s before the line $y = \delta_g$ intersects the AP flame, because no chemical reaction is included in Eq. 27. The adjustment distance is open to some doubt because the solid phase can only adjust in distance scales of the order of unity, while the gas phase adjusts over distances of the order of $1/\xi$. If $\theta_{AP} > 0$, then clearly as $s \to -\infty$ the AP flame will be penetrated by the line $y = \delta_g$. To this time $s = -\infty$ has been defined to be at distances of the order of a few $1/\xi$ units from the origins, so that this problem has not arisen.

The distressing point is that to this time the procedure does not yield a solution. This is a two point, nonlinear boundary value problem with an eigenvalue r. There is mathematically no guarantee of a solution. However, the original partial differential equations should yield a physically meaningful solution. Unless the physics have been so distorted with the approximate method of solution, it would be anticipated that a solution would exist because of course, experimentally, one does exist.

There are several things which could be wrong, and these will be examined. First, the profile choices were shown in the previous section to yield an unrealistic interface condition when compared with experiment. The use of more complex profiles in the solid phase, however, negates the possibility of a simple analytical solution in this vicinity. The use of more complex profiles in either the gas or solid phases increases the number of required differential equations. If the number of differential equations increase the algebraic complexity mounts, computer time soars, and the problem is compounded when chemical reaction and the attendant mass fraction equations are considered. The gas phase temperature profile is especially suspect, but if more strips in y were considered, the solution could be made as accurate as desired. But each strip introduces a new differential equation to which the above objections are raised. Second, the presumption of a pyrolysis law for AP may be constraining the solution and forcing the unrealistic interface condition. However, physically a solution should exist to the problem as formulated. Third, the region bounds employed, artificially imposing the parabolic condition at $y = \delta_g$, may be at fault. It is clearly in error as one proceeds toward the pure AP deflagration in regions of strong y gradients. As the binder is approached, the approximation should be adequate. This condition, coupled with the potential inadequacy of gas phase profiles is considered one of the weakest points in the analysis. Fourth, there could be errors in the computer program, of course.

Assuming that the last cause is not dominant, the question remains in future work as to what direction to take. It may readily be shown that the shape of the sandwich, in the case of no contribution from the BO flame, is dependent upon the nature of the ignition transient. For uniform ignition the slope of the AP should be horizontal, away from the binder. It is first recommended that a one strip integral method be used, abandoning the parabolic condition, to investigate the allowable solutions for the pure AP to relax to a horizontal state. A more sophisticated analysis of the solid phase heat transfer condition in the interface vicinity should then be performed. Work is currently under way in these two areas. If it becomes apparent that the integral techniques are requiring too much sophistication to yield a solution, it is recommended that a direct numerical integration be attempted, or at least a study of the difficulty of such an attempt should be made. This represents a formidable task, and there is a real question concerning the probability of success using a reasonable amount of computer time. Nevertheless, the interpretation difficulty of the experimental results warrants continued attempts at analytical modeling.

SECTION 6

SUMMARY, SIGNIFICANCE AND CONCLUDING REMARKS

This program has produced many and diverse results. Any attempt to summarize would be redundant to the summaries found in each section. The summary here is in outline form giving the primary results and the significance of the finding. This last section then is intended to be a ready and handy reference. It is hoped that the information contained here will be useful for guiding others in planning and executing their future efforts, both experimental and analytical, to understand the combustion of solid propellants.

UNALUMINIZED, UNCATALYZED AP-BINDER SANDWICH

Result: All binders tested--CTPB, HTPB, PBAN and polyurethane--became liquid as the combustion front approached.

Significance: No analytical model has considered the possibility of liquid phase binder; most investigators thought binders burned "dry." Some investigators have gone so far as to classify wet and dry burning binders when in fact all the binders tested were "wet."

Result: The surface structure and subsurface profile of the AP was identical to that reported for AP self-deflagration.

Significance: The results from AP self-deflagration studies can be applied; e.g., as boundary conditions, to the case of combustion of sandwiches and perhaps to the case of composite propellant combustion.

Result: No evidence for interfacial reaction between AP and binder was obtained.

Significance: At least for the case where no catalyst was present, the class of reactions which have been hypothesized to occur at the interface could be considered non-important. This class of reactions would include subsurface heterogeneous as well as reactions of the type proposed by Fenn in his Phalanx Flame Model and by Hermance in his Crevice Model.

Result: The maximum regression always occurred in the AP.

Significance: At least two mechanisms must be operant: (1) energy feedback from a diffusion flame and (2) energy from the self-deflagration of AP. The binder behaves as an inert heat sink near the interface.

Result: Two types of flame were observed and can be related to the low pressure deflagration rate of AP: (1) at $p < 300$ psia (the low pressure deflagration limit of AP) the AP and binder pyrolysis products form a classic diffusion flame of several millimeters extent, and (2) at $300 < p < 1500$ psia, many spatially and temporally variant flames exist in the diffusion region.

Significance: At least two specific regimes can be defined with the low pressure deflagration limit serving as the criteria. In the upper region, $p > 300$ psia, the old arguments about laminar or turbulent transport properties become meaningless: the system is truly intrinsically turbulent in the full generic meaning of the word turbulence (Ref. 30). Thus, an analytical treatment of the combustion must include consideration for the change in flame structure and transport properties.

Result: At pressures greater than 1000 psi the AP regresses several times faster than does the binder.

Significance: The relevance of results of sandwich studies to propellant combustion (where due to the heterogeneity of oxidizer and binder, the binder would not have the long residence time of the sandwich situation) must be questioned for cases where the pressure exceeds 1000 psi. The relation between sandwich and propellant combustion can be improved by using thin binder layers in the sandwiches.

Result: The liquid formed from the polyurethane (PU) of the AP-PU sandwich during combustion was of low viscosity and readily flowed over the AP.

Significance: At high pressures ($p = 800$), where the AP regresses significantly faster than the PU, AP-PU propellants often self-quench. It had been postulated (Ref. 13 and 14) that this was due to liquid PU flowing over and "smothering" the AP. The low viscosity of PU coupled with its ability to wet AP seems to confirm the previous hypothesis.

Result: The liquid resulting from the combustion heating of HTPB, CTPB and PBAN was more viscous and flow was limited to a few hundred micrometers of the original interface.

Significance: In analytical modeling it could be assumed that there was little mixing of the fuel-oxidizer species except by gas phase diffusion. Models based on a statistical representation of the surface may be subject to some error, however, due to the flow and accumulation of binder.

UNALUMINIZED, CATALYZED AP-BINDER SANDWICHES

Result: Addition of Fe_2O_3 or Harshaw catalyst Cu0202 to the binder was ineffective in changing the burning rate or sample regression pattern from that of uncatalyzed sandwiches.

Result: Addition of Harshaw Cu0202 to the AP increases the burning rate greatly. The primary effect up to 1600 psi seems to be catalysis of the AP self-deflagration. Above 1600 psi it seems that interfacial phenomena increase in importance.

Result: At low pressure ($p < 1200$ psi) iron oxide inhibits the deflagration rate of the AP. Above 1000 psi, iron oxide augments the AP rate and the interfacial rate.

Significance: The results indicate two items of importance in the catalysis of real propellants: (1) because of the importance of interfacial phenomena and the usual practice of mixing the catalyst in the binder, the smaller the oxidizer grind the greater should be the catalytic effect and (2) if ways could be found to load the oxidizer or coat the oxidizer with these catalysts their effectiveness would increase markedly.

UNCATALYZED, AP-ALUMINIZED HTPB SANDWICH

Result: As-received aluminum residing on areas of AP will not readily ignite or agglomerate. It will sinter together.

Result: The behavior of as-received aluminum existing on areas of binder is characterized by accumulation/agglomeration. Each accumulate or agglomerate may contain several hundred original aluminum particles. The binder provides the "stickiness" necessary for accumulation.

Result: Ignition and combustion of the as-received aluminum occurs in the oxidizer rich portion adjacent to the diffusion flame.

Result: The accumulation/agglomeration of as-received aluminum differs markedly depending on whether the pressure is above or below the low pressure deflagration limit of AP.

Result: A special preoxidized aluminum (see Task ORD-331-001/200-1/URO 240 202) prevents agglomeration, and results in much more fine particle aluminum combustion.

Significance: The above results illustrate that the aluminum behavior is strongly affected by:

1. The environment surrounding the aluminum
2. The quality and quantity of Al_2O_3 skin surrounding the aluminum
3. The loading level and particle size of the aluminum
4. The prevailing flame structure

ANALYSIS, ANALYTIC MODELING

Result: A model was developed but a solution to the sandwich deflagration problem was not obtained.

Significance: Even in the more simple, two-dimensional sandwich configuration, analysis is at best difficult and must be compromised with respect to reality if a tractable analysis is to be performed.

Result: Order of magnitude analyses indicate that heat transfer processes adjust on quite disparate distance scales and that there is reason to suspect that binder-oxidizer reactions do not substantially affect the interface behavior for uncatalyzed situations.

Significance: The interface in these situations should be dominated by heat transfer from the AP reactions.

APPENDIX

THE DEFLAGRATION RATES OF CATALYZED AMMONIUM PERCHLORATE

Naval Weapons Center

The deflagration rates for pellets incorporating 2 w% Fe_2O_3 and 2, 4, 6 and 8 w% Harshaw catalyst Cu0202 are presented in Fig. A-1 through A-5. The pellets were prepared as follows:

1. As-received ultra-pure AP (300-500μm diameter) was ground using a mortar and pestle.
2. This powder was screened and the portion between 44-74μm was saved.
3. Catalyst was screened and the 44-74μm portion was saved.
4. AP and catalyst were mixed for 24 hours.
5. Pellets were pressed at 48,600 psi for 30 minutes. The densities of the samples were 1.91-1.94 g/cc.

The data of Fig. A-1 through A-5 show increased burn rates for the catalyzed AP (with often a higher value for the low pressure deflagration limit) and an increased temperature sensitivity of deflagration rate.

Another form of sensitivity has been graphically demonstrated in the window bomb tests. The light source for photography employed at NWC consists of a 2500 watt xenon source operated at a 72 amp current. A heat absorbing filter is used to remove that portion of the xenon spectrum not useful for photography. This system provides ample light for photography but did not contribute enough energy to alter the burn rate--the edge of the sample in the "shadow" had the same burn rate as the edge directly exposed to the radiation--for the pure AP samples. When this same illumination was used for the Fe_2O_3 and Harshaw Cu0202 catalyzed pellets, a pronounced effect was observed. The portion of the sample receiving the most illumination regressed much more rapidly than did the portion which was in the shadow. In order to overcome this problem, the radiant flux was decreased by decreasing the current to the xenon source (from 72 amps to ∿69 amps) and by inserting a #4 wire mesh attenuating screen between the xenon source and the heat filter. A #4 screen results in approximately a six-fold decrease in flux density. These modifications resulted in a planar regression of the catalyzed sample.

Thus it is shown that the addition of catalyst makes the catalyzed mixture more responsive to an increment of energy increase (both radiation and sensible enthalpy changes) than is the uncatalyzed AP. This observation should be considered in future explanations of the combustion of sandwiches or propellants which incorporate these catalysts.

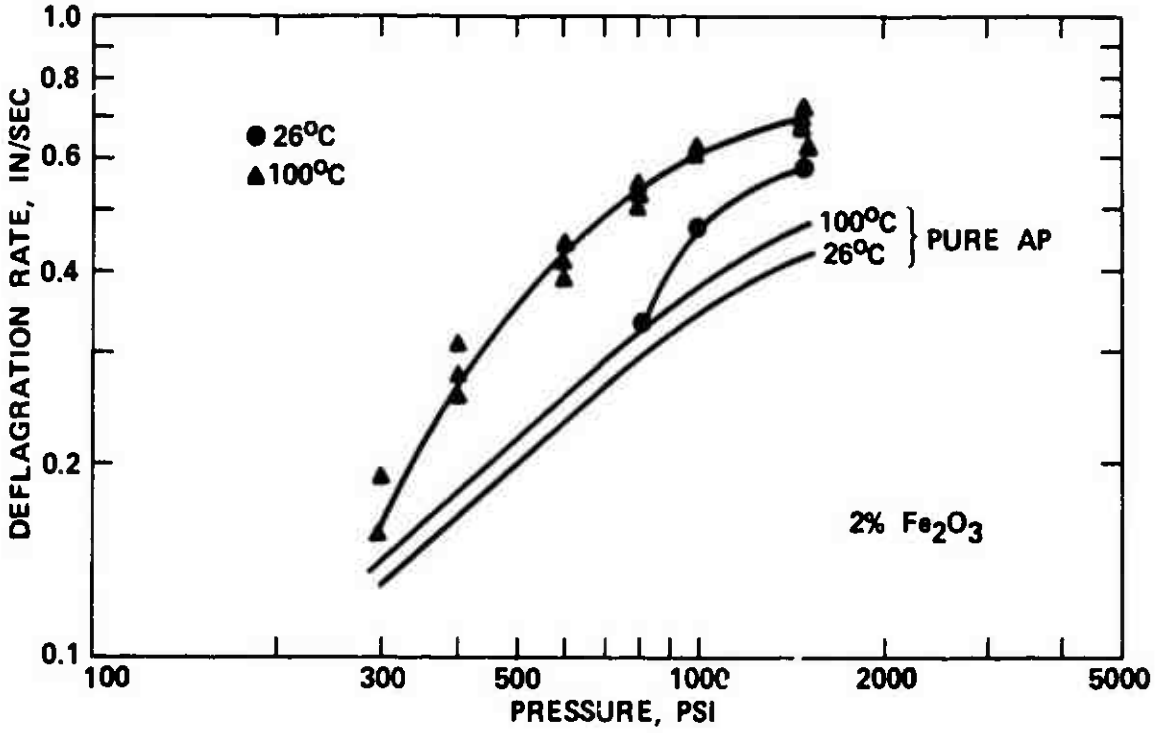

Fig. A-1. Deflagration Rate as a Function of Pressure and Initial Sample Temperature for Pure AP Plus 2 w% Fe_2O_3.

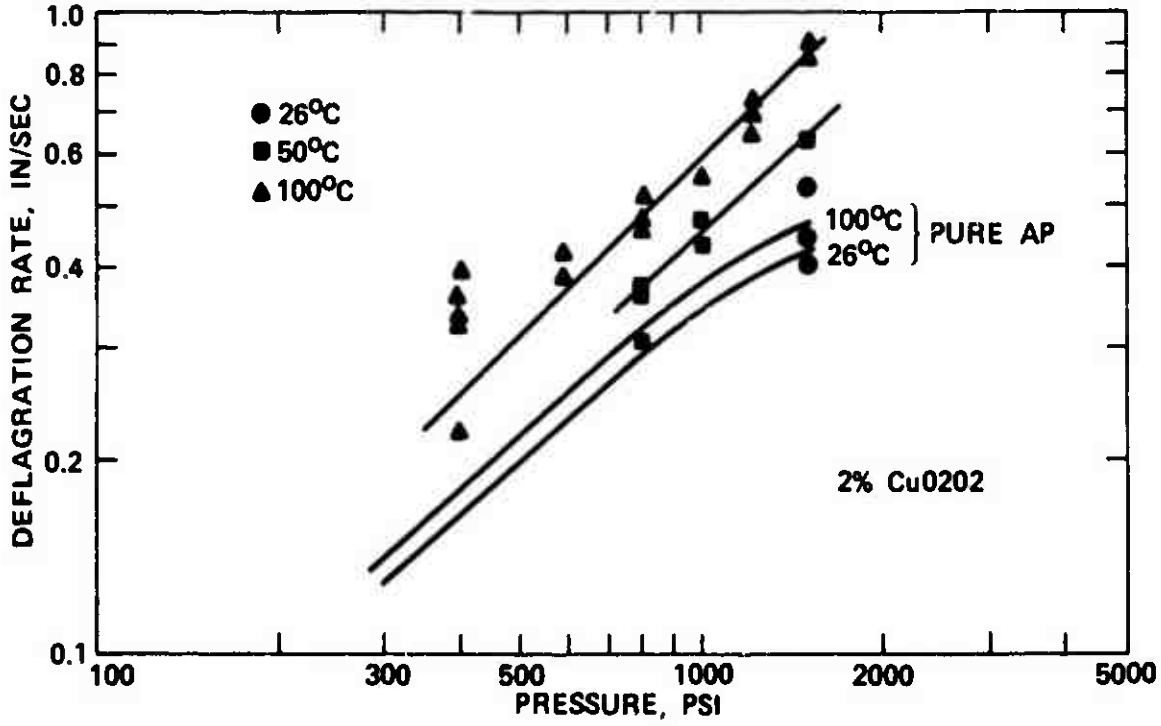

Fig. A-2. Deflagration Rate as a Function of Pressure and Initial Sample Temperature for Pure AP Plus 2 w% Cu0202.

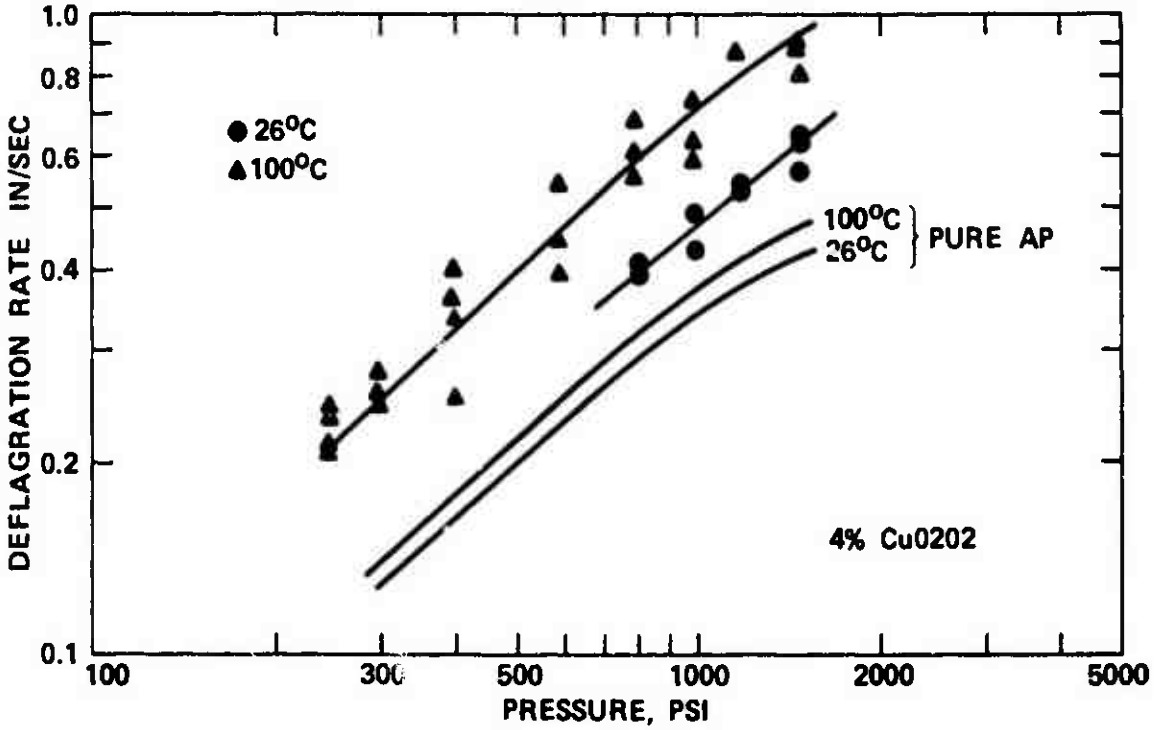

Fig. A-3. Deflagration Rate as a Function of Pressure and Initial Sample Temperature for Pure AP Plus 4 w% Cu0202.

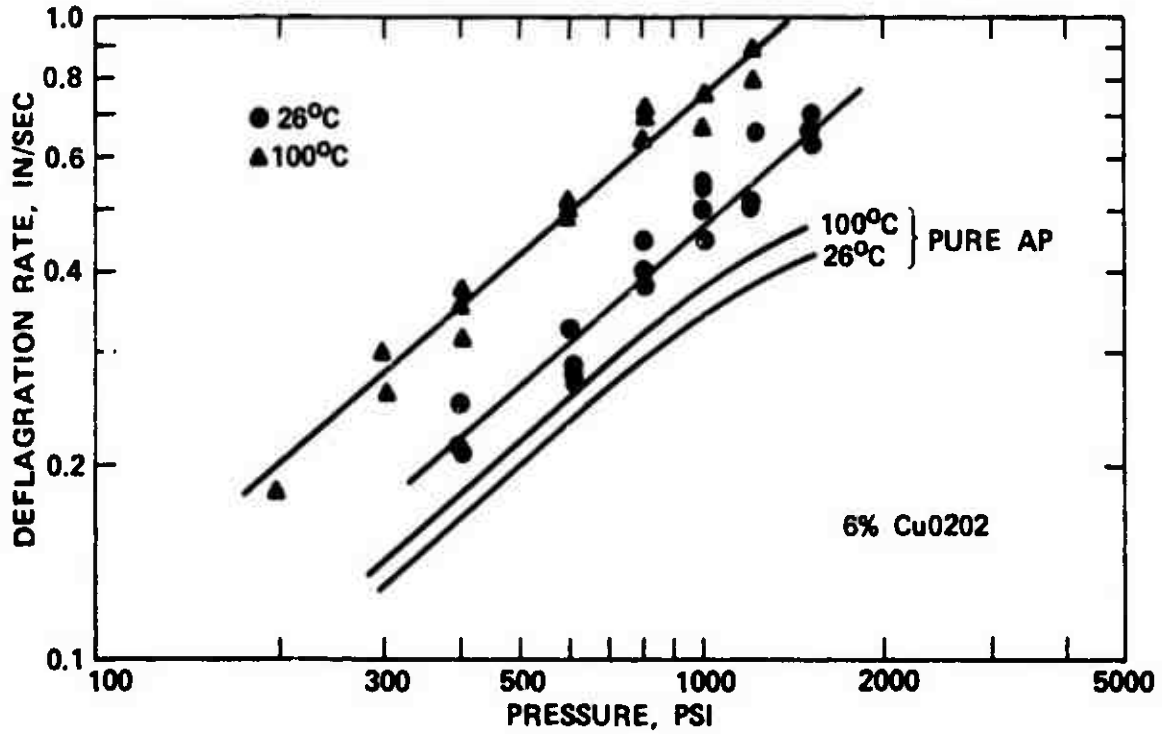

Fig. A-4. Deflagration Rate as a Function of Pressure and Initial Sample Temperature for Pure AP Plus 6 w% Cu0202.

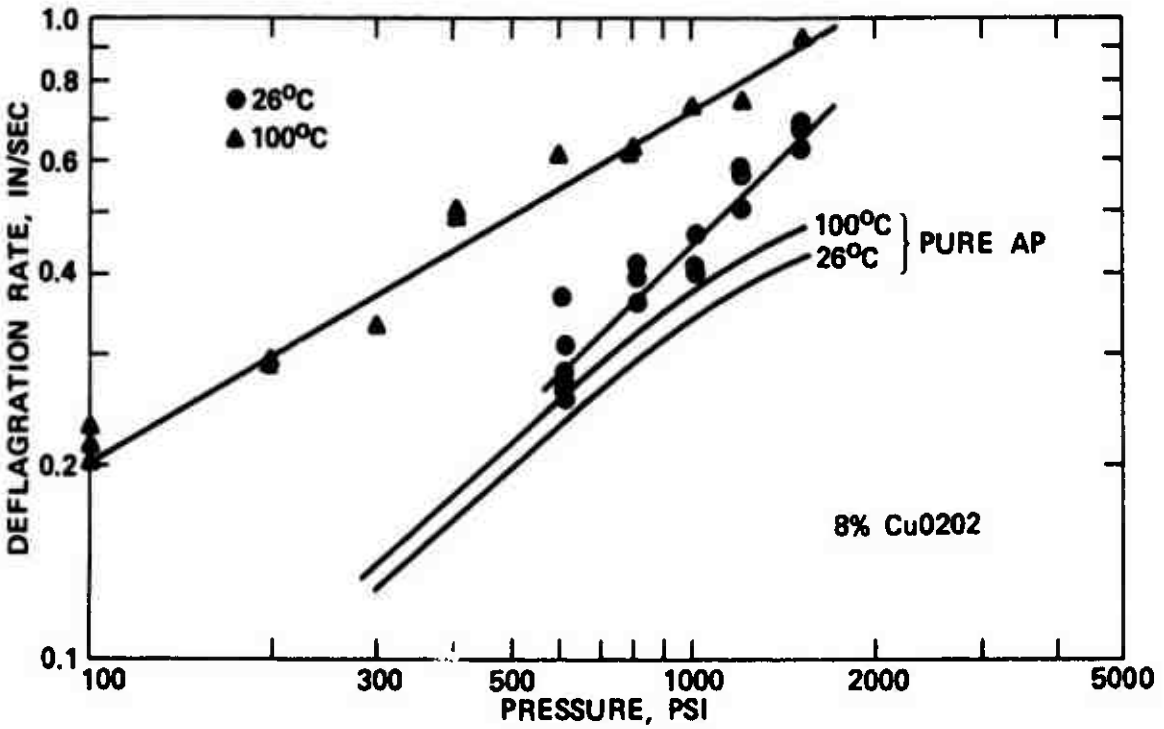

Fig. A-5. Deflagration Rate as a Function of Pressure and Initial Sample Temperature for Pure AP Plus 8 w% CuO202.

REFERENCES

1. Hightower, J. D., and E. W. Price. "Combustion of Ammonium Perchlorate," in *Eleventh Symposium (International) on Combustion.* Pittsburgh, Pa., The Combustion Institute, 1967. Pp. 463-72.

2. Boggs, T. L. "The Deflagration Rate, Surface Structure and Subsurface Profile of Self-Deflagrating Single Crystals of Ammonium Perchlorate," AMER INST AERONAUT ASTRONAUT J, Vol. 8, No. 5 (May 1970), pp. 867-73.

3. Boggs, T. L., and K. J. Kraeutle. "Role of the Scanning Electron Microscope in the Study of Solid Rocket Propellant Combustion, I. Ammonium Perchlorate Decomposition and Deflagration," COMBUST SCI & TECH, Vol. 1, No. 2 (September 1969), pp. 75-93.

4. Boggs, T. L., E. W. Price, and D. E. Zurn. "The Deflagration of Pure and Isomorphously Doped Ammonium Perchlorate," in *Thirteenth Symposium (International) on Combustion.* Pittsburgh, Pa. The Combustion Institute, 1971. Pp. 995-1008.

5. Povinelli, Louis A. "Summary Report on the Nature of Ammonium Perchlorate Deflagration," in *6th ICRPG Combustion Conference,* Chemical Propulsion Information Agency, Silver Spring, Md., December 1969. CPIA Publ. No. 192, Vol. 1, pp. 371-74.

6. Shannon, L. J., and J. E. Erickson. "Thermal Decomposition of Composite Solid Propellant Binders," in *Sixth ICRPG Combustion Conference,* Chemical Propulsion Information Agency, Silver Spring, Md., December 1969. CPIA Publ. No. 192, Vol. 1, pp. 519-30.

7. Varney, A. M. "An Experimental Investigation of the Burning Mechanisms of Ammonium Perchlorate Composite Solid Propellants," Ph.D. Thesis, Georgia Institute of Technology, May 1970. 226 pp.

8. Fleming, R. W., R. L. Derr, and N. S. Cohen. "Role of Binder in Solid Propellant Combustion," New York, N. Y., American Institute of Aeronautics and Astronautics, November 1972. (AIAA Paper No. 72-1121.)

9. Bouch, L. S. "A High-Heating-Rate Thermal Analysis of Solid-Propellant Reactions," Ph.D. Thesis, University of Utah, August 1971. 169 pp.

10. Pokhil, P. F., and L. D. Romodanova. *Investigation of the Structure of Surface of Burning of Model Mixtures of Solid Fuels*, tr. by Foreign Technology Division, Air Force Systems Command. Wright-Paterson Air Force Base, Ohio, 1967. 8 pp. (AD 671873.)

11. Bastress, E. K. "Modification of the Burning Rates of Ammonium Perchlorate Solid Propellants by Particle Size Control," Ph.D. Thesis, Princeton University, Princeton, N. J., 1961.

12. Selzer, H. "Surface Reactions in Solid Propellants," in *AGARD 34th Propulsion and Energetics Panel's Meeting*, 13-17 October 1969, Dayton, Ohio.

13. Boggs, T. L., R. L. Derr, and M. W. Beckstead. "Surface Structure of Ammonium Perchlorate Composite Propellants," AMER INST AERONAUT ASTRONAUT J, Vol. 8, No. 2 (February 1970), pp. 370-72.

14. Derr, R. L., and T. L. Boggs. "Role of Scanning Electron Microscopy in the Study of Solid Propellant Combustion: Part III. The Surface Structure and Profile Characteristics of Burning Composite Solid Propellants," COMBUST SCI & TECH, Vol. 1, No. 5 (April 1970), pp. 369-84.

15. Naval Ordnance Test Station. *Combustion of Solid Propellants and Low Frequency Combustion Instability*, by Aerothermochemistry Division, China Lake, Calif., NOTS, June 1967. (NOTS TP 4244.)

16. Hightower, J. D., and E. W. Price. "Experimental Studies Relating to the Combustion Mechanism of Composite Propellants," ASTRONAUT ACTA, Vol. 14, No. 1 (November 1968), pp. 11-21.

17. Austin, T. D. "Flame Temperature Profile of Ammonium Perchlorate Fuel Binder Sandwiches," in *Fourth Combustion Conference*, Chemical Propulsion Information Agency, Silver Spring, Md., December 1967. CPIA Publ. No. 162, Vol. 1, pp. 487-90.

18. Powling, J. "The Combustion of Ammonium Perchlorate Based Composite Propellants: A Discussion of Some Recent Experimental Results," Explosives Research and Development Establishment, Waltham Abbey, Essex, England, 1965. (ERDE Report No. 15-R-65.)

19. Nadaud, L. "Models Used at ONERA to Interpret Combustion Phenomena in Heterogeneous Solid Propellants," COMBUST AND FLAME, Vol. 12, No. 3 (June 1968), pp. 177-95.

20. Varney, A. M., and W. C. Strahle. "An Experimental Investigation of the Combustion Mechanisms of Ammonium Perchlorate-Based Composite Solid Propellants," New York, N. Y., American Institute of Aeronautics and Astronautics, 1971. (AIAA Paper No. 71-170.)

21. Nachbar, W. "A Theoretical Study of The Burning of a Solid Propellant Sandwich," in *Solid Propellant Rocket Research*, ed. by Martin Summerfield. Vol. 1, Progress in Astronautics and Rocketry, a series of volumes sponsored by ARS. New York, London, Academic Press, 1960. Pp. 207-26.

22. Boggs, T. L., and D. E. Zurn. "The Deflagration of Ammonium Perchlorate-Polymeric Binder Sandwich Models," COMBUST SCI TECH J, Vol. 4, No. 6 (February 1972), pp. 279-92.

23. Varney, A. M., and W. C. Strahle. "Experimental Combustion Studies of Two-Dimensional Ammonium Perchlorate-Binder Sandwiches," COMBUST SCI & TECH, Vol. 4, No. 5 (January 1972), pp. 197-208.

24. Jones, H. C., and W. C. Strahle. "The Effects of Copper Chromite and Iron Oxide Catalysts on AP/CTPB Sandwiches," in *14th Symposium (International) on Combustion*. Pittsburgh, Pa., The Combustion Institute, 1972.

25. Fenn, J. B. "A Phalanx Flame Model for the Combustion of Composite Solid Propellant," COMBUST AND FLAME, Vol. 12, No. 3 (June 1968), p. 201.

26. Steinz, J. A., and H. Selzer. "Depressurization, Extinguishment of Composite Solid Propellants: Flame Structure, Surface Characteristics and Restart Capability," COMBUST SCI & TECH, Vol. 3, No. 1 (April 1971), pp. 25-36. See also: Steinz, J. A., and H. Selzer, "Depressurization, Extinguishment for Various Starting Pressure and Solid Propellant Types," New York, N. Y., American Institute of Aeronautics and Astronautics, June 1971. (AIAA Paper No. 71-631.)

27. Brown, W. E., J. R. Kennedy, and D. W. Netzer. "A Study of AP/PBAA Sandwich and AP Pellet Combustion," in *8th JANNAF Combustion Meeting*, Chemical Propulsion Information Agency, Silver Spring, Md., December 1972. CPIA Publ. No. 231, Vol. II, pp. 169-86.

28. Brown, W. E., J. R. Kennedy, and D. W. Netzer. "An Experimental Study of Ammonium Perchlorate-Binder Sandwich Combustion in Standard and High Acceleration Environments," COMBUST SCI & TECH, Vol. 6 (1972), pp. 211-22.

29. Naval Postgraduate School. *Nonmetallized Composite Propellant Combustion*, by D. W. Netzer, J. R. Kennedy, G. M. Biery, II, and W. E. Brown. Monterey, Calif. 1 March 1972. (NPS-57NT72031A.)

30. Derr, R. L. "Review of the Workshop on Steady-State Combustion and Modeling of Composite Solid Propellants, in *7th JANNAF Combustion Meeting*, Chemical Propulsion Information Agency, Silver Spring, Md., February 1971. CPIA Publ. No. 204, Vol. 1, pp. 1-8.

31. Hermance, C. E. "A Model of Composite Propellant Combustion Including Surface Heterogeneity and Heat Generation," AMER INST AERONAUT ASTRONAUT J, Vol. 4, No. 9 (September 1966), pp. 1629-37.

32. Princeton University. *The Burning Mechanism of Ammonium Perchlorate-Based Composite Solid Propellants,* by J. A. Steinz, P. L. Stang, and M. Summerfield, February 1969. (Aerospace and Mechanical Sciences Report No. 830.)

33. Jones, H. E. "An Experimental Investigation Relating to the Combustion Mechanisms of Ammonium Perchlorate Composite Propellants," Ph.D. Thesis, Georgia Institute of Technology, 1971.

34. Boggs, T. L., and D. E. Zurn. "The Temperature Sensitivity of the Deflagration Rates of Pure and Doped Ammonium Perchlorate," COMBUST SCI & TECH, Vol. 4, No. 5 (January 1972), pp. 227-32.

35. Levy, J. B., and Friedman, R. "Further Studies of Ammonium Perchlorate Deflagration," in *8th Symposium (International) on Combustion,* Williams and Wilkens, Baltimore, 1962. Pp. 663-72.

36. Pittman, C. U., Jr. "Location of Action of Burning Rate Catalysts in Composite Propellant Combustion," AMER INST AERONAUT ASTRONAUT J, Vol. 7, No. 2 (February 1969), pp. 328-34.

37. Pearson, G. S. "Composite Propellant Catalysts: Copper Chromate and Chromite," COMBUST AND FLAME, Vol. 14, No. 1 (February-June 1970), pp. 73-84.

38. Pearson, G. S., and D. Sutton. "Composite Solid Propellant Ignition: Ignition of Ammonia and Other Fuels by Perchloric Acid Vapor," AMER INST AERONAUT ASTRONAUT J, Vol. 5, No. 2 (February 1967), pp. 344-46.

39. Beckstead, M. W., Derr, R. L., and Price, C. F. "A Model of Composite Solid Propellant Combustion Based on Multiple Flames," AMER INST AERONAUT ASTRONAUT J, Vol. 8, No. 12 (December 1970), pp. 2200-07.

40. Crump, J. E. "Photographic Survey of Aluminum Combustion in Solid Propellants," in *Proceedings of 1st ICRPG Combustion Instability Conference,* Chemical Propulsion Information Agency, Silver Spring, Md., January 1965. CPIA Publ. No. 68, Vol. 1, pp. 367-71.

41. Naval Weapons Center. *Behavior of Aluminum in Solid Propellant Combustion,* by E. W. Price, J. E. Crump, K. J. Kraeutle, J. L. Prentice, and D. E. Zurn. To be published. See also: Naval Weapons Center Technical Note 608-121.

42. Naval Weapons Center. *Combustion of Solid Propellants and Low Frequency Combustion Instability Progress Report, 1 April- 30 September 1967*, by Aerothermochemistry Division. China Lake, Calif., NWC, April 1968. 108 pp. (NWC TP 4478.)

43. Crump, J. E., J. L. Prentice, and K. J. Kraeutle. "Role of the Scanning Electron Microscope in the Study of Solid Propellant Combustion: II. Behavior of Metal Additives," COMBUST SCI & TECH, Vol. 1, No. 3 (November 1969). pp. 205-23.

44. Willoughby, P. G., K. L. Baker, and R. W. Hermsen. "Photographic Study of Solid Propellants Burning in an Acceleration Environment," United Technology Center Contractor Report for NASA CR-66824 (undated.)

45. Crump, J. E. "Aluminum Combustion in Composite Propellants," in *2nd Combustion Conference*, Interagency Chemical Rocket Propulsion Group, Chemical Propulsion Information Agency, Silver Spring, Md., May 1966. CPIA Publ. No. 105, Vol. 1, pp. 321-29

46. U. S. Naval Ordnance Test Station. *Aluminum Particle Combustion Progress Report*, by Metal Combustion Study Group. China Lake, Calif., NOTS, April 1966. (Technical Progress Report 415, NOTS TP 3916.)

47. Naval Weapons Center. *Metal Particle Combustion Progress Report*, by Metal Combustion Study Group, Edited by J. L. Prentice, China Lake, Calif., NWC, August 1968. 118 pp. (NWC TP 4435.)

48. Prentice, J. L. "On the Combustion of Single Aluminum Particles," COMBUST SCI & TECH, Vol. 9, No. 2 (June 1965), pp. 208-10.

49. Prentice, J. L., C. M. Drew, and H. C. Christensen. "Preliminary Studies of High-Speed Photography of Aluminum Particle Combustion in Flames," PYRODYNAMICS, Vol. 3, No. 1 and 2 (July 1965), pp. 81-90.

50. Drew, C. M. "Some Further Comments on the paper 'Estimating Aluminum Particle Combustion Kinetic,'" COMBUST AND FLAME, Vol. 9, No. 2 (June 1965), pp. 205-8.

51. Christensen, H. C., R. H. Knipe, and Alvin S. Gordon. "Survey of Aluminum Particle Combustion," PYRODYNAMICS, Vol. 3, No. 1 and 2 (July 1965), pp. 91-119.

52. Kraeutle, K. J. "The Behavior of Aluminum During Subignition Heating and Its Dependence on Environmental Conditions and Particle Properties," in *9th JANNAF Combustion Conference*, Chemical Propulsion Information Agency, Silver Spring, Md., December 1972. CPIA Publ. No. 231, Vol. 1, pp. 325-40.

53. Price, E. W. "Review of the Combustion Instability Characteristics of Solid Propellants," in *Advances in Tactical Rocket Propulsion, AGARD Conference Proceedings No. 1*, ed. by S. S. Penner, Maidenhead, England, Technivision Services, August 1968. Pp. 147-53, 165-67, 181.

54. -----. "Relevance of Analytical Models for Perturbation of Composite Solid Propellants," AMER INST AERONAUT ASTRONAUT J., Vol 7, No. 1 (January 1969), pp. 153-54.

55. U. S. Naval Ordnance Test Station. *Low-Frequency Combustion Instability of Solid Rocket Propellants, 1 July - 1 September 1962*, by E. W. Price. China Lake, Calif., NOTS, December 1962. Pp. 3-4. (TPR 301, NOTS TP 3107.)

56. -----. *Low-Frequency Combustion Instability of Solid Rocket Propellants, 1 September 1962 - 1 May 1963*, by M. D. Horton, J. L. Eisel, and E. W. Price. China Lake, Calif., NOTS, May 1963. Pp. 2-6. (TPR 318, NOTS TP 3248.)

57. -----. *Status of Solid Rocket Combustion Instability Research*, by E. W. Price. China Lake, Calif., NOTS, February 1967. Pp. 5-6. (NOTS TP 4275.) See also: Pages 12-14 of Ref. 15.

58. Guirao, C., and F. A. Williams. "A Model for Ammonium Perchlorate Deflagration Between 20 and 100 atm," AMER INST AERONAUT ASTRONAUT J, Vol. 9, No. 7 (July 1971), pp. 1345-56.

59. Williams, F. A. *Combustion Theory*, Addison-Wesley, Reading, Mass., 1965, p. 37.

60. Myers, B. F., and C. R. Bartle. "Reaction and Ignition Delay Times in the Oxidation of Propane," AMER INST AERONAUT ASTRONAUT J, Vol. 7, No. 10 (October 1969), pp. 1962-69.

61. Bakhman, N. N., and V. B. Librovich. "Flame Propagation Along Solid Fuel-Solid Oxidizer Interface," COMBUST AND FLAME, Vol. 15, No. 2 (October 1970), pp. 143-55.

62. Culick, F. E. C., and G. L. Dehority. "An Elementary Calculation for the Burning Rate of Composite Solid Propellants," COMBUST SCI & TECH, Vol. 1, No. 3 (November 1969), pp. 193-204.

63. Strahle, W. C. "One-Dimensional Stability of AP Deflagrations," AMER INST AERONAUT ASTRONAUT J, Vol. 9, No. 4 (April 1971), pp. 565-69.

3 Lewis Research Center
Dr. R. J. Priem (1)
Dr. L. A. Povinelli (1)
Technical Library (1)
2 Lyndon B. Johnson Space Center
J. G. Thibodaux (1)
Technical Library (1)
1 Science & Technology Information Facility, Bethesda (NASA Representative, CRT)
3 Aerojet Solid Propulsion Company, Sacramento, Calif, via AFPRO
Head, Technical Information Office (1)
P. Micheli (1)
W. Schmidt (1)
1 Aerospace Corporation, Los Angeles, Calif. (Technical Library)
4 Allegany Ballistics Laboratory, Cumberland, Md.
K. O. Hartman (1)
R. Miller (1)
R. Yount (1)
Technical Library (1)
1 Applied Physics Laboratory, JHU, Silver Spring, Md.(Technical Library)
1 ARO, Incorporated, Arnold Air Force Station, Tenn.(N. S. Dougherty, Jr.)
3 Atlantic Research Corporation, Alexandria, Va.
M. King (1)
A. Macek (1)
Technical Library (1)
1 Bermite Division of Tasker Industries, Saugus, Calif.(Technical Library)
2 Brigham Young University, Provo, Utah
Dr. Marvin D. Horton (1)
R. L. Coates (1)
1 Brookhaven National Laboratory, Upton, N. Y. (P. W. Levy)
2 California Institute of Technology, Pasadena, Calif.
Dr. F. E. C. Culick (1)
Dr. Frank E. Marble (1)
2 Chemical Propulsion Information Agency, Applied Physics Laboratory, Silver Spring, Md.
T. W. Christian, 1II (1)
Technical Library (1)
2 Davidson Laboratory, Stevens Institute of Technology, Hoboken, N.J.
Mechanical Engineering Department
Dr. R. F. McAlevy, 1I1 (1)
Dr. R. B. Cole (1)
1 Factory Mutual Research Corporation, Norwood, Mass.
(Dr. G. H. Markstein)
12 Georgia Institute of Technology, Atlanta, Ga.
Dr. W. Strahle (10)
Dr. B. Zinn (1)
Technical Library (1)

3 Hercules, Inc., Bacchus Works, Magna, Utah
M. Beckstead (1)
K. B. Isom (1)
Technical Library (1)
1 Institute for Defense Analyses, Arlington, Va. (Technical Library)
3 Jet Propulsion Laboratory, CIT, Pasadena, Calif.
Warren Dowler (1)
Leon Strand (1)
Tachnical Library (1)
1 Lockheed Missiles & Space Company, Sunnyvale, Calif.(Technicsl Library)
4 Lockhaed Propulsion Company, Redlands, Calif.
Dr. N. S. Cohen (1)
Dr. R. L. Derr (1)
R. W. Fleming (1)
Technical Library (1)
1 Martin Marietta Corp., Baltimore, Md. (Research Institute for Advanced Studies, J. N. Maycock)
4 Princeton University, Forrestal Campus Library, Princeton, N. J.
Dr. I. Glassman (1)
Dr. M. Summerfield (1)
L. Caveny (1)
3 Purdue University, West Lafayette, Ind.
A. M. Mellor (1)
J. R. Osborn (1)
Technical Library (1)
1 Rocket Research Corporation, Redmond, Wash. (Technical Library)
2 Rocketdyne, Canoga Park, Calif.
J. E. Flanagan (1)
Technical Library (1)
3 Rocketdyne, McGregor, Tex.
W. Haymes (1)
G. D. Sammons (1)
Technical Library (1)
4 Sandia Corporation, Albuquerque, N. Mex.
H. S. Levine (1)
R. T. Meyer (1)
L. S. Nelson (1)
Tachnical Library (1)
1 Stanford Research Institute, Manlo Park, Calif.(Technical Library)
1 University of Delaware, Newark, Dal.(Prof. H. C. Beachell)
2 University of Denver, Danver Rasearch Institute, Denver, Colo.
W. McLain (1)
R. Williams (1)
1 University of Illinois, Urbana, Ill. (H. Krier)
3 University of Utah, Salt Laks City, Utah
Prof. A. Baer (1)
Prof. N. W. Ryan (1)
Technical Library (1)
2 Yale University, New Haven, Conn.
Prof. J. Fenn (1)
Prof. Daniel Rosner (1)